ELUCIDATING THE MECHANISM OF ACTION OF SELECTIVE HISTONE DEACETYLASE INHIBITORS IN CANCER

By

Christina Elizabeth Wells

Dissertation

Submitted to the Faculty of the

Graduate School of Vanderbilt University

in partial fulfillment of the requirements

for the degree of

DOCTOR OF PHILOSOPHY

in

Biochemistry

May, 2013

Nashville, Tennessee

Approved:

Professor Scott Hiebert

Professor Lawrence Marnett

Professor Christopher Williams

Professor Kevin Schey

Professor Utpal Dave

This dissertation is dedicated to my Granny, Papa, Grandpa Wells, and Grandma Wells. You were not here to experience this time in my life but I know you were always watching over me. Thank you for your unconditional love and for wonderful memories. I miss you every day.

In Loving Memory of

Lona Yawn

DW Yawn

Harold Wells

Audrey Wells

ACKNOWLEDGEMENTS

Graduate school has been a challenging but rewarding experience and many thanks are owed to the people who have helped me through it. First, I would like to thank Dr. Scott Hiebert for allowing me to join his lab 4 years ago. Thank you, Scott, for pushing me to work hard and not give up. It has definitely not been an easy ride here in graduate school and Scott helped me work through failed or negative result-projects to ultimately end up working on the project in this dissertation. Also, thanks for being supportive of my career choices. I will definitely take the skills and knowledge I learned here in this lab to my future career.

Also, thank you to my thesis committee members, Drs. Larry Marnett, Chris Williams, Utpal Dave, and Kevin Schey, and my former committee members, Drs. Zu-Wen Sun and Stacey Huppert. Thank you for discussing my work with me and helping me come up with ideas to move forward with my project. Thank you for sticking with me through project changes and changing paper submission dates. Thank you for your time and commitment to my project.

I must thank the Hiebert lab members for all the support over the years. A special thanks goes out to Dr. Kristy Stengel for basically putting up with my shenanigans. Thank you to Kristy for letting me vent about experiments and life, for laughing with me, discussing science with me, eating lunch with me every day, and just being an overall great friend. I'll miss you very much! Also, thanks to Steven Pierce for being a great lab manager and watching over my mice for

me when I have too much to do, and to Dr. Yue Zhao for being such a great lab mate and always willing to help me out. Also, thanks to all the new members of the Hiebert lab for all of your help and support. I wish all of the Hiebert lab members the best of luck on experiments and your futures!

I also want to thank previous Hiebert lab members, Jonathan Kaiser, Dr. Melissa Fischer, Dr. Laura DeBusk, Marion Hills, and Dr. Aubrey Hunt. I shared this lab space for the greatest length of time with these people and I could not have made it through graduate school without them. Thank you, Jonathan, for joking with me and always making me smile. Thank you for helping me out so many times and being my buddy. We endured so many obstacles together and I know we will always have a great friendship because of it. I miss you and wish you were here.

Thank you to Melissa for letting me rotate with her forever ago and helping me learn so much. Thank you for the long talks and the endless support. I know we do not get to see each other near as much as we use to but I still cherish our friendship as much as when we saw each other every day. Thanks for being such a great friend. Thank you to Laura for being such a wonderful person and always knowing how to cheer me up. Thank you to Marion for all the “sewing” talks, the laughs, the support, and for sticking with me when times were tough in the lab. I wish you and your new family the best of wishes! Thanks to Aubrey for all the help and especially keeping me company when you came back to the lab during the winter. I really enjoyed having you back!

I also would like to thank my undergraduate mentor, Dr. Tom Rybolt at the University of Tennessee at Chattanooga and my high school chemistry teacher, Mrs. Anita Pippin. Thank you for getting me interested in chemistry and teaching me more than I thought was possible. Thank you for your supportive teachings and kind criticism. I am where I am today because of your influences on my life and I thank you for that.

Last but not least, I want to thank my family. Without the support of my family I would not have made it through graduate school. I thank you for understanding when I miss Sunday dinners and holidays and making me always feel loved when I finally do get to come home. Thank you for keeping me in the loop of family happenings. I have the greatest family in the world and I cherish each and every one of you. Thank you to my dad, Randy Wells, for all of the encouragement and advice. Thank you for putting up with my delayed responses to emails and sporadic visits home. I know we don't get to see each other as much as we use to but I love you and thank you for being such a great dad. My last thank you goes to my mom, Connie Wells. Frankly, there are no words big enough for the thank you that is coming your way. Thank you for everything from house work, to cooking, to late nights helping me stay awake to finish my work. Thank you for giving up your time at your home to be with me and help me through these challenging times. Thank you for your love and always knowing that I could do it. Just thank you and know that I love you.

TABLE OF CONTENTS

LIST OF FIGURES

LIST OF TABLES

ABBREVIATIONS

ac - acetylated

Alb - albumin

AML1 - acute myeloid leukemia 1

ATRA - all trans retinoic acid

BET - bromodomain and extra-terminal

BrdU - bromo deoxyuridine

CALCL - cutaneous anaplastic large cell lymphoma

CBP - CREB-binding protein

CldU - chloro deoxyuridine

CoA - coenzyme A

CoREST - corepressor of repressor element 1 silencing transcription

CTCL - cutaneous T cell lymphoma

DAD - deacetylase activation domain

Depsi - Depsipeptide

DNA - deoxynucleic acid

EdU - ethynyl deoxyuridine

EST - expressed sequence tag

GCN5 - general control nonderepressible 5

GNAT - Gcn5 N acetyltransferases

HAT - histone acetyltransferase

HDAC - histone deacetylase

HDIs - histone deacetylase inhibitors

HMBA - hexamethylenebisacetamide

IdU - iodo deoxyuridine

IP4 - Ins(1,4,5,6)P_4

iPOND - isolation of proteins on nascent DNA

LyP - lymphomatoid papulosis

MEF - mouse embryonic fibroblast

MEF2 - myocyte enhancing factor 2

MEL - murine erythroleukemia

MF - mycosis fungoides

Mi2/NURD - nucleosome remodeling and deacetylase

MTG8 - myeloid translocation gene 8

MYST - MOZ YBF2/SAS3-SAS2-TIP60

NaB - sodium butyrate

NAD - nicotinamide adenine dinucleotide

NCoR - nuclear corepressor

NES - nuclear export signal

NLS - nuclear localization signal

PDB - protein database

PI - propidium iodide

PUVA - psoralen plus ultraviolet A

RAR - retinoic acid receptor

redFK - reduced form of Romidepsin

ROS - reactive oxygen species

Rpd3 - reduced potassium dependency 3

RXR - retinoid x receptor

SAHA - suberoylanilide hydroxamic acid

SANT - Swi3/Ada2/NCoR/TFIIIB

Sin3 - Swi independent 3

SIR - silent information regulator

SMRT - silencing mediator of retinoic and thyroid receptors

SS - Sézary Syndrome

T_{CM} - central memory T cell

T_{EM} - effector memory T cell

Th1 - T helper 1

Th2 - T helper 2

TSA - trichostatin A

TSEBT - total skin electron beam therapy

VPA - valproic acid

WCL - whole cell lysate

WT - wildtype

Zn^{2+} - zinc

CHAPTER I

INTRODUCTION

In order for a cell to undergo proliferation, DNA must be faithfully replicated each cell cycle. DNA is packaged tightly and neatly with histones into chromatin in order to fit into the nucleus of a cell. Chromatin modifications play important roles in crucial cell processes such as DNA replication, DNA repair, and transcription. Chromatin modifications can regulate recruitment of chromatin remodeling factors or chromatin modifiers, recruitment of DNA replication machinery, and transcription. Due to the important role that chromatin modifications play in these crucial cell processes, it is logical that aberrations in chromatin modifiers can have detrimental effects on cells, such as the development of cancer and disease.

Chromatin

Nucleosome Structure

Over a meter of DNA is condensed into the nucleus of each cell. This is accomplished by compacting the DNA into condensed chromatin fibers. The nucleosome is the basic building block of chromatin. Each nucleosome is composed of 147 base pairs of DNA that is wrapped around a core histone octamer. Each histone octamer is made up of two copies of histones H2A, H2B,

H3, and H4 [1-4] (Figure 1). The N-terminal histone tail of the core histone octamer is unstructured while the rest of the core histone is globular [4, 5]. Linker DNA, or short DNA segments, link nucleosomes together and these linked nucleosomes undergo short-range interactions with other neighboring nucleosomes to form chromatin fibers [4-6]. These fibers then interact with other chromatin fibers and compact into condensed chromatin. Chromatin can be divided into two major states, either heterochromatin or euchromatin. Heterochromatin is highly condensed and thought of as in a “closed” state, which is associated with transcriptional repression [1]. Euchromatin is in a relaxed, more open state and corresponds to regions of active transcription [1]. Histone modifications alter chromatin structure and switch the chromatin between these open and closed states.

Histone Modifications

Histone modifications occur predominantly on the N-terminal tails of histones and to a lesser extent on the globular regions of histones [1, 3, 5]. These modifications are regulated in a dynamic fashion and are added and removed by specific enzymes. These modifications appear to alter chromatin structure by affecting non-covalent interactions between and within nucleosomes to condense or unravel the chromatin. Also, proteins with specialized domains can recognize certain histone modifications and bind to these sites to then recruit additional proteins and chromatin modifying enzymes. These specialized domain

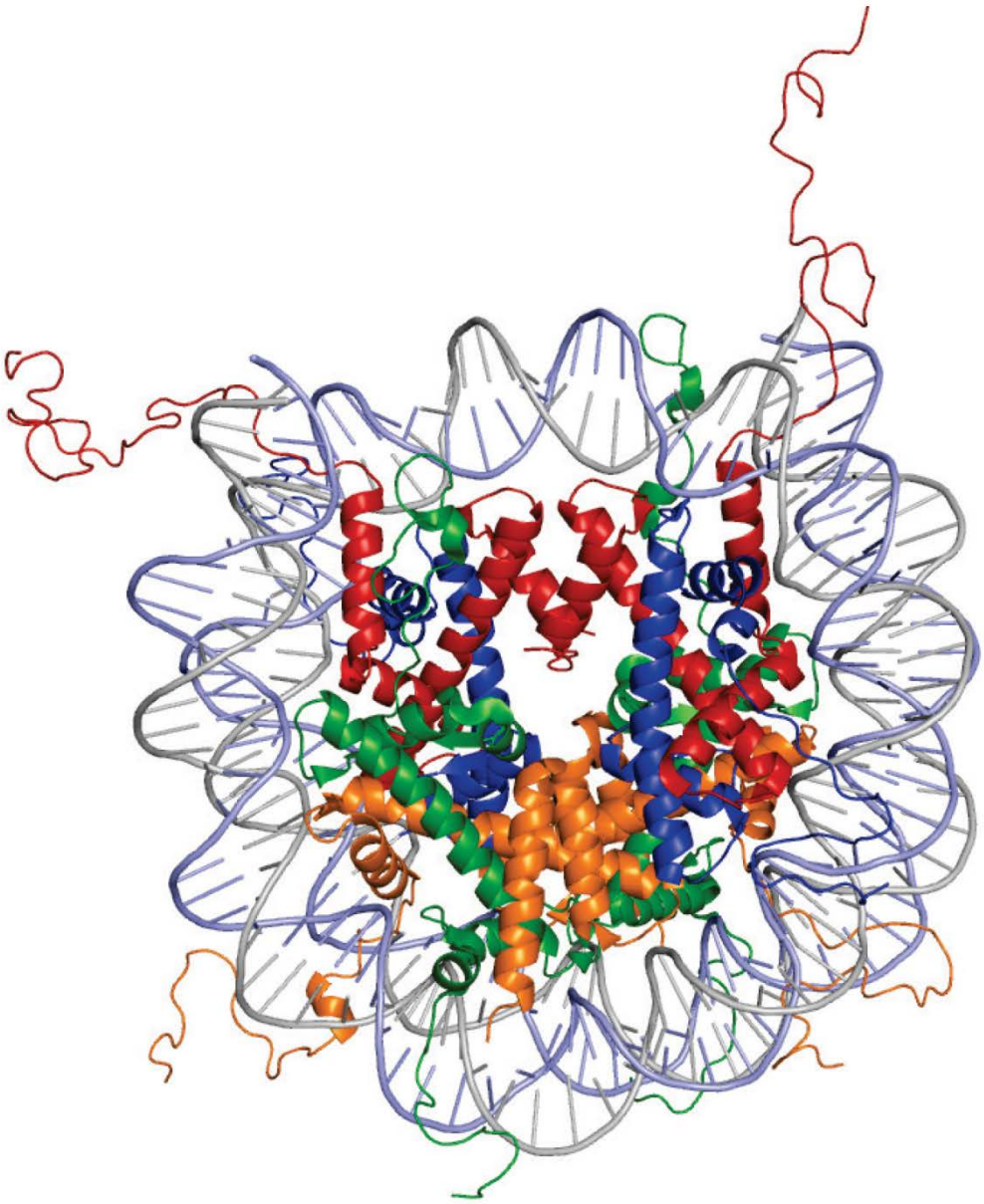

Figure 1. Structure of a nucleosome. DNA (purple and gray strands) is wrapped around an octamer of histones H2A (green ribbons), H2B (orange ribbons), H3 (red ribbons), and H4 (blue ribbons). The N-terminal tails are shown protruding out of the nucleosome core. (PDB 1KX5)

proteins are referred to as chromatin “readers” that bind specific histone modifications [6-8]. One example of “reader” proteins are those proteins that possess bromodomains, such as the BET (bromodomain and extra-terminal) family of proteins (BRD2, 3, 4, and BRDT) that specifically recognize singly or multiply acetylated histones and are associated with processes such as transcriptional activation and transcriptional elongation [9, 10]. There are also proteins known as “writers” and “erasers” [6]. Histone writers can be the histone acetyltransferases that add acetyl groups to lysines and histone erasers can be histone deacetylases that remove these acetyl groups, thus affecting processes such as DNA replication, repair, and transcription. These histone modifications can also serve to block recruitment or binding of proteins to a particular site. There are at least 16 different classes of histone modifications (shown in Table 1-modified from [1]).

The most well studied histone modifications are phosphorylation, methylation, acetylation and ubiquitylation. Histone phosphorylation can occur on serine, threonine, and tyrosine residues and can alter the charge of the nucleosome, thus altering the structure of chromatin. Phosphorylation plays a role in many processes such as replication, transcription, apoptosis, and repair [1, 3]. While methylation can occur on lysine, arginine, and histidine, the best studied of these modifications is lysine methylation, which can be associated with active/euchromatic regions (H3K4, H3K36, and H3K79) or repressed/heterochromatic regions (H3K9, H3K27, and H4K20) [1, 3].

Table 1. Histone Modification Classes

Histone Modifications	Attributed Function
Acetylation	transcription, repair, replication, and condensation
Methylation (lysine)	transcription and repair
Methylation (arginine)	transcription
Phosphorylation (serine & threonine)	transcription, repair, and condensation
Phosphorylation (tyrosine)	transcription and repair
Ubiquitylation	transcription and repair
Sumoylation	transcription and repair
ADP ribosylation	transcription and repair
Deimination	transcription and decondensation
Proline isomerisation	transcription
Crotonylation	transcription
Propionylation	unknown
Butyrylation	unknown
Formylation	unknown
Hyroxylation	unknown
O-GlcNAcylation (serine & threonine)	transcription

In addition, lysine residues can be either mono-, di-, or tri- methylated, which can have varying degrees of function because of the different methylation states. For example, repression is normally associated with tri-methylation. Often during the switch from transcriptional activation to repression, a lysine residue that is acetylated during activation is then deacetylated and replaced by a methyl group to silence the gene. Ubiquitylation is a very large modification that targets lysines on histones H2A and H2B. This modification can serve as an active (H2BK120) or repressive (H2AK119) transcription mark [1, 3]. Sumoylation is also a large modification and occurs on all four core histones [3]. Specific sites on H2A, H2B, and H4 are sumoylated and appear to repress transcription in yeast [3]. Acetylation (more specifically, deacetylation) is a focus of this dissertation and is described in more detail below.

Acetylation

Lysine residues primarily occur in the basic N-terminal tails of histones but can also occur in the core domains of histones (such as H3K56ac). The presence of these positively charged residues in the core attracts the negatively charged nucleosome cores, thus causing the chromatin to maintain a tight conformation. Acetylation of these lysine residues neutralizes the positive charge of the tails and causes the chromatin to loosen through disruption of electrostatic interactions between nucleosomes. This open chromatin state allows for recruitment of transcription factors or other proteins to promote gene transcription.

Histone acetyltransferases (HATs) are the enzymes that transfer an acetyl group from coenzyme A to the lysine residues. HATs can also target non-histone substrates, but histone acetylation will be discussed here. Most HATs are components of multisubunit complexes and these complexes contain subunits that regulate HAT activity such as by targeting HAT activity to specific chromosomal regions or regulating the substrate specificity of HATs [11-13]. Three of the main families of HATs are the GNAT (Gcn5 N acetyltransferases), MYST (MOZ YBF2/SAS3-SAS2-TIP60), and CBP/p300 (CREB-binding protein) families [11, 14, 15]. These families contain different HAT complexes that are composed of different protein subunits but can contain the same HAT for the catalytic activity of the complex. Many HATs are unable to acetylate nucleosome histones when the HAT is alone i.e. not in complex [11]. However, when in complex the HAT is able to acetylate nucleosome histones and specific subunits of the complexes are required for targeting the HAT to the specific histones [11]. For example, yeast Gcn5 (general control nonderepressible 5) cannot acetylate nucleosome histones unless it is present in either the ADA or SAGA complex. These two complexes contain two common subunits, Ada2 and Ada3, which are required for the association and acetylation of nucleosomal histones [11, 16].

The multisubunit HAT complexes also affect the substrate specificity of HATs. For example, the GNAT family has specificity primarily toward the lysine residues on histones H3, H4, and H2B while the MYST family displays specificity for histone H3, H4, and H2A [11-13]. As mentioned, HATs are associated with active transcription, however they are also implicated in other processes such as

DNA replication and repair. For example, HAT activity can allow for the enhanced retention of ATP-dependent chromatin remodeling complexes during replication or repair by acetylating lysines for that recruit or retain these remodeling factors [17]. This would allow for sustained or further chromatin remodeling that allows additional replication or repair machinery to access DNA.

Due to the importance of acetylation and HAT activity in many major cell processes, a balance between acetylation (activation) and deacetylation (repression), needs to be maintained. The enzymes that aid in maintaining this balance and remove acetyl group from lysines are the histone deacetylases (HDACs).

Histone Deacetylases

Classification of HDACs

HDACs target both histone and non-histone substrates, but histone deacetylation will be the focus of this dissertation. HDACs remove the acetylation present on the ε-amino group of lysine residues on histones. This deacetylation, then allows for other modifications such as methylation, ubiquitylation, or sumoylation to occur on the amino group, thus affecting transcriptional regulation.

There are currently 18 human HDACs that are classified into 4 different classes (with one class being subdivided into two subclasses) based on their sequence similarities to each other and to yeast HDACs, subcellular localization,

tissue specific expression, and domain organization. The mammalian HDACs are also classified based on their homology to 3 yeast proteins, Rpd3, Hda1, and Sir2. Rpd3 was first identified in genetic screens for transcriptional repressors and later the deacetylase function of Rpd3 was determined along with the identification of another yeast deacetylase enzyme, Hda1, through purification and analysis of the HDA and HDB yeast HDAC complexes [18, 19].

The SIR (silent information regulator) gene was discovered many years ago through studies that examined mating type interconversion in yeast [20]. The expression of genes necessary for mating and sporulation are controlled by the mating type loci in yeast and mutations in the mating type loci can regulate the expression of genes [20, 21]. The SIR gene was found to suppress, or silence, the mating and sporulation defects in mutations in the mating type loci [20]. There were four SIR genes isolated in yeast (SIR1, 2, 3, and 4) but SIR2 was the only gene that is highly conserved from archaea to humans [22].

Sir2 was originally identified from a genomic library in 1985 by complementation of sir mutations [21]. The Sir2 family of proteins are responsible for repressing transcription at telomeres, mating-type loci, and ribosomal DNA and regulating longevity in yeast [6, 23, 24]. However, the mechanism by which they repressed transcription was unclear until research in 2000 used NAD/nicotinamide exchange reactions to test whether these enzymes could cleave the glycosidic bond in NAD to generate nicotinamide and ADP-ribose [23]. They found that Sir2 proteins could cleave this bond but only if acetylated lysines were present [23] . Histone deacetylase experiments then revealed that these

proteins could also catalyze histone deacetylation but this reaction absolutely required NAD [23]. Thus, these proteins were histone deacetylases that were unlike the previously characterized zinc-dependent Rpd3/Hda1 HDACs. Each class of HDACs is discussed below in more detail.

Class I

Class I includes HDACs 1, 2, 3, and 8 and these HDACs are homologous to yeast Rpd3 (reduced potassium dependency 3) [25-27]. The class I HDACs are ubiquitously expressed and predominantly localized to the nucleus. They are between 350 and 500 amino acids in length. Class I HDACs require Zn^{2+} to mediate the release of acetate and form a free lysine [28]. The zinc ion is chelated by side chains of histidine and aspartic acid in the catalytic center of the HDAC structure [29]. These HDACs do not bind directly to DNA but instead are usually the catalytic components of multiprotein corepressor complexes. HDAC8 is the only class I HDAC that does not require a multiprotein complex for its function.

HDACs 1 and 2 share 82% identity with each other and are the most similar of all the class I HDACs (Figure 2) [30-32]. Not only do they share homologous catalytic domains, they also share homology in their C terminal domains. HDACs 1 and 2 have similar functions and can interact with each other. They are also found in the same multiprotein complexes, containing Sin3 (Swi independent 3), Mi2/NuRD (nucleosome remodeling and deacetylase), and CoREST (corepressor of repressor element 1 silencing transcription) [29, 33, 34].

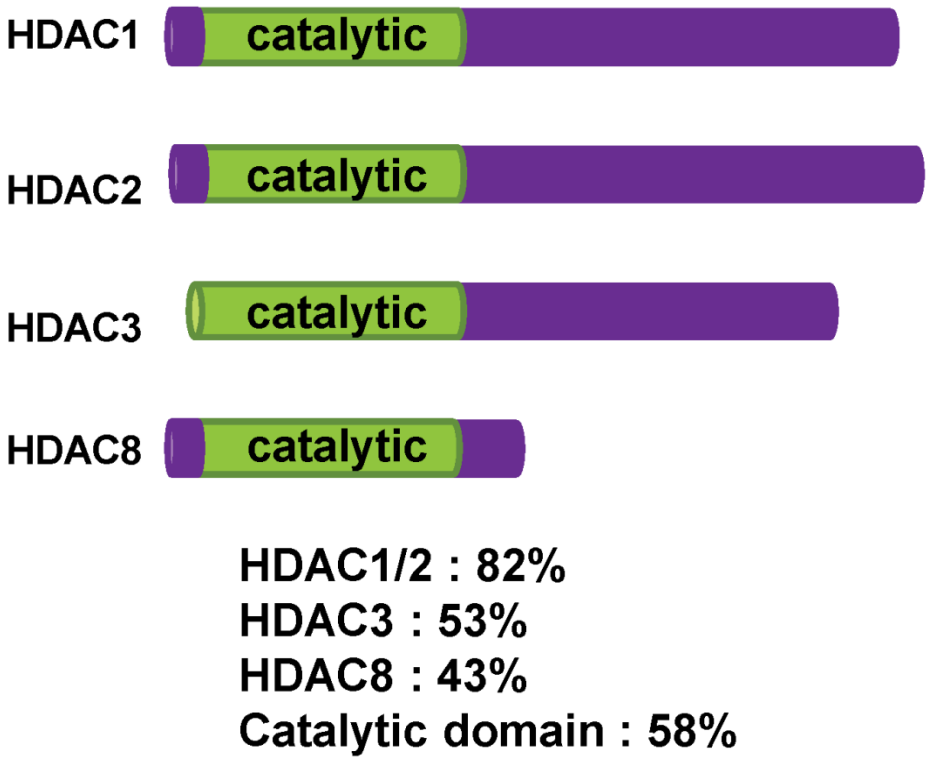

Figure 2. Class I HDACs are classified based on sequence conservation and contain a highly conserved catalytic domain. The catalytic domain is shown in green and identity percentages are based on similarity to HDAC1.

Sin3 and many of the subunits that make up Sin3 complexes are conserved from fungi to mammals [29]. There are two Sin3 homologs in mammals, Sin3A and Sin3B. The Sin3A complex is composed of HDAC1 and 2 as the catalytic components as well as 9 other subunits including the histone binding proteins, RbAp46 and RbAp48 [33, 35]. The Sin3A complex interacts with many DNA sequence-specific transcription factors and adapter proteins that target the complex to specific regions of DNA for repression activity [35]. The Sin3A complex is involved in repression by nuclear hormone receptors when the receptor is not bound by ligand.

The Mi-2/NuRD complex contains HDAC1 and 2, RbAp46, RbAp48, and other subunits including MBD2 (methyl CpG-binding domain-2) and Mi-2 [29, 36, 37]. Besides the histone deacetylation properties of the complex, Mi-2 is responsible for ATPase activity of the complex, which plays a role in nucleosome mobilization and condensation [37]. MBD2 allows this complex to be recruited for DNA methylation-dependent gene silencing [29] and associate with methylated DNA binding proteins.

The CoREST complex is referred to as a neuronal corepressor complex and along with HDAC 1 and 2 contains other proteins such as LSD1 (a H3K4 demethylase). By being in complex together, HDAC1/2 and LSD1 are able to stimulate each other's activities. The histone demethylation stimulates deacetylation of nucleosomes, which in turn is required for optimal demethylation [29].

HDAC3 was identified in 1997 using an expressed sequence tag (EST) database search looking for DNA and protein sequences that had high homology with HDACs 1 and 2 in a fetal liver library [31]. HDAC3 is 428 amino acids in length and has a molecular weight of 49 kDa. HDAC3 shares 53% and 52% identity, respectively, with HDAC1 and HDAC2 [30-32] (Figure 2). The class I HDACs also contain a highly conserved central catalytic domain [31, 32] that is 58% identical between HDAC1 and HDAC3. The C-terminal tail of HDAC3 differs from any other HDAC and the last 30 amino acids of the C-terminal tail is required for the deacetylase activity of HDAC3 [32, 38]. HDAC3 forms a separate complex with the nuclear corepressor proteins, NCoR (nuclear corepressor) or SMRT (silencing mediator of retinoic and thyroid receptors).

HDAC3 requires the interaction with NCoR or SMRT for activity while the NCoR/SMRT complex requires HDAC3 for deacetylase activity and transcriptional repression. NCoR and SMRT are highly related to one another in function and sequence. These two proteins were first identified based on their roles in repressing transcription involving retinoic acid receptors, retinoid X receptors, thyroid hormone receptors, etc [39]. NCoR and SMRT both have the conserved deacetylase activation domain (DAD) that interacts with HDAC3 and a SANT (Swi3/Ada2/NCoR/TFIIIB) domain that is necessary and sufficient for interacting with and activating HDAC3 [40].

In 2012, HDAC3 was crystallized with the DAD from the human SMRT [40]. The crystal structure of HDAC3 revealed that upon binding HDAC3, the DAD undergoes extensive conformational changes where the DAD no longer

forms part of the core of the SMRT structure but lies along the surface of HDAC3 [40]. A second surprise was that between HDAC3 and DAD-SMRT, there was an essential inositol tetraphosphate molecule, Ins(1,4,5,6)P_4) or IP4. This IP4 molecule acts as “intermolecular glue” holding the proteins together [40]. The discovery of the structure of HDAC3 provides critical information about how HDAC3 and its corepressor complexes interact and may provide new insights into therapeutics involving HDAC3 in disease.

To study the function of individual HDACs, mouse models harboring deletions of the class I HDACs have been generated. Deletion of *Hdac1* led to embryonic lethality by embryonic day 10.5 thus establishing a vital role for HDAC1 in embryogenesis [41-43]. *Hdac1*-null embryonic stem cells showed a proliferation defect associated with an increase in the cell cycle inhibitors p21 and p27 [41-43]. An increase in *Hdac2* and *Hdac3* levels were observed but only *Hdac2* could partially compensate for the loss of *Hdac1* [41, 42]. *Hdac2* deletion did not lead to embryonic lethality but caused perinatal lethality with many of the mice dying by three weeks after birth. The cause of death of these mice was cardiac malformations where there was thickening of the ventricle walls of the heart due to increased proliferation [44]. Global *Hdac8* deletion also led to perinatal lethality due to skull instability [45], suggesting a vital role for *Hdac8* in skull patterning.

Hdac3 deletion caused embryonic lethality before embryonic day 7.5 proving that HDAC3 is vital for normal embryonic development [46] . To elucidate why these mice were dying, conditional HDAC3$^{-/-}$ mouse embryonic

fibroblasts (MEFs) were harvested, and studies revealed that these MEFs had increases in apoptosis, cell cycle delay, and S phase associated-DNA damage [46]. Deletion of HDAC3 in MEFs also resulted in increases in histone H4K5, H4K12, and H4K16 acetylation levels with a modest increase in histone H3 K9/K14 acetylation in *Hdac3*-null MEFs [46].

To study HDAC3 function in adult animals, a liver-specific deletion of HDAC3 using Cre recombinase under the control of the albumin promoter (Alb-Cre) was made [43]. These mice were viable but developed liver hypertrophy, disrupted metabolism, and elevated levels of histone H4K5ac and H4K12ac with modest increases in H3K9ac [43, 47]. Further analysis of these mice revealed a decrease in heterochromatin and alteration of chromatin structure and a requirement for HDAC3 in genomic stability [47]. As mentioned, S phase associated DNA damage was observed in HDAC3 null cells [46]. Analysis of HDAC3 null livers recapitulated the DNA damage and genomic instability seen in HDAC3 null MEFs along with defects in DNA repair [47] (Figure 3). Long term observation of these *Hdac3*$^{-/-}$*:Alb-Cre* mice found that these mice developed hepatocellular carcinoma [47].

Another HDAC3 conditional mouse model developed was the HDAC3:Vav-Cre mouse that allowed for the study of HDAC3 in hematopoiesis [48]. These mice had hypocellular bone marrow, anemia, a dramatic loss of lymphoid cells, decreased stem and progenitor cell proliferation, and DNA replication defects [48] (Figure 4). These studies suggest that long-term inactivation of HDAC3 could lead to detrimental effects on normal cells but that

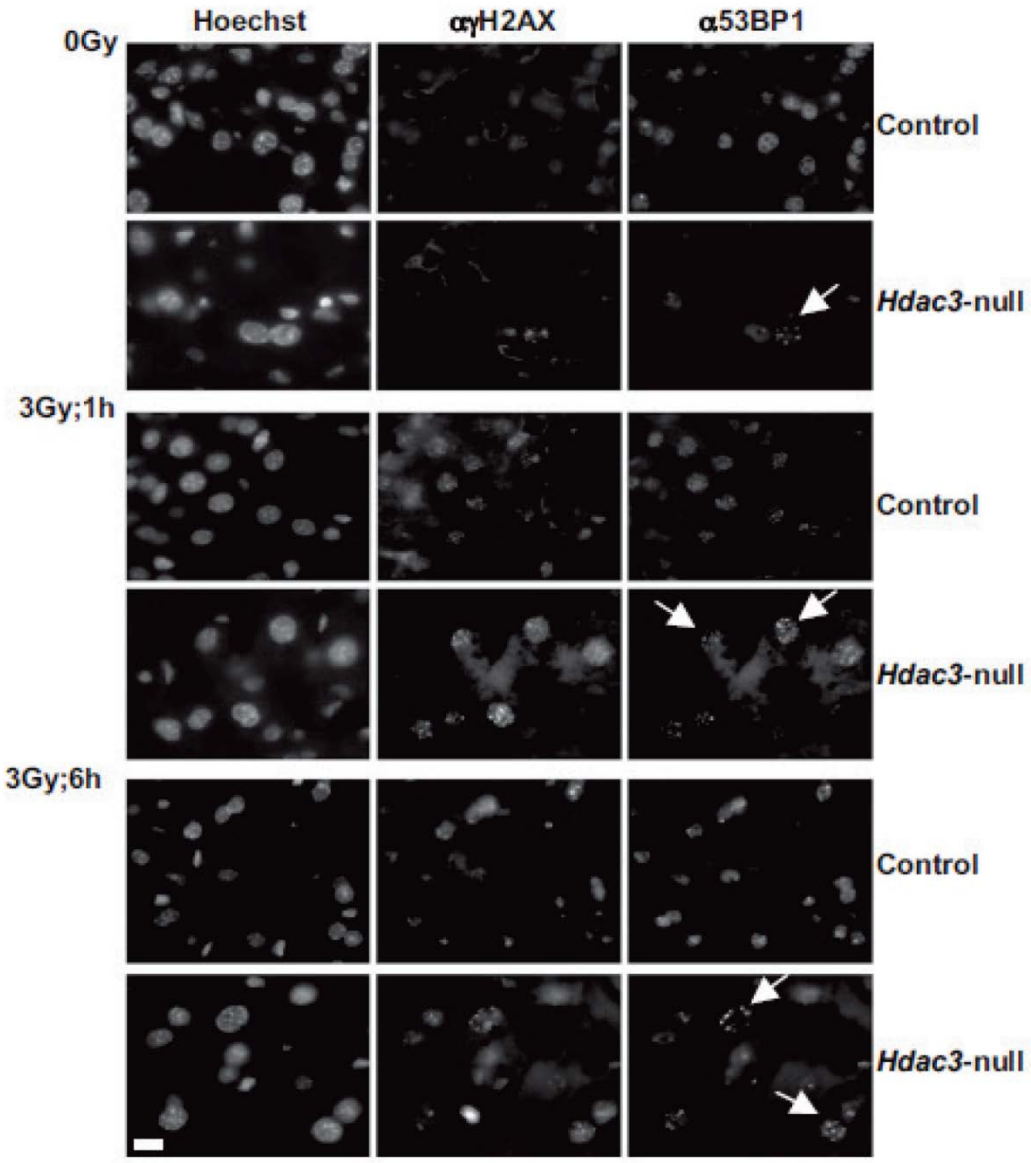

Figure 3. DNA repair is impaired in Hdac3-null livers. Hdac3-null hepatocytes are defective in DNA repair. Mice were irradiated with a 3 Gy dose of IR, and frozen sections of livers collected immediately or 1 or 6 hr later were prepared for immunofluorescence analysis of γH2AX and 53BP1. Arrows indicate Hdac3-null nuclei with 53BP1 foci. The scale bar represents 20 mm. Figure from [47].

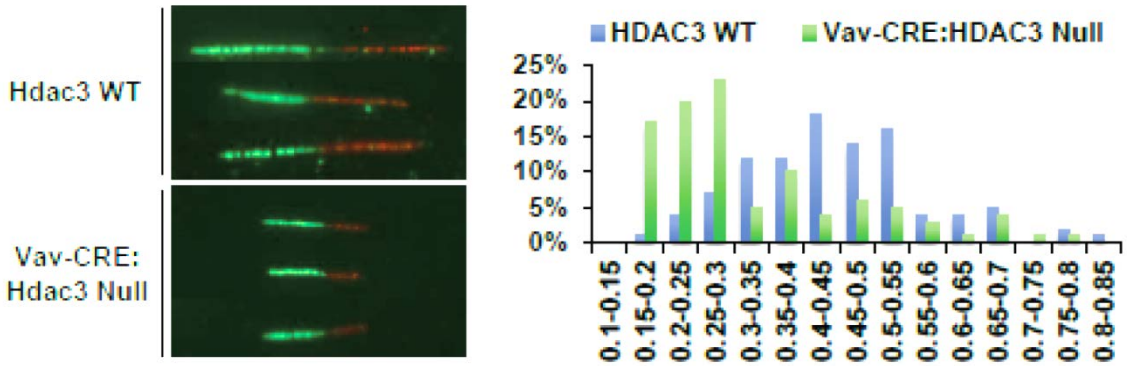

Figure 4. *Hdac3*-null stem cells show defects in DNA replication. DNA fiber labeling with IdU (green) and CldU (red) was used to assess DNA replication fork progression in LSK/Flt3- cells from control and Hdac3-/- bone marrow. Graphical representation of the length of replication tracks taken from 100 DNA fibers is shown in the graph. Figure from [48]

shorter term inactivation may provide a window of opportunity to target only proliferating cells (S phase dependent DNA damage and defects in DNA replication) and leave the normal, non-cycling cells alone.

Class IIa and IIb

The class II HDACs are subdivided into class IIa and class IIb based on sequence homology and organization of domains. Figure 5 shows the two subclasses and they are described below. All of the class II HDACs share homology with the yeast Hda1 enzyme and like the class I HDACs, require Zn^{2+} for enzymatic activity [29, 49, 50]. However, interestingly, these HDACs often require HDAC3 for their activity.

Class IIa consists of HDACs 4, 5, 7, and 9. These enzymes share a highly conserved C terminal domain (homologous to Hda1) and an N terminal domain that is not similar to other proteins [29, 49, 50] (Figure 5). They are also approximately twice the size of the class I HDACs (about 1000 amino acids in length) due to this elongated N terminal region that is required for coregulator binding. Class IIa HDACs also differ from class I HDACs, in that class IIa members are expressed in a more tissue-specific manner instead of being ubiquitously expressed [29, 49, 50]. HDACs 4, 5, and 9 have the highest expression in heart, skeletal muscle, and brain while HDAC7 has high expression in heart, lung, thymus and skeletal muscle [29, 49, 50].

The four members of class IIa were thought to have redundant or partially redundant functions in the tissues in which they are expressed, but deletion in

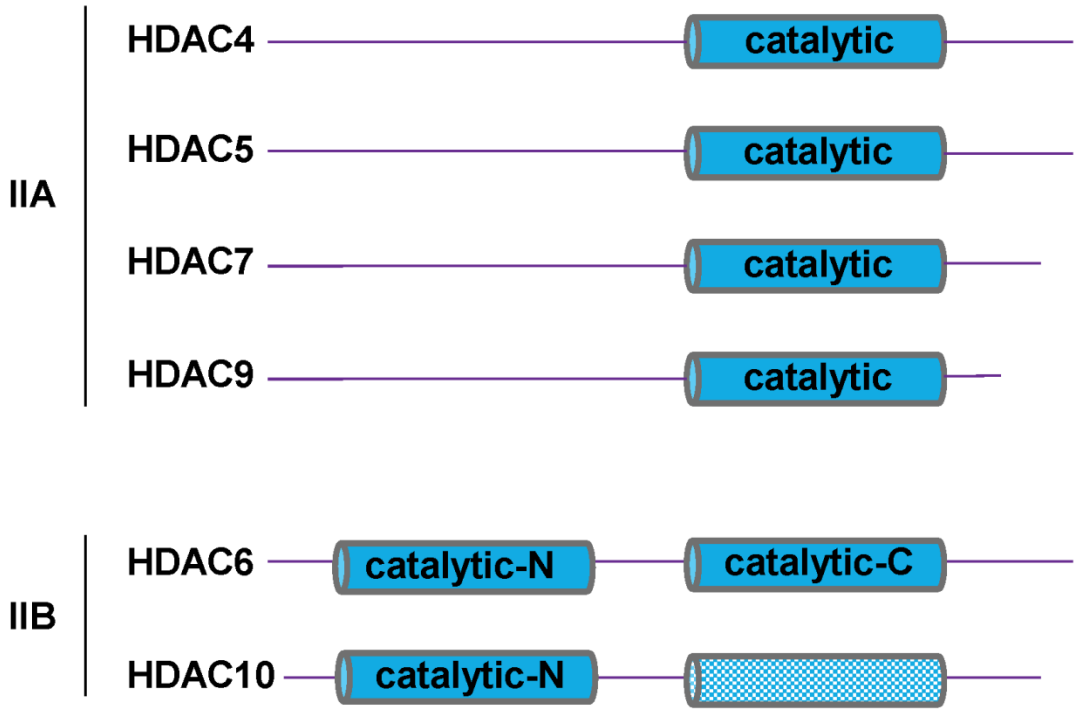

Figure 5. The class II HDACs are subdivided into class IIa and class IIb based on sequence homology and organization of domains. Class IIa share a highly conserved C terminal domain while the class IIb HDACs have duplicated catalytic domains. Both catalytic domains are functional in HDAC6 while only the first domain is functional in HDAC10.

mice showed that these HDACs have separate functions from one another. Deletion of either HDAC5 or HDAC9 resulted in viable mice but these mice displayed cardiac hypertrophy induced by stress [51]. HDAC4$^{-/-}$ mice were also viable but had increased chondrocyte hypertrophy during bone development [52]. HDAC7 deletion resulted in the most severe phenotype with embryonic lethality observed by embryonic day 11 due to a weakened vascular structure [53].

The class IIa HDACs are able to regulate many processes due to their interactions with many different transcription factors. Class IIa HDACs are able to shuttle between the nucleus and cytoplasm through phosphorylation and interaction with the 14-3-3 proteins [49, 50]. Each of the class IIa HDACs possess nuclear export signals (NES) to export them from the nucleus and a nuclear localization signal (NLS) to import them into the nucleus [49]. Phosphorylation of the class II family members by CaMK (calcium/calmodulin-dependent kinase) results in a conformational change of the HDACs and the exposure of the NES, thus exporting the HDAC from the nucleus [54]. The 14-3-3 chaperone proteins bind to the class IIa HDACs to keep the HDACs in the cytoplasm by covering the NLS [55, 56]. This shuttling between the nucleus and cytoplasm is important for transcription factors that interact with the class IIa HDACs. When the class II HDACs are shuttled out of the nucleus, they are unable to bind to their substrates and activating complexes, thus they are unable to repress transcription. For example, a major transcription factor that interacts with the class IIa HDACs is myocyte enhancer factor 2, or MEF2. MEF2 plays a major transcriptional role in myogenesis, neuronal cells, and negative selection of

developing thymocytes [49, 50, 57, 58]. Also, aberrant MEF2 expression has been linked to coronary heart disease and T cell lymphoma [50]. MEF2 requires the nuclear localization and binding of class IIa HDACs through a conserved binding region for MEF2 in the N terminal domain of the HDACs to repress transcription [49, 55, 57]. When both MEF2 and the HDACs are phosphorylated, MEF2 is released from the HDACs and MEF2 can then interact with transcriptional coactivators [49, 55, 57].

The class IIb HDACs include HDAC6 and HDAC10. This class differs from the class IIa HDACs in their domains, localization pattern, and tissue specificity. Class IIb is characterized by duplicated HDAC domains [49] (Figure 5). HDAC6 contains two tandem deacetylase domains and both are functional. Only the first domain in HDAC10 has a catalytically active site [49]. The leucine-rich C terminal domain of HDAC10 is homologous to the second domain of HDAC6 but lacks an active pocket site for enzymatic activity [49, 50]. Both HDACs are primarily localized to the cytoplasm but HDAC10 can shuttle to the nucleus. Like the class IIa HDACs, HDAC6 and HDAC10 have tissue specific expression but the tissues they are expressed in differ from those that express class IIa family members. HDAC6 is expressed in liver, kidney, pancreas, and heart, while HDAC10 is expressed in liver, kidney, and spleen [29, 49, 50]. HDAC10 does not have deacetylase activity *in vivo* but does have the ability to repress transcription when present in the nucleus and tethered to a promoter [29, 49, 50]. The activity of HDAC6 is confined to the cytoplasm where it localizes

with the microtubule network [49]. HDAC6 functions as a specific deacetylase of tubulin and plays a role in cell motility and structure.

Class III

The class III HDACs were originally identified in yeast as Silent Information Regulators (SIR), also known as sirtuins [20, 21] and have very little conservation to the class I, II, or IV family members. The SIR complex is responsible for repressing transcription at telomeres, mating-type loci, and ribosomal DNA in yeast [20, 22-24]. Unlike the class I and II HDACs, the class III enzymes require NAD^+ (nicotinamide adenine dinucleotide) instead of Zn^{2+} for activity [23, 59] Another unique feature is that class III can also transfer an ADP-ribose moiety to amino acids [23, 59]. When an acetyl lysine is deacetylated, a NAD^+ molecule is cleaved producing nicotinamide and O-acetyl-ADP ribose. SIR2 is highly conserved from archaea to humans and has 7 homologs in human, SIRT 1-7 [22].

The sirtuins have been linked to many age-related and metabolic diseases such as cardiovascular disease, type II diabetes, cancer, and neurodegeneration [22, 60]. They also affect lifespan in yeast with SIR2 mutants exhibiting an approximately 50% shorter lifespan than controls. Each of the 7 mammalian SIRT family members have been deleted in mice. Most of these mouse models produced viable mice but had different phenotypes based on which sirtuin was deleted. SIRT1 deletion had a severe phenotype with some $SIRT1^{-/-}$ mice being born but at much lower ratios than expected and most of these mice died within a

few months. Interestingly, SIRT1$^{-/-}$ mice did not open their eyelids for many weeks after normal controls opened their eyes and when these mice did open their eyes, the eyes were generally misshapen [22, 61]. These mice were much smaller and usually died due to abnormal heart development and cardiac defects. SIRT7 deletion also resulted in cardiac defects and decreased life span [22]. In SIRT7$^{-/-}$ mice, there was an increase in the levels of apoptosis in cardiac tissue through hyperacetylation of p53 [62]. SIRT6$^{-/-}$ mice were born but died within a month due severe metabolism defects and increased thymocyte apoptosis. These mice had very little adipose tissue and very low to no blood glucose levels [22, 63]. Deletion of SIRT3 or SIRT4 caused less severe phenotypes. SIRT3$^{-/-}$ and SIRT4$^{-/-}$ mice were viable but had defects in metabolism that increased reactive oxygen species that correlated with increases in cancer and aging [22, 64, 65]. There was an increase in mitochondrial acetylation specifically in the enzyme, glutamate dehydrogenase [64, 65]. This led to disruptions in insulin signaling. Deletion of SIRT2 and SIRT5 produced viable mice with no observed phenotypes [22, 64].

Class IV

The only member of class IV is HDAC11. HDAC11 displays similarity to both the class I and class II HDAC family members, which is why it was given a class of its own. HDAC11 is more similar in size and exhibits nuclear localization like the class 1 HDACs, but is expressed in a more tissue specific manner like the class II HDACs. HDAC11 is expressed in brain, heart, kidney, and skeletal

muscle [66]. There is little known about the function of HDAC11; however, it is evolutionarily conserved, suggesting a fundamental role for HDAC11 in various organisms.

HDACs in Disease

As stated in the beginning of this introduction regulation of chromatin and transcription is crucial for normal development and life. Histone deacetylation by HDACs plays a major role in maintaining a balance between open and closed chromatin and access to DNA. HDACs are tightly regulated by their recruitment and interaction with multiprotein complexes that are required for HDAC enzymatic activity, and deregulation of these proteins and processes can cause catastrophic effects as seen in the knockout mouse models described above. However, increased activation of HDACs has been linked to many types of diseases and inhibition of HDACs is gaining use in the clinics. Cancer is the main disease that involves inappropriate recruitment and function of HDACs, but other diseases such as neurodegenerative disorders, heart disease, muscular dystrophy, and spinal muscular atrophy have shown increased activation of HDACs [29, 67, 68]. Many of the cancers that are the most affected by inappropriate recruitment and function of HDACs are blood cancers such as promyelocytic leukemia, acute myeloid leukemia, and acute lymphoblastic leukemia, however, solid tumor cancers such as glioblastomas, breast, cervical, and GI cancers have been associated with HDAC deregulation [69-73].

For example, in acute myeloid leukemia HDAC3 is inappropriately recruited by a fusion protein consisting of a translocation between the co-repressor MTG8 (myeloid translocation gene 8) and the hematopoietic transcription factor, AML1 (acute myeloid leukemia 1). This inappropriate recruitment results in unregulated repression of AML1 target genes and the development of AML [73, 74]. One cancer that has shown tremendous improvement with treatment involving histone deacetylase inhibitors is cutaneous T cell lymphoma.

Cutaneous T cell lymphoma

Cutaneous T cell lymphoma (CTCL) is a heterogeneous group of non-Hodgkin's lymphoma that is characterized by an initial accumulation of malignant, mature T cells in the skin [75-77]. The incidence of CTCL is 6.4 per million persons with the highest incidence being in males and African Americans [76]. Generally, CTCL incidence increases with age and is confined to adults but certain types of childhood and adolescent CTCLs have been seen. Early-stage CTCL is generally confined to the skin resulting in an indolent nature and good prognosis. However, advanced or refractory disease has skin, peripheral blood and lymph node involvement, is aggressive, and has shortened survival [75-77]. The most common types of CTCL are mycosis fungoides and Sézary syndrome, followed by the $CD30^+$ lymphoproliferative disorders. Together, these types of CTCL make up 95% of CTCL cases [78].

Mycosis Fungoides and Sézary Syndrome

Mycosis fungoides (MF) and Sézary syndrome (SS) make up approximately two-thirds of CTCL. MF normally has an indolent, stable course that can persist for many years. The malignant T cells in MF are primarily localized in the skin as patches or plaques that vary in size, shape, color, and distribute in a bathing suit type pattern [75, 76, 78]. Sometimes these plaques or patches can progress to tumors with deeper infiltration of malignant cells into the skin. Patients that are diagnosed with early stage MF can have a normal life expectancy.

SS is thought of as the leukemic version of CTCL due to not only skin infiltration by malignant T cells, but also circulating malignant T cells in the peripheral blood and lymph node involvement. In SS there is a high number of malignant T cells in the peripheral blood that have cerebriform (grooved/lobulated) nuclei, termed Sézary cells [78, 79]. SS is characterized by erythroderma (covering approximately 80% of the patient's skin), lymphadenopathy, and thickening of the skin [79]. Patients generally have high morbidity with SS due to intense itching and discomfort. The prognosis of SS is usually poor with the 5-year survival rate of 24% and a median survival of 3 years [78, 79].

Originally, MF and SS were thought to be the same disease but at different stages of progression. However, MF and SS arise from different cell origins [76, 80], which is consistent with different clinical behaviors and disease courses. There are approximately 2x as many T cells in the skin as there are in

the peripheral blood and when a naïve T cell is activated by an antigen, this cell differentiates into either an effector memory cells or a central memory T cell that have different patterns of migration due to their different expression levels of homing addressins, chemokines, and chemokine receptors [76, 80, 81]. Effector memory (T_{EM}) T cells are skin resident T cells and express chemokine receptors (CCR4, CCR6, and CCR10) that are required for T-cell migration into the skin [76, 80, 81]. Central memory (T_{CM}) T cells express CCR7 and L-selectin that are necessary for homing to the lymph nodes and circulation in the blood [76, 80-82]. T cells that were isolated from MF patient skin lesion were found not to express CCR7 or L-selectin but did express high levels of CCR4 and CLA (skin homing addressin) suggesting a T_{EM} phenotype [76, 82]. SS patient cells show a T_{CM} phenotype by expressing high levels of CCR7 and L-selectin for homing to lymph nodes and peripheral blood [76, 80-82].

$CD30^+$ Lymphoproliferative Disorders

After MF and SS, $CD30^+$ lymphoproliferative disorders are the next most common type of CTCL. The prognosis of this type of CTCL is generally good with patients having a normal life expectancy compared to age and sex matched control populations [83, 84]. These CTCL types express high levels of the cell surface receptor, CD30. CD30, or tumor necrosis factor death receptor member 8, expression is absent on normal cells and is only found on activated T and B cells, usually more commonly in T cell lymphomas [83, 84]. CD30 expression is

generally associated with a better outcome and can lead to increased Fas signaling, triggering apoptosis [83, 84].

Two of the most common types of $CD30^+$ lymphoproliferative disorders are lymphomatoid papulosis (LyP) and cutaneous anaplastic large cell lymphoma (cALCL). LyP is confined to the skin and characterized by chronic, recurrent and self-regressing red papules and nodules that can occur singly, but usually in clusters, and normally form on the trunk and limbs of patients [83]. These papules can be small pinpoint sizes or can grow larger into papulonodules. Papules can become necrotic and normally regress within 3-12 weeks, possibly leaving scars. The duration of the cycle of recurrent and regressing disease can last several months to years after the initial onset. In CALCL, the skin manifestations are larger and more tumor-like in appearance. These tumors tend to present solitarily and not in clusters. Like LyP, CALCL tumors may ulcerate and regress and overall the prognosis is favorable [83].

Complications of CTCL

A major complication of CTCL is increased risk and susceptibility to secondary malignancies and infections. A large majority of CTCL patients die due to infection complications and not due to tumor burden [76]. The skin lesions on CTCL patients can become necrotic and ulcerated, disrupting the normal protective skin barrier. This allows an increased chance of invasion of pathogens and infection. Advanced-stage CTCL patients are unable to fight off infections

like early-stage and uninfected individuals due to a compromised immune system.

The most important risk factor for infections (both cutaneous and systemic) is advanced disease [85]. Advanced stage disease is characterized by the expansion of malignant $CD4^+$ T cells and a decrease in normal, reactive $CD8^+$ cytotoxic T cells and non-malignant T helper 1 (Th1) cells [86]. A decreased number of $CD8^+$ T cells and Th1 cells corresponds to a decreased survival rate due to decreased cell mediated immunity. $CD8^+$ T cells and Th1 cells control malignant T cells to a certain degree by cytotoxicity and secreting cytokines such as interferon α directed towards the malignant T cells that express tumor associated antigens. The decreased number of normal blood T cells in erythrodermic patients (SS patients) has been compared to patients with advanced AIDS (acquired immunodeficiency syndrome) where AIDS patients usually have very low numbers of circulating normal T cells [87]. With the expansion of these malignant T cells, there is also a skewing toward T helper 2 (Th2) cell cytokine expression (IL-5, IL-10, IL-13, and IL-17) corresponding to immune deregulation, increased susceptibility to infection, impaired anti-tumor immunity, and increased tumor cell proliferation due to Th2 cytokines suppressing T cell mediated immunity [86].

In early stage disease, Th1 cytokines are more highly expressed (IL-2, IL-4, and IFNɣ) that aid in anti-tumor immune response and cell mediated immunity [86]. As disease progresses, Th2 cytokines are highly expressed, and as this change in immune function occurs, the body does not recognize and properly

respond to tumor antigens, thus losing this anti-tumor response and ability to fight the malignant T cell expansion contributing to the immune failure. Some current therapies are aimed towards increasing the Th1 response and increase host immunity.

Treatments in CTCL

Besides an allogeneic stem cell transplant, there is no cure for MF and SS CTCL. However, there are different types of treatments for both early and late stage disease. Early stage or limited disease (MF, $CD30^+$ disorders) with few or infrequent lesions can be treated with a "watch and wait" approach or skin directed therapies. These therapies can include topical bexarotene, nitrogen mustard (an alkylating agent), and corticosteroids [75, 77]. If lesions are recurrent and cover a large amount of the skin, then skin treatments can also be combined with low dose oral methotrexate and phototherapy. Psoralen plus ultraviolet A (PUVA) is highly effective. Upon photoactivation, psoralen, which accumulates in lymphocytes, will form DNA adducts [75]. The complete response rate exceeds 90% in limited disease.

Another possible treatment is to deliver electrons to the skin surface using Total Skin Electron Beam Therapy, TSEBT. TSEBT is effective due to malignant T cells being radiosensitive [75]. Advanced, systemic, or refractory disease, such as SS, has a more aggressive treatment course involving combinations of skin directed therapies as well as systemic therapies. Some of these systemic therapies include oral bexarotene, oral methotrexate or pralatrexate, histone

deacetylase inhibitors (HDIs) (such as Vorinostat and Romidepsin) (discussed in detail below), immunomodulatory cytokines (such as interferon α that maintains a Th1 skewing and enhance the host anti-tumor immunity) or cytotoxic chemotherapy. Chemotherapy is delayed as long as possible to try and limit toxicity and keep from further diminishing the quality of life of patients. Data involving Bexarotene, ATRA, and Methotrexate will be discussed in Chapter III and are discussed in more detail below.

ATRA and Bexarotene

All trans retinoic acid (ATRA) and Bexarotene are retinoids that are able to bind and activate retinoid receptors. Retinoids are derivatives of vitamin A and belong to the steroid hormone family. They are regulators of many processes including metabolism, differentiation, apoptosis, proliferation, and hematopoiesis [88]. Retinoids are able to regulate these processes through interaction with the above mentioned retinoid receptors. There are two families of retinoid receptors, the retinoic acid receptors (RARs) and the retinoid X receptors (RXRs). These receptors are ligand activated and can bind to DNA. RARs have two endogenous ligands, ATRA and 9 cis retinoic acid (9 cis RA), while RXRs are activated by 9 cis RA [88]. Bexarotene is the first synthetic retinoid for the RXRs (highly selective for RXRs), resulting in Bexarotene being termed a “rexinoid” and was approved in 1999 for treatment in CTCL [78, 88]. Bexarotene has had success in CTCL treatment as both a topical gel used in early stage disease and orally in late stage disease.

Even though retinoids that activate RARs have been used in treatment (like ATRA, Isotretinoin, Etretinate, and Acitretin) they have not seen the same success as Bexarotene due to modest and short response rates. Rapid metabolism of retinoids causes insufficient levels of drug in target tissues. Bexarotene has had longer and better response rates than the RAR drugs due to its binding to RXRs instead of RARs. The ability to bind the RXRs allows Bexarotene to cause different biological functions than the RAR ligands. Upon ligand binding and activation of the retinoid receptors, the RARs and RXRs form heterodimers and together they bind specific DNA sequence RAREs, or retinoic acid response elements leading to gene activation through interaction with coactivators [88]. In the absence of ligands, the RAR/RXR heterodimers can interact with corepressors such as NCOR/SMRT and HDAC3 resulting transcriptional repression [88]. A unique feature of the RXRs is that not only can they heterodimerize with RARs, they can also homodimerize and then these homodimers can form heterodimers with over 20 other nuclear receptors [88]. These nuclear receptors include thyroid hormone receptors, vitamin D receptors, etc. This unique feature of the RXRs is thought to contribute to Bexarotene's success in CTCL treatment.

Bexarotene causes a G_1 arrest and apoptosis with activation of caspase 3 and PARP cleavage in CTCL cells [89]. A key feature of retinoid treatment, including Bexarotene, is that this treatment is not immunosuppressive and may even boost immune function in patients, which is helpful due to the immunosuppressive nature of CTCL and increased susceptibility of infection.

Bexarotene may downregulate Th2 cytokines by suppressing CCR4 expression among malignant T cells, resulting in increased immune function. For refractory CTCL patients, Bexarotene can be given at a dose of 300mg/m^2 with response rates of approximately 30-40% and a duration of 3-17 months [78]. Some of the major side effects of Bexarotene treatment that have to be closely monitored during treatment are hypertriglyceridemia and central hypothyroidism [78]. During treatment, patients are sometimes put on cholesterol lowering drugs to help with the hypertriglyceridemia.

Methotrexate

Methotrexate is an antifolate used at low doses in recurrent early stage CTCL and at higher doses and in combination with other treatments in advanced CTCL. Methotrexate inhibits de novo purine and pyrimidine synthesis through competitive inhibition of dihydrofolate reductase and inhibition of AICAR (aminoimidazole carboxamide ribonucleotide) transformylase [90-92]. By inhibiting dihydrofolate reductase, the reduction of folate cofactors is prevented, resulting in a loss of the tetrahydrofolate essential for purine and pyrimidine synthesis [90-92]. Methotrexate is cell cycle specific and only active in S phase. By depleting the levels of activated folate, this disrupts cell replication and leads to cell cycle arrest [90-92]. Adverse effects of Methotrexate treatment include nausea, fatigue, hepatotoxicity, and reproductive toxicity. Pralatrexate is a new antifolate that is targeted towards the reduced folate carrier in cancer cells, which

in cancer cells is overexpressed resulting in accumulation of the drug, thus resulting in a more potent antifolate drug [90-92].

Histone Deacetylase Inhibitors

Many cancers involve the inappropriate recruitment and function of HDACs. Two HDIs that have shown tremendous efficacy in CTCL treatment are Vorinostat and Romidepsin [75, 93-95]. These HDIs will be described in brief here but will be described in more detail in the next section. Vorinostat, or suberoylanilide hydroxamic acid (SAHA), was the first HDI that was FDA approved (2006) for treatment in CTCL and is used in refractory/relapsed patients. Vorinostat inhibits the class I and class II HDACs. Vorinostat is orally available and is usually given at 400mg per day [93]. Some of the side effects that can occur during treatment include fatigue, nausea, and thrombocytopenia [93].

Romidepsin, also known as Depsipeptide, is a class I and HDAC6 inhibitor and was FDA approved in 2009 for the treatment of CTCL patients that had undergone and failed one prior systemic treatment (refractory disease)[95]. Romidepsin is only available intravenously and is usually given on days 1, 8, and 15 of a 28 day cycle at 14mg/m^2. In clinical trials, the average overall response rate was 34%. Side effects of Romidepsin treatment that can limit treatment duration and success include cardiac toxicity, thrombocytopenia, anemia, and GI toxicities [95].

Histone Deacetylase Inhibitors

Classes of HDIs

Shortly after the isolation and characterization of histone deacetylation, naturally occurring histone deacetylase inhibitors (HDIs) were discovered. However, when the first natural HDI, n-butyrate, was found to cause increased acetylation in cells (described below), HDACs had not been isolated yet and the exact mechanism of histone acetylation caused by n-butyrate, was not known. N-butyrate would later be classified as the first HDI when HDACs were discovered 12 years later. Along with naturally occurring HDIs, synthetic HDIs have been made to decrease toxicity issues and target specific HDACs. HDIs are classified based on structure and differ in the concentration with which activity is seen, specificity, and toxicity. Some of the major classes of HDIs are described below and the structures can be seen in Figure 6 (Modified from [96, 97] and Sigma Aldrich).

Aliphatic Acids

The aliphatic acids (or short-chain fatty acids) include n-butyrate and valproic acid (VPA). They are the smallest and simplest types of HDIs with activity seen at millimolar concentrations. As mentioned, n-butyrate was one of the first HDIs discovered and is a naturally occurring bacterial byproduct in fiber fermentation. n-butyrate treatment of HeLa, neuroblastoma, and other cell types caused morphological changes and decreases in cell proliferation, both of which

Aliphatic Acids

***n*-butyrate**

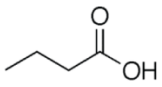

VPA

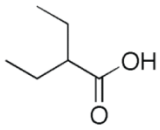

Hydroxamates

TSA

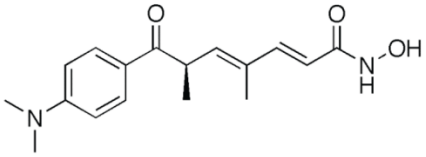

SAHA

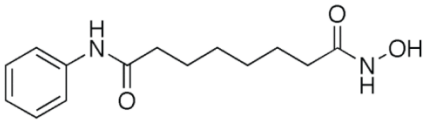

Cyclic Peptides

Depsipeptide

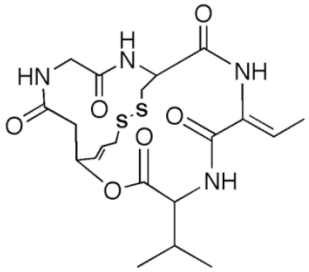

Benzamide

MS-275

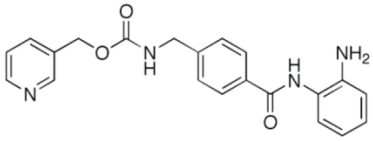

Pimelic diphenylamides/
N-(o-amino-phenyl) carboxamides

RGFP136

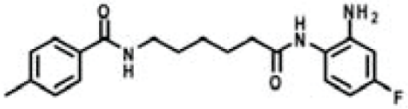

RGFP966

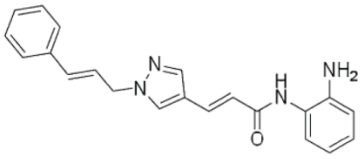

Figure 6. Histone deacetylase inhibitors.

were irreversible [98-100]. Treatment with n-butyrate in HeLa and Friend erythroleukemia cells also caused rapid accumulation of histone acetylation on histone H4 [98-100]. In both of these cell lines, when n-butyrate was removed from the cell culture medium and the cells are cultured in fresh medium, the acetylation levels returned to normal levels seen in control cells, proving that this acetylation increase due to n-butyrate was reversible [98]. Another impressive finding was that n-butyrate could induce differentiation in Friend erythroleukemia cells, which normally have a block in differentiation. Valproic acid differs from n-butyrate in that VPA is a synthetic compound. VPA was first used as an anti-convulsant in epilepsy and bipolar disorder treatment but in 2001 was found to relieve HDAC-dependent repression and cause hyperacetylation, thus identifying it as an HDI [101]. n-butyrate and VPA both work by inhibiting the class I and class II HDACs and studies of these aliphatic acids have provided important information on HDAC function. However, as mentioned, n-butyrate and VPA are active at millimolar concentrations due to their weak binding to HDAC binding pockets [102]. This requirement of high concentrations of drug makes the aliphatic acids the least effective class of HDIs resulting in the desire to find more potent HDIs.

Hydroxamates

Approximately 10 years after the discovery of n-butyrate as a HDI, the anti-fungal compound, trichostatin A (TSA), was found to induce differentiation of Friend cells and could inhibit cell cycle progression in rat fibroblasts [103]. TSA

treatment was then shown to cause increased histone acetylation accumulation in a TSA-sensitive cell line and was determined to be a potent HDI [104]. TSA has activity in the nanomolar concentration range but has undesirable toxic side effects. A synthetic hydroxamate compound was made in 1996 using the hybrid polar compound, hexamethylenebisacetamide (HMBA), as a model. This new compound was called suberoylanilide hydroxamic acid (SAHA) and upon its development, was a potent inducer of differentiation of murine erythroleukemia (MEL) cells [105, 106]. It was not until two years later that SAHA was found to be a histone deacetylase inhibitor and cause increased acetylation levels of histones[106]. SAHA is also known as Vorinostat in the clinics, and inhibits both the class I and class II HDACs using micromolar concentrations. As mentioned in the CTCL section of this introduction, SAHA has had great success in cancer treatment, specifically CTCL and was FDA approved in 2006 for treatment in CTCL.

Cyclic Peptides

The other HDI approved for treatment in CTCL, Depsipeptide (also known as Romidepsin or FK-228), belongs to the cyclic peptides class of HDIs. Depsipeptide is a naturally occurring compound that was isolated from the fermentation broth of *Chromabacterium violaceum* during a screen to identify compounds that could selectively reverse the phenotype in Ras transformed cells [95]. Depsipeptide was shown to be lipophilic and contain a noncystine disulfide linkage. During circulation in the serum, Depsipeptide remains inactive until it

penetrates the membrane of a tumor cell and is converted to its active, reduced form (redFK) by intracellular antioxidants [95]. Depsipeptide works in the nanomolar concentration range leading to potent HDAC inhibition of class I HDACs and HDAC6. It is thought that one of the sulfhydryl groups in the redFK form of Depsipeptide interacts with the zinc ions in the active site of the zinc dependent HDACs [95]. One downfall of Depsipeptide, as well as SAHA, is that since these HDIs inhibit multiple HDACs, they may be inhibiting targets that are not integral to CTCL survival and progression resulting in adverse toxicities in patients (see CTCL section). Additionally, the roles of HDACs in tumorigenesis and the mechanisms by which HDAC inhibition is effective against cancer remain unclear. Therefore, selective inhibition of HDACs may decrease side effects by inhibiting only one or two HDACs at a time and allow for further elucidation of the roles of individual HDACs in cancer. This led to the synthesis of selective HDIs known as the pimelic diphenylamides and N-(o-amino-phenyl) carboxamide.

Pimelic diphenylamides and the N-(o-amino-phenyl) carboxamides

The benzamide family of HDIs (reviewed in [107, 108]) includes such drugs as MS-275 that cause anti-proliferative effects in both cell culture and xenografts nude mouse models of 7 different human tumor lines, including human leukemia, colorectal, lung, ovary, pancreatic, oral, and gastric cancer [109] and is more isoform-specific in its HDAC inhibition (HDAC1/2 being the most inhibited). However, even though this HDI was more selective, it lacked the potency of other HDIs. Recently, a family of benzamide-based HDIs was

identified as possessing class I specific inhibition and less toxicity when compared to the hydroxamates [110-112]. These HDIs are known as the pimelic diphenylamides. It is not known how these HDIs bind to HDACs or how they are inhibiting HDAC activity. Compound 106 was one of the first pimelic diphenylamides and exhibited inhibition of HDACs 1, 2, and 3 through tight binding with inhibition of HDAC3 be the greatest [110]. Through kinetic studies, this class of HDIs was found to be slow on/ slow off inhibitors unlike the fast on/fast off hydroxamates. This slow on/slow off inhibition results in prolonged increases in acetylation and HDAC inhibition. A derivative of compound 106, RGFP136, was used to study Frataxin upregulation in Friedreich's ataxia cells and long term memory formation by examining the role of HDAC3 specifically [96].

Most recently, a new HDAC3 selective inhibitor has been identified and is also a derivative of the pimelic diphenylamide family. It is an N-(o-amino-phenyl) carboxamide HDI known as RGFP966 and exhibits the greatest inhibition of HDAC3 with an IC_{50} of 0.08μM in *in vitro* substrate assays, and importantly, inhibition of other HDACs by RGFP966 was not seen at concentrations up to 15μM [97]. This class of HDIs provides a new approach to studying the individual role of HDACs in cancer. The focus of Chapter III will be the effects of this new HDI, RGFP966 in CTCL cells and elucidation of the mechanism of action of this inhibitor. Chapter IV will then explore the effects of some of the other pimelic diphenylamides that possess different selectivities towards the class I HDACs.

Mechanisms of Cell Killing of HDIs

Although HDIs have been extensively studied and some have been FDA approved for treatment in cancer, it is unclear of the exact mechanism of action of these inhibitors. SAHA and Depsipeptide, for example, can induce cell cycle arrest, apoptosis, and decreased proliferation in cancer cells [113-115] . SAHA also causes increases in ROS production and may have anti-angiogenic properties as well [116, 117]. Studies with Depsipeptide revealed that nude mice xenografted with lymphoma cells had prolonged life when treated with Depsipeptide, suggesting decreased cancer burden in these mice [118]. A key beneficial feature of many of the HDIs is their ability to kill rapidly proliferating tumor cells but leave the non-malignant quiescent cells unharmed [113, 114, 119-121]. Deletion of HDAC3, as well as HDAC1/2, leads to DNA damage and apoptosis is cycling cells but not in non-proliferating cells [46, 47, 122]. This suggests that mechanisms other than altered transcription may account for the anti-cancer activity of these HDIs, both selective and broad inhibitors. In particular, the S-phase dependent cell killing suggests possible effects of HDAC inhibition on DNA replication.

HDACs in Replication and Chromatin Condensation

Proper DNA replication and reorganization of chromatin is critical for normal development. During each round of the cell cycle, DNA and histones need to be synthesized and packaged correctly into chromatin. During replication, chromatin is remodeled ahead of the fork so that DNA replication

machinery can gain access to the DNA and then chromatin is reassembled behind the fork [2, 123]. The newly synthesized histones are acetylated at histone H4K5 and H4K12 and histone H3K56 and these marks may influence chromatin structure after incorporation or help in certain assembly steps [2]. For proper chromatin maturation, these lysine residues need to be deacetylated to allow compaction of the chromatin. Failure to compact newly produced chromatin may lead to defects in replication fork progression, DNA damage, or DNA replication.

HDACs are usually thought of exclusively as transcriptional repressors. However, as discussed above, HDACs are crucial for normal cell cycle progression and deletion of these HDACs can lead to disruption of cell proliferation, S phase associated DNA damage and DNA replication defects, thus providing evidence that HDACs are important in other functions. Indeed, HDACs 1 and 2 regulate deacetylation of histones deposited on newly synthesized DNA during S phase and are enriched at replication forks [47, 124, 125] through association with histone chaperones like RbAp48 and CAF1 [25, 33, 126, 127]. Also, as discussed earlier HDAC3 targets the histone deposition marks H4K5ac and H4K12ac. Loss of HDAC3 activity using siRNA or gene deletion showed a requirement for HDAC3 for proper DNA replication fork progression [48, 128]. However, these methods do not allow examination of the acute effects of HDAC inhibition on DNA replication.

Scope of dissertation

Given the fundamental roles of histone deacetylases (HDACs) in the regulation of DNA repair, replication, transcription and chromatin structure, it is understandable that therapies targeting HDACs are being studied as anti-cancer agents. However, even though some HDIs have been FDA approved for treatment in cancer, it is unclear how exactly these HDIs work. Also, many of the HDIs being tested in clinics are broad spectrum HDIs and inhibit multiple HDACs at one time. This may lead to unnecessary side effects due to the inhibition of non-integral targets. A new class of selective HDIs has been developed and is the focus of Chapter III of this dissertation. Chapter III aims to determine the effects and the mechanism of action of a first in class HDAC3 selective inhibitor in CTCL cells. Chapter IV is a discussion of two other HDIs that have different HDAC selectivities than the HDAC3 selective inhibitor and Chapter V is a summary and discussion of this work.

CHAPTER II

MATERIALS AND METHODS

Cell culture

HH ($CD30^+$ lymphoproliferative disorder) cells (ATCC) were cultured in RPMI supplemented with 10% heat inactivated fetal bovine serum (FBS), 50 U/ml penicillin, 50µg/ml streptomycin, and 2mM $_L$-glutamine. Hut78 (Sézary Syndrome) cells (ATCC) were cultured in Iscove's Modified Dulbecco's Medium (IMDM) supplemented with 20% heat inactivated FBS, 50 U/ml penicillin, 50µg/ml streptomycin, and 4mM $_L$-glutamine. Cells were maintained between $2x10^5$ – $1x10^6$ cells/mL.

Antibodies

The following antibodies were purchased from Abcam: Histone H4 [EP10000Y] (acetyl K5) (ab51997), Histone H3 (acetyl K27) (ab4729), HDAC 1 (ab19845), HDAC 2 [Y461] (ab32117), HDAC 3 (ab16047) and Histone H2B (ab1790). Histone H3 [96C10] (3638S) and Histone H4 [L64C1] (2935S) were used as loading controls and purchased from Cell Signaling. Anti-acetyl histone H3 (or H3K9K14ac) (06-599) and Anti-phospho-Histone H2A.X (Ser 139) clone JBW301 (05-636) were purchased from Millipore. Histone H3 (acetyl K56) (2134-1) was purchased from Epitomics, and anti-actin (A2066) was purchased from Sigma Aldrich. PCNA [FL261] was purchased from Santa Cruz (SC7907).

Histone deacetylase inhibitors (HDIs) and CTCL therapeutic drugs

Depsipeptide (aka Romidepsin, FK228, Depsi) was kindly provided by Celgene. The HDIs RGFP233, RGFP136, and RGFP966 were synthesized and kindly given to us by Repligen Corporation. These compounds are analogs of previously published compounds [96] but have different HDAC inhibition selectivity [96, 97, 110, 111]. In purified enzyme assays, RGFP966, 233, and 136 had the following HDAC inhibition IC_{50} values for HDAC1, HDAC2, and HDAC3: RGFP966: >15, >15, 0.08μM; RGFP233: 0.034, 0.059, 3.33μM; and RGFP136: 5.2, 3.0, 0.4μM. Bexarotene (SML0282), Methotrexate (M8407), and ATRA (R2625) were purchased from Sigma Aldrich.

Protein preparation and western blot analysis

For preparation of whole cell protein lysates, cell pellets were washed with PBS and then sonicated in radioimmunoprecipitation assay (RIPA) buffer containing protease inhibitors (Roche) and phosphatase inhibitors (Roche). For preparation of liver lysates, livers were minced in RIPA buffer with protease inhibitors with a razor blade and then homogenized using a dounce homogenizer. Samples were sonicated and then cleared by centrifugation. Then samples were diluted 1:2 in Laemmli's sample buffer (Bio-Rad) and subjected to 13% sodium dodecyl sulfate-polyacrylamide gel electrophoresis. Western blot analyses were performed using primary antibodies listed above and for histone modification or γH2ax westerns, fluorophore conjugated secondary antibodies and the Odyssey system (LiCor) were used. For the iPOND experiment, a HRP secondary

antibody and Western Lightning Plus enhanced chemiluminescence substrate (PerkinElmer, NEL103001EA) was used.

For protein separation, soluble chromatin obtained from HeLa cells was fractionated using a Superose 6 10/300 GL (GE Healthcare) gel filtration column. Fractions (0.5ml) were collected, concentrated using trichloroacetic acid precipitation, and analyzed by western blotting using the antibodies indicated in Figure 15. Molecular weight standards were added to the sample as controls. Their elution fractions are indicated at top of the figure.

Growth curves

Alamar blue was purchased from Invitrogen (DAL1100). Cells were counted and split into T25 (Corning) flasks at $2x10^5$ cells/mL. Cells were then treated with DMSO or HDIs once at hour 0. 100µl aliquots were taken in triplicate from each flask at 0hr, 24 hrs, 48 hrs, and 72 hrs after treatment, distributed into a flat bottom 96-well plate, and 10µl of alamar blue added to each well. After a 4 hr incubation, fluorescence was measured using the Biotek Synergy MX Microplate Reader. For the dual treatment curves, the same protocol was followed except ATRA was re-administered at 48hrs after the initial treatment.

Annexin V staining

Annexin V analysis of HH and Hut78 cells was performed using annexin V-fluorescein isothiocyanate (annexin V-FITC) apoptosis detection kit I (BD Pharmingen - 556547) per the manufacturer's instructions. Briefly, cells were

treated with DMSO, Depsi, or HDIs for 24 hrs, pelleted, washed with PBS, and counted. Cells were then resuspended in annexin V binding buffer, labeled with annexin V-FITC and propidium iodide (PI), and then analyzed by flow cytometry using the 5-laser BD LSRII instrument in the Vanderbilt Flow Cytometry Core. Here propidium iodide (PI) is used as a vital dye.

BrdU staining

Cell cycle status was analyzed using the FITC Mouse Anti-BrdU set (BD Pharmingen-556028). Cells were treated with DMSO, Depsi, or HDIs for 24 hrs and then BrdU (20μM final concentration) was added to each flask one and a half hours before harvesting. The cells were then pelleted, washed with PBS, and counted. $1x10^6$ cells per sample were pelleted, resuspended in 200μl cold PBS and 5mls of cold 100% ethanol, covered with foil, and stored at 4˚C overnight. The next day cells were pelleted, resuspended in 1mL 2N HCl supplemented with 0.5mg/mL pepsin, and then incubated for exactly 30 mins at 37˚C. Samples were then neutralized with 3mL 0.1M Sodium Tetraborate (pH 8.5) and pelleted for 7mins. Then samples were washed 1x with 1mL of PBS + 0.5% BSA, pelleted, washed 1x with PBS + 0.5% BSA + 0.5% Tween 20, and pelleted again. Samples were then resuspended in FITC-Conjugated anti-BrdU and incubated for 45 mins at room temperature in the dark. Samples were washed one more with PBS + 0.5% BSA + 0.5% Tween 20 and resuspended in 400μL of PBS. Propidium iodide and RNase A were added to each sample and then analyzed

by flow cytometry using the 5-laser BD LSRII instrument in the Vanderbilt Flow Cytometry Core.

iPOND

Analysis of proteins associated with DNA replication forks was performed using the iPOND (isolated proteins on nascent DNA) method described previously [129]. Briefly, Hut78 cells were pulsed with EdU for 15 mins followed by either no thymidine chase or a 60 minute thymidine chase. The protein-DNA complexes were then crosslinked with 1% (wt/vol) formaldehyde, nascent DNA was conjugated to biotin using click chemistry, and then protein-DNA complexes were purified using Streptavidin beads. The eluted proteins were then analyzed using western blot analysis. A no click reaction sample (No Clk) that did not include biotin azide was used as a negative control. 0.1% input samples were included for positive controls of each protein analyzed. PCNA served as a positive control for a replication fork associated protein and H2B served as a loading control and positive control for a chromatin associated protein.

DNA fiber labeling

DNA fiber labeling analysis was used to assess DNA replication fork progression [130] in Hut78 cells treated with DMSO, 10nM Depsipeptide or 10μM 966. For experiments where DMSO or HDIs were added prior to labeling, DMSO or HDIs were added 5 mins or 4 hrs prior to the addition of IdU (green). Following a 20 min IdU pulse (20μM final concentration), cells were washed and drug re-

administered along with 100μM CldU for 20 mins. Cells were then washed with equilibrated HBSS, resuspended in cold PBS at $1x10^6$ cells/ml, and mixed with non-labeled cells for better spreading results (20μL labeled cells + 60μL non-labeled cells). 2μL of cell suspension and 10μL of spreading buffer (0.5% SDS, 200mM Tris-HCl ph 7.4, 50mM EDTA) was added to each slide, let sit for 6 mins at RT and then tilted to 15 degrees to allow the DNA to run slowly down the slide. 5 slides were made for each sample. Slides were then air dried for at least 40mins, fixed in 3:1 methanol:acetic acid for 2 mins, air dried again for 20 mins, and then stored at 4˚C overnight.

The next day, slides were submerged in 2.5M HCl for 30mins, rinsed 3x in PBS and then incubated in 10% goat serum/0.1%Triton in PBS for 1 hr. Then slides were incubated in the dark for 1 hr in rat monoclonal anti-CldU (Accurate Chemical OBT0030G) and mouse anti-IdU (Becton Dickinson 347580) diluted 1/100 in 10% goat serum/0.1% Triton in PBS. Slides were then rinsed 3x in PBS and incubated 30 min with secondary antibodies (Invitrogen Alexa Fluor 568 goat anti-rat-IgG A-11077 and Alexa Fluor 488 goat anti-mouse-IgG A-11029) in 10% goat serum/0.1% Triton in PBS in the dark. Slides were then rinsed 3x in PBS, air dried in the dark, mounted with 110μL of Prolong Gold with no Dapi (Invitrogen P36930) using whole slide coverslips, let dry overnight at RT and then stored at 4˚C. Samples were imaged at 1000x and 100 fibers were measured for each sample.

Fork velocity was determined by the total length of fibers (IdU plus CldU) divided by 40 min. The above listed protocol was followed for all experiments

except for changes in the labeling scheme as listed below: For experiments where DMSO or HDIs were added after labeling with IdU followed by CldU, cells were labeled with IdU for 20mins followed by 20 mins of CldU, washed, and then either immediately treated with DMSO or HDIs for 25 mins or incubated in fresh medium for 4hrs and then treated with DMSO or HDIs for 25 mins. Fork Velocity was determined by the total length of fibers (IdU plus CldU) divided by 40 min pulse or by the length of either the IdU label or CldU label divided by 20 min pulse.

CHAPTER III

INHIBITION OF HISTONE DEACETYLASE 3 CAUSES REPLICATION STRESS IN CUTANEOUS T CELL LYMPHOMA

Background and Significance

Cutaneous T cell lymphoma (CTCL) is a heterogeneous group of non-Hodgkin's lymphoma that is characterized by accumulation of malignant T cells in the skin [75-77]. The most common subtypes of CTCL are mycosis fungoides, Sézary Syndrome, and the $CD30^+$ lymphoproliferative disorders, comprising 95% of CTCL [76-78, 131]. Histone deacetylase (HDAC) inhibitors have become an important treatment option for CTCL that progresses to the more aggressive stages of disease. Histone deacetylases are likely to serve as valuable therapeutic targets as they contribute to genomic stability and cell cycle control through their fundamental roles in cell proliferation including the regulation of DNA repair, replication, transcription, and chromatin structure. In fact, due to their success in the treatment of CTCL, HDACs are now being explored as therapeutic targets for multiple cancers [132-135].

Two histone deacetylase inhibitors (HDIs), SAHA (Vorinostat) and Depsipeptide (Romidepsin), are FDA approved for the treatment of refractory CTCL [75, 77, 93, 94, 136]. Both of these compounds inhibit multiple HDACs with SAHA inhibiting class I and II HDACs while Depsipeptide inhibits the class I HDACs and HDAC6 [94, 136, 137]. However, since these HDIs inhibit multiple

HDACs, they may be inhibiting targets that are not integral to CTCL survival and progression, thereby causing unnecessary side effects. Treatment with SAHA or Depsipeptide is less toxic than standard chemotherapy but can be associated with negative impacts on quality of life [77, 93, 137]. Adverse effects of SAHA and Depsipeptide include nausea, fatigue, gastrointestinal and cardiac toxicity, and hematologic impairment [77, 93, 137]. Additionally, the roles of HDACs in tumorigenesis and the mechanisms by which HDAC inhibition is effective against cancer remain unclear. Therefore, selective inhibition of HDACs may decrease side effects by inhibiting only one or two HDACs at a time and allow for further elucidation of the roles of individual HDACs in cancer.

An important target of these HDIs is histone deacetylase 3, or HDAC3. HDAC3 (a class I HDAC) is involved in the regulation of chromatin structure and gene expression, which controls DNA repair, metabolism, and even tumorigenesis [43, 46, 47, 138, 139]. While HDACs are often thought of exclusively as transcriptional repressors, mouse embryonic fibroblasts (MEFs) lacking HDAC3 displayed S phase dependent DNA damage accumulation, deregulation of transcription, and apoptosis [46]. Due to this role in DNA damage, selective HDAC3 inhibition could potentially target the rapidly proliferating tumor cells while not harming the surrounding quiescent, non-malignant cells [113-115, 119-121].

HDACs are classified based on sequence conservation. The Class I HDACs 1 and 2 share 82% identity while these HDACs share 53% and 52% identity, respectively, with HDAC3 [30-32]. The class I HDACs also contain a

highly conserved central catalytic domain [31, 32] that is 58% identical between HDAC1 and HDAC3. Given the high level of homology between the class I HDACs, it is understandable why a selective inhibitor would be difficult to identify. However, a new class of inhibitors, N-(*o*-aminophenyl) carboxamides, can show 10-fold or higher selectivity for HDAC3, over HDACs 1 and 2 [[97] and Vincent Jacques, Repligen, unpublished data]. This family of inhibitors includes RGFP966 [96, 97, 110, 111], which has an IC_{50} of 0.08μM in *in vitro* substrate assays and inhibition of other HDACs by RGFP966 was not seen at concentrations up to 15μM [97]. Therefore, we set out to determine the effects of selective HDAC3 inhibition using RGFP966 on cancer cell growth.

In this chapter, CTCL cell lines were treated with a selective HDAC3 inhibitor and it was found that these cells exhibited sensitivity to selective HDAC3 inhibition as demonstrated by decreased cell growth and increased apoptosis. These cells also had increased DNA damage upon HDAC3 inhibition and did not progress normally through the cell cycle due to impaired S phase progression. Consistently, DNA fiber labeling assays demonstrated that inhibition of HDAC3 caused a 50% reduction in DNA replication fork velocity. Through isolation of proteins on nascent DNA (iPOND), we determined that HDAC3 is associated with chromatin and present at and around DNA replication forks. Thus, HDAC3 inhibition caused replication stress in CTCL cells, and selective inhibition of HDAC3 through novel inhibitors may be useful in the treatment of CTCL.

Results

Selectivity of novel histone deacetylase inhibitors

The development of selective class I HDAC inhibitors has been challenging due to the conservation of the deacetylase domains of HDACs1-3, yet recently some selectivity has been achieved [96, 97, 110, 112]. To further assess the action of these inhibitors, we sought a histone mark that separates the functions of HDAC1/2 from HDAC3. Deletion of *Hdac3* caused increases in the acetylation of H4K5, H4K8, H4K12, H4K16, H3K9K14, and H3K27 [47], which are also targeted by Hdac1/2 [125]. However, we noted that *Hdac3* deletion did not cause the accumulation of the modification recognized by the rabbit monoclonal antibody to H3K56ac (Figure 7A). While this antibody can also cross react with H3K9ac [140], anti-H3K9ac signal did increase in *Hdac3*$^{-/-}$ cells, suggesting that under the conditions used here we did not detect H3K56ac (Figure 7A; note that all samples were run on the same gel, but we removed intervening lanes for side by side comparison of WT and *Hdac3*$^{-/-}$ samples). In contrast, inhibitors of class I HDACs (SAHA, Trichostatin A and sodium butyrate (NaB)), caused a more dramatic accumulation of H3K56ac than nicotinamide, which impairs the Sirtuins (Figure 7B). Therefore, we used siRNAs directed to *Hdac1* and *Hdac2* and found that co-suppression of the expression of both enzymes was necessary to cause H3K56ac to accumulate, suggesting that both

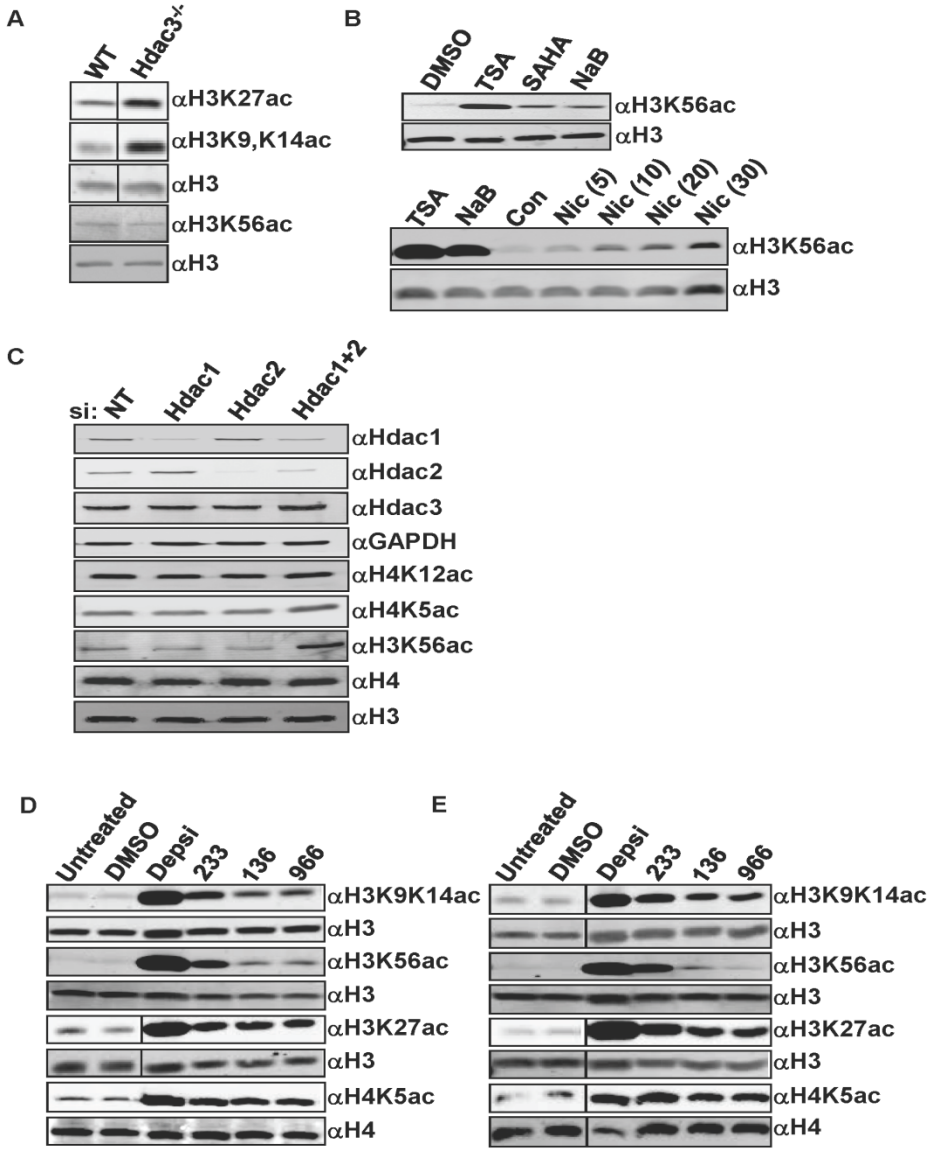

Figure 7. HDIs show selective inhibition of HDACs in CTCL cell lines. Western blot analysis. (A)Whole cell lysates from Wild-type (WT) and *Hdac3*-null livers. (B) Upper Panel: NIH 3T3 cells following treatment with various HDIs (indicated above each lane). Lower panel: NIH 3T3 cells treated with either Trichostatin A (TSA) (1μM), sodium butyrate (NaB) (5mM), or increasing concentrations of nicotinamide (mM). (C) Whole cell lysates prepared from cells that were transfected with either non-targeting siRNAs (NT) or siRNAs directed to the indicated Hdacs. (D & E) (D) HH or (E) Hut78 cell lines treated with DMSO, 10 nM Depsipeptide (Depsi), 10 μM 233, 10 μM 136, or 10 μM 966. Cells were treated for 24 hrs and then harvested for protein isolation. Samples were run on the same gel and probed on the same membrane. Intervening lanes (represented by a black bar) were removed for side by side comparison of DMSO and Depsipeptide. Histones H3 and H4 were used as loading controls.

of these enzymes can target this mark, but that *Hdac3* fails to deacetylate this residue (Figure 7C).

Given that H3K56ac separates the action of HDAC1/2 from HDAC3, we tested selective HDAC1/2 (RGFP233) and HDAC3 selective inhibitors (RGFP136 and RGFP966) for specificity. RGFP233 (233) showed 100- and 50-fold selectivity respectively towards HDAC1 and HDAC2 over HDAC3, and RGFP136 (136) and RGFP966 (966) were 10- and >100-fold respectively more selective for HDAC3 in *in vitro* deacetylase assays [Vincent Jacques, Repligen unpublished data]. Treatment of two CTCL cell lines, HH and Hut78, with the HDAC3-selective inhibitors 966 and 136, for 24 hours prior to western blot analysis resulted in increased acetylation at H3K9/K14, H3K27, and H4K5, but not H3K56ac (even at 10μM, Figure 7D and E). In contrast, Depsipeptide, an inhibitor of the class I HDACs (HDACs 1, 2, 3, and 8) [136, 137], caused the robust accumulation of all of the histone acetylation marks tested, whereas the HDAC1/2-selective inhibitor, 233, caused a less robust accumulation of these same marks. Using the Odyssey imaging system, we measured the fluorescence (integrated intensity units) of each band and found that 966 and 136 were 8-fold selective for HDAC3 inhibition by these criteria, even when used at relatively high levels (Figure 7D and E), confirming the *in vitro* data that 136 and 966 are selective for HDAC3 inhibition [Vincent Jacques, Repligen unpublished data]. Importantly, 966 was determined to have no inhibition of other HDACs at concentrations up to 15 μM in *in vitro* assays [97], which is consistent with our finding of only modest increases in H3K56ac at 10 μM.

HH and Hut78 CTCL cell lines show sensitivity to novel, selective HDIs and additive effects with CTCL clinical drugs

To determine how treatment with selective HDIs affects CTCL cell lines, we first performed cell proliferation assays using alamar blue to measure cell growth and viability in the presence of different HDIs. HH and Hut78 cells were treated at hour 0 with either DMSO, Depsipeptide, 233, or 966 and then analyzed at hours 0, 24, 48, and 72 for changes in cell proliferation as measured by changes in alamar blue-dependent fluorescence. Both cell lines were sensitive to treatment with 10 μM 233 or 966, as demonstrated by decreases in cell growth over time (Figure 8A). However, Hut78 cells exhibited a greater sensitivity to these HDIs than HH cells. Both cell lines were sensitive to Depsipeptide, while unaffected by the DMSO control. Dose curves were performed on each cell line to determine the optimal dose for dual treatment with drugs that are used or have been used to treat CTCL (Figure 8B). Cells were treated with varying concentrations of 233, 136, or 966 at hour 0 and again analyzed using alamar blue cell viability assays. CTCL cells showed dramatic sensitivity to 233 at each concentration, with Hut78 cells again exhibiting heightened sensitivity when compared to HH cells (Figure 9A). Treatment of cells with 136 had only modest effects on cell growth when compared to 966 treatment (Figure 9B and Figure 8B) in both cell lines. Through discussion with Repligen, we discovered that the IC_{50} for 136 was 8 times less potent than 966. Thus, we discontinued the analysis of 136 in subsequent experiments and focused on the inhibition of Hdac3 using 966.

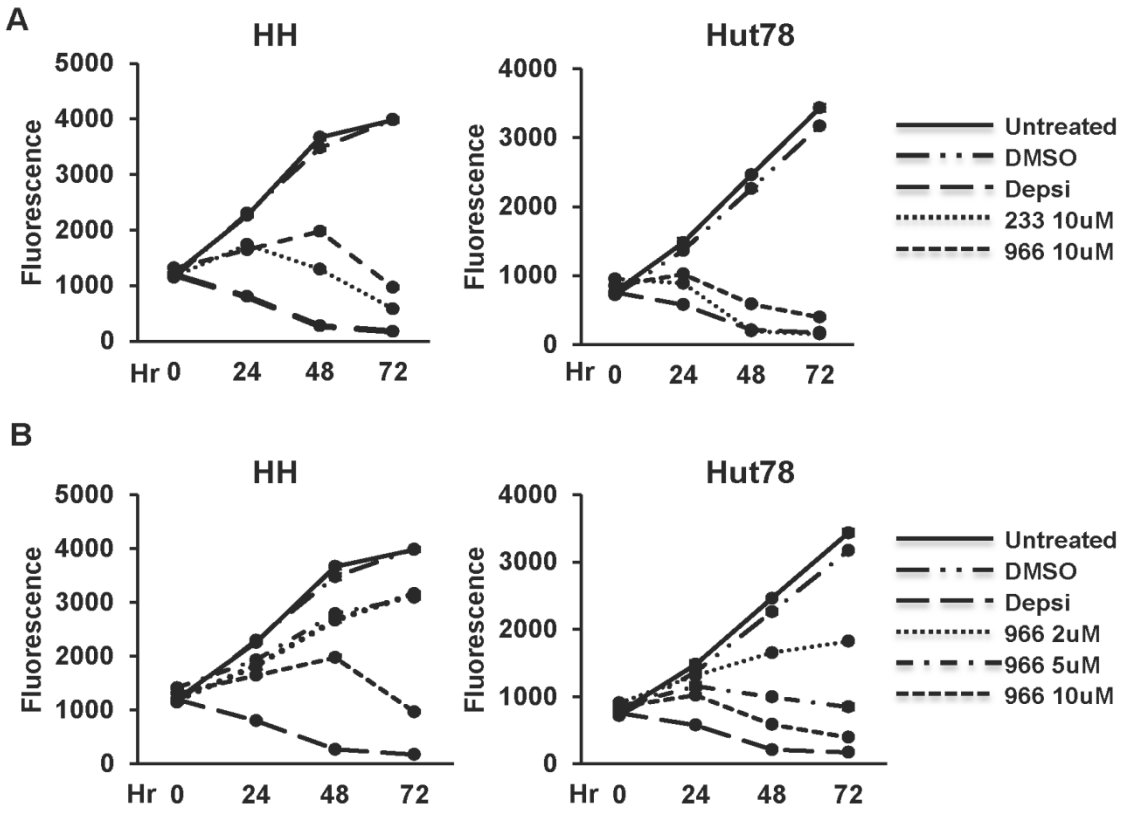

Figure 8. CTCL cell lines are sensitive to pan and selective HDIs. (A) Growth curves of HDI treated HH cells (left) or Hut78 cells (right). Cells were treated once with DMSO, 10 nM Depsipeptide (Depsi), 10 μM 233, or 10 μM 966 at hour 0. Untreated cells and DMSO treated cells were used as controls. Cell growth was assessed at 0, 24, 48, and 72 hours after treatment. (B) Dose curves of 966 treated HH cells (left) and Hut78 cells (right). The experiment was performed in the same manner as (A) except that the cells treated were treated once with 2 μM, 5 μM, or 10 μM of 966 at hour 0. For both (A) and (B), representative curves are shown from experiments performed in triplicate that are consistent with other biological replicates. Statistical analysis was performed using a two-tail paired T-test and comparing the HDI treated cells to DMSO treated cells resulting in the following p values: (A) HH cells (left), Depsi: p=0.0008, 233: p=0.004, and 966: p=0.006. For the Hut78 cells (right), Depsi: p=0.002, 233: p=0.006, and 966: p=0.006. (B) HH cells (left), Depsi: p=0.0008, 966 2 μM: p=0.02, 966 5 μM: p=0.01, and 966 10 μM: p=0.006. For the Hut78 cells (right), Depsi: p=0.002, 966 2 μM: p=0.03, 966 5 μM: p=0.01, and 966 10 μM: p=0.006.

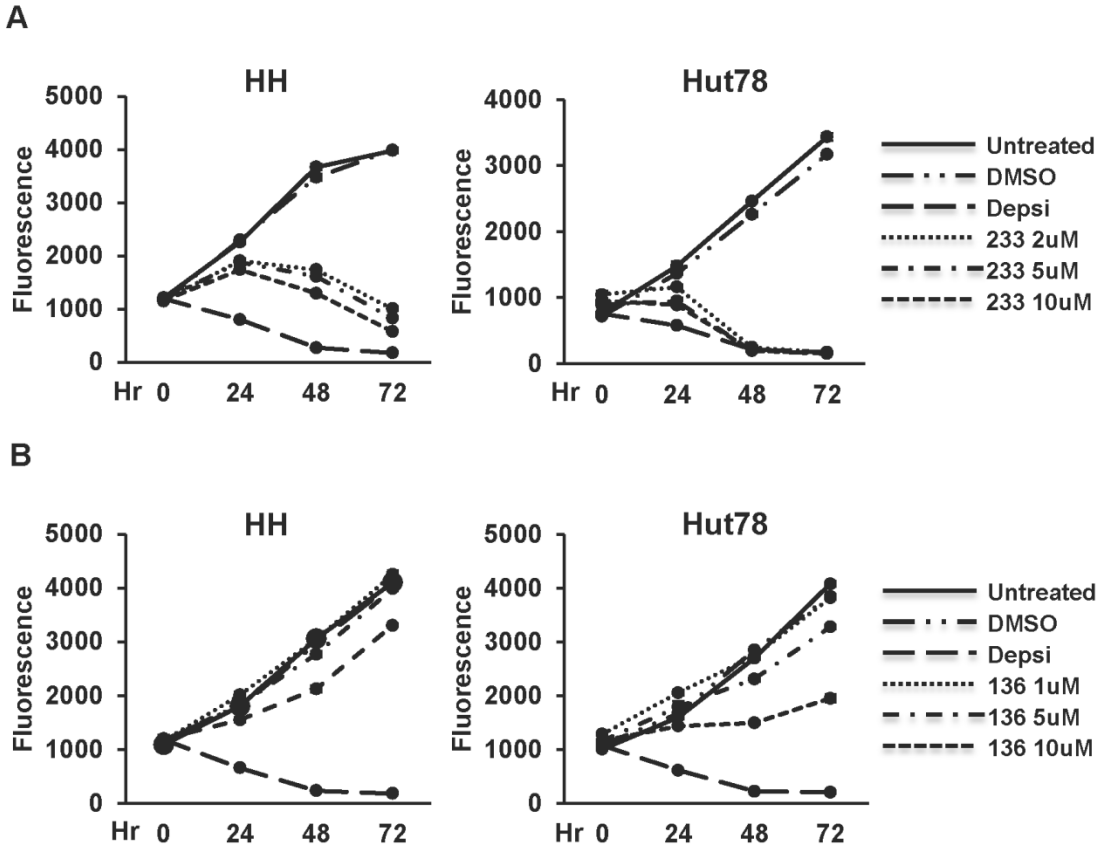

Figure 9. CTCL cell lines exhibit sensitivity to multiple concentrations of 233 and high dose 136. Dose curves of HH cells (left) or Hut78 cells (right) treated with 10 μM 233 (A) or 966 (B). Cells were treated once with DMSO, 10 nM Depsipeptide (Depsi), or different concentrations of either 233 or 136 at hour 0. Untreated cells and DMSO treated cells were used as controls. Cell growth was assessed at 0, 24, 48, and 72 hours after treatment using alamar blue. For both (A) and (B), representative curves are shown from experiments performed in triplicate that are consistent with other biological replicates. P values: (A) HH cells (left), Depsi: p=0.0008, 233 2 μM: p=0.005, 233 5 μM: p=0.005, and 233 10 μM: p=0.004. For the Hut78 cells (right), Depsi: p=0.002, 233 2 μM: p=0.01, 233 5 μM: p=0.005, and 233 10 μM: p=0.006. (B) HH cells (left), Depsi: p=0.001, 136 1 μM: p=0.1, 136 5 μM: p=0.1, and 136 10 μM: p=0.006. For the Hut78 cells (right), Depsi: p=0.001, 136 1 μM: p=0.08, 136 5 μM: p=0.02, and 136 10 μM: p=0.005.

A number of therapies are currently used for the treatment of CTCL and given that single agent therapy is rarely beneficial, we tested Bexarotene (highly selective retinoid x receptor agonist), Methotrexate (inhibitor of dihydrofolate reductase), or ATRA (All Trans Retinoic Acid, a retinoic acid receptor agonist) [75, 88, 91, 141] for cooperative cell killing with 966. A dose of 2μM for 966 was selected for dual treatment experiments so that we could assess additive or synergistic effects when 966 was combined with these drugs. Dose curves for Bexarotene, Methotrexate, and ATRA were performed and concentrations near the IC_{50} were chosen (Figure 10). Both HH and Hut78 cells exhibited increased sensitivity to dual treatment of 966 plus Bexarotene (Figure 11A), while only Hut78 cells showed increased sensitivity to 966 plus Methotrexate or ATRA (Figure 11B and C).

CTCL cell lines undergo apoptosis, have increased DNA damage, and exhibit cell cycle defects

We next determined whether the decreased cell growth seen when HH and Hut78 cells were treated with selective HDIs (Figures 8 and 9) was due to increased apoptosis. Flow cytometry analysis using Annexin V and propidium iodide (PI) was performed on HH and Hut78 cells that had been treated for 24 hours with DMSO, 10 nM Depsipeptide, 10 μM 233, or 10 μM 966. HH and Hut78 cells displayed significant increases in Annexin V levels following treatment with HDIs, with Hut78 cells exhibiting the highest Annexin V levels (Figure 12A and Figure 12B). Therefore, these cells undergo apoptosis when

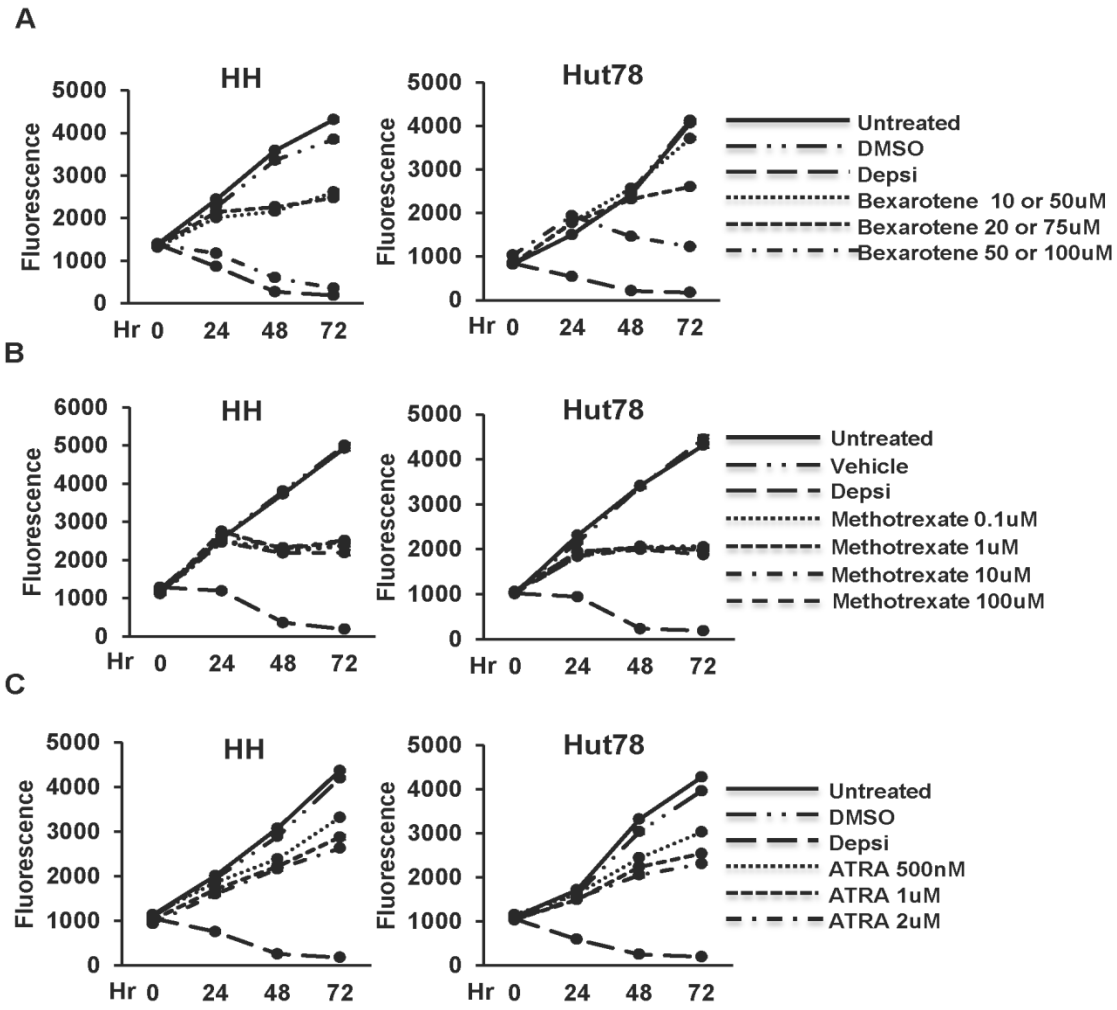

Figure 10. Dose curves for Bexarotene, Methotrexate, and ATRA reveal optimal concentrations for combination treatments**.** (A) Bexarotene (B) Methotrexate (C) ATRA treated HH cells or Hut78 cells. Cells were treated at hour 0 with DMSO, 10 nM Depsipeptide, or varying concentrations of Bexarotene, Methotrexate, or ATRA. Untreated cells and DMSO treated cells were used as controls. (A) HH cells were treated with 10, 20, or 50 μM of Bexarotene. Hut78 cells were treated with 50, 75, or 100 μM of Bexarotene. (B) DMSO and a solution containing Na_2CO_3 served as vehicle controls. (C) ATRA was re-dosed at 48 hr after treatment. For (A-C), representative curves are shown from experiments performed in triplicate that are consistent with other biological replicates. P values: (A) HH cells (left), Depsi: p=0.0007, Bexarotene 10 μM: p=0.001, Bexarotene 20 μM: p=0.004, and Bexarotene 50 μM: p=0.001. For the Hut78 cells (right), Depsi: p=0.002, Bexarotene 50 μM: p=0.8, Bexarotene 75 μM: p=0.1, and Bexarotene 100 μM: p=0.04. (B) HH cells (left), Depsi: p=0.001, Methotrexate 0.1 μM: p=0.007, Methotrexate 1 μM: p=0.01, Methotrexate 10 μM: p=0.01, and Methotrexate 100 μM: p=0.006. For the Hut78 cells (right) Depsi: p=0.001, Methotrexate 0.1 μM: p=0.005, Methotrexate 1 μM: p=0.006, Methotrexate 10 μM: p=0.004, and Methotrexate 100 μM: p=0.004. (C) HH cells (left), Depsi: p=0.001, ATRA 500 nM: p=0.008, ATRA 1 μM: p=0.002, and ATRA 2 μM: p=0.003. For the Hut78 cells (right) Depsi: p=0.001, ATRA 500 nM: p=0.02, ATRA 1 μM: p=0.005, and ATRA 2 μM: p=0.006.

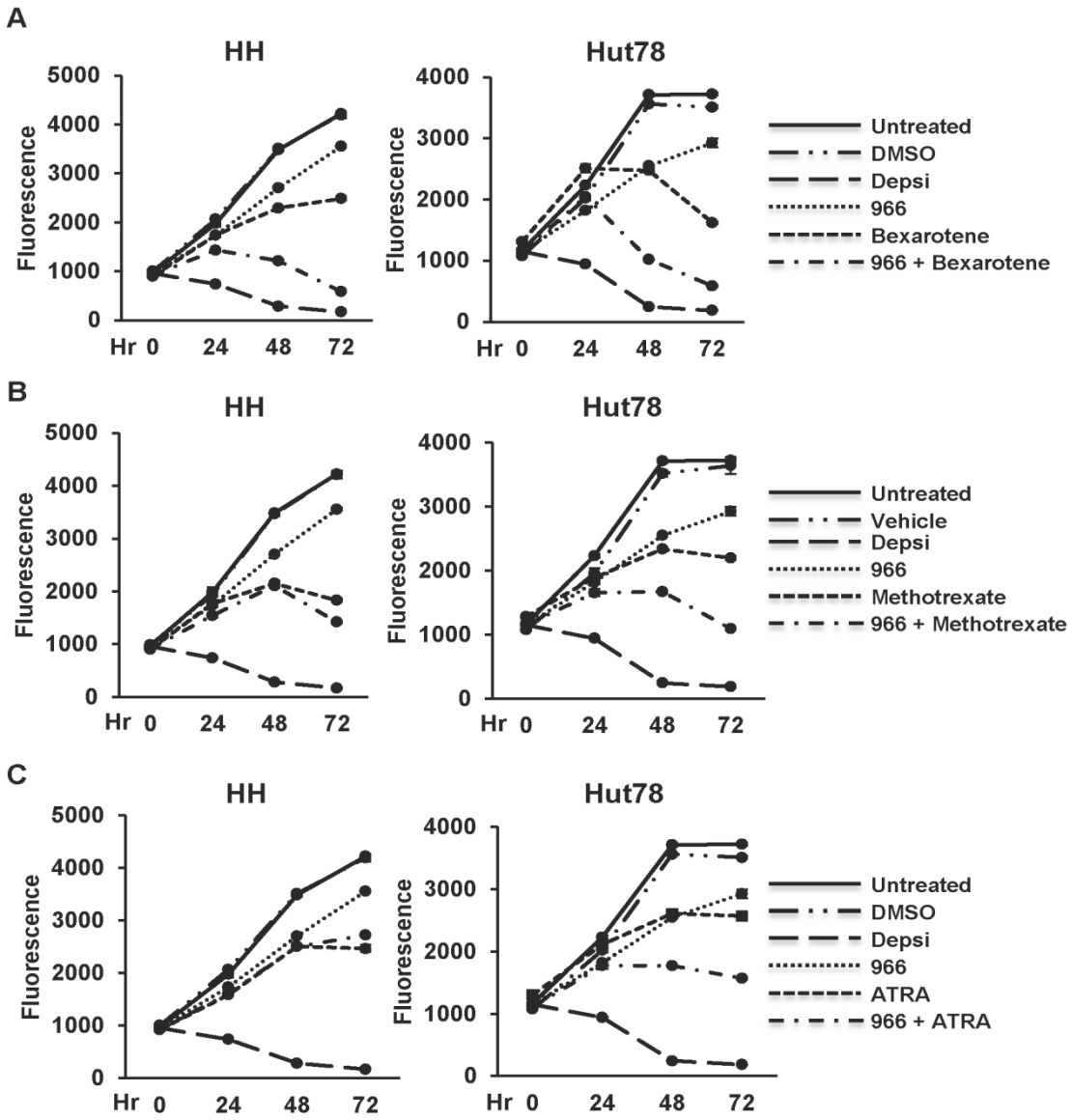

Figure 11. Dual treatment with RGFP966 and CTCL drugs has an additive effect on cell growth. HH cells or Hut78 cells were treated once at hour 0 with DMSO, 10 nM Depsipeptide, 2 μM 966, or a combination of 2 μM 966 and either Bexarotene, Methotrexate, or ATRA. (A) HH cells (left) or Hut78 cells (right) were treated with 20 μM or 75 μM Bexarotene alone or in combination with 966. (B) Treatment with 0.1 μM Methotrexate alone or in combination with 966. DMSO and 1 M Na_2CO_3 served as vehicle controls. (C) Treatment with 2 μM ATRA alone or in combination with 966. ATRA was re-dosed at 48 hours after treatment. For (A-C), representative curves shown performed in triplicate and consistent with other biological replicates. P values: (A) HH cells, Depsi: p=0.0008, 966: p=0.003, Bexarotene: p=0.003, and 966 + Bexarotene: p=0.002. Hut78 cells, Depsi: p=0.001, 966: p=0.08, Bexarotene: p=0.01, and 966 + Bexarotene: p=0.009. (B) HH cells, Depsi: p=0.0008, 966: p=0.003, Methotrexate: p=0.003, and 966 + Methotrexate: p=0.003. Hut78 cells Depsi: p=0.001, 966: p=0.01, Methotrexate: p=0.01, and 966 + Methotrexate: p=0.004. (C) HH cells, Depsi: p=0.0008, 966: p=0.003, ATRA: p=0.002, and 966 + ATRA: p=0.0007. Hut78 cells Depsi: p=0.001, 966: p=0.01, ATRA: p=0.02, and 966 + ATRA: p=0.004.

treated with HDIs. In both cell lines, Depsipeptide treatment resulted in the greatest cell killing, followed by 233 and 966. This trend may reflect the fact that Depsipeptide inhibits all three class I HDACs, 233 inhibits two HDACs, and 966 selectively inhibits a single HDAC.

Deletion of *Hdac3* caused increased DNA damage and cell cycle delays in an S phase dependent manner in fibroblasts [46]. To determine if the apoptosis occurring in Hut78 and HH cells when cells were treated with HDIs was associated with increased DNA damage, we treated cells for 8 hours with DMSO, Depsipeptide, 233 or 966 and performed western blot analysis using anti-γH2aX, which is localized to sites of DNA double-strand breaks [142]. Both cell lines showed approximately a 2.4-fold increase in the amount of γH2aX in samples treated with 966, indicative of an increase in DNA damage when HDAC3 was inhibited in CTCL cells (Figure 12C and Figure 12D). Treatment with Depsipeptide or 233 also caused increased γH2aX levels in both cell lines, with Depsipeptide being the most robust. When HH and Hut78 cells were treated with DMSO, Depsipeptide, 233, or 966 for 24 hours and pulsed with BrdU for 90 min before harvest, Hut78 cells treated with HDIs exhibited decreased BrdU incorporation, and also an increase in cells that were present in S phase but were not incorporating BrdU (Figure 13A-C and Figure 14A-C). These S phase cells that did not incorporate BrdU represent cells that have not completed DNA replication and are arrested in the S phase, suggesting that HDI treatment caused replication stress in CTCL cell lines.

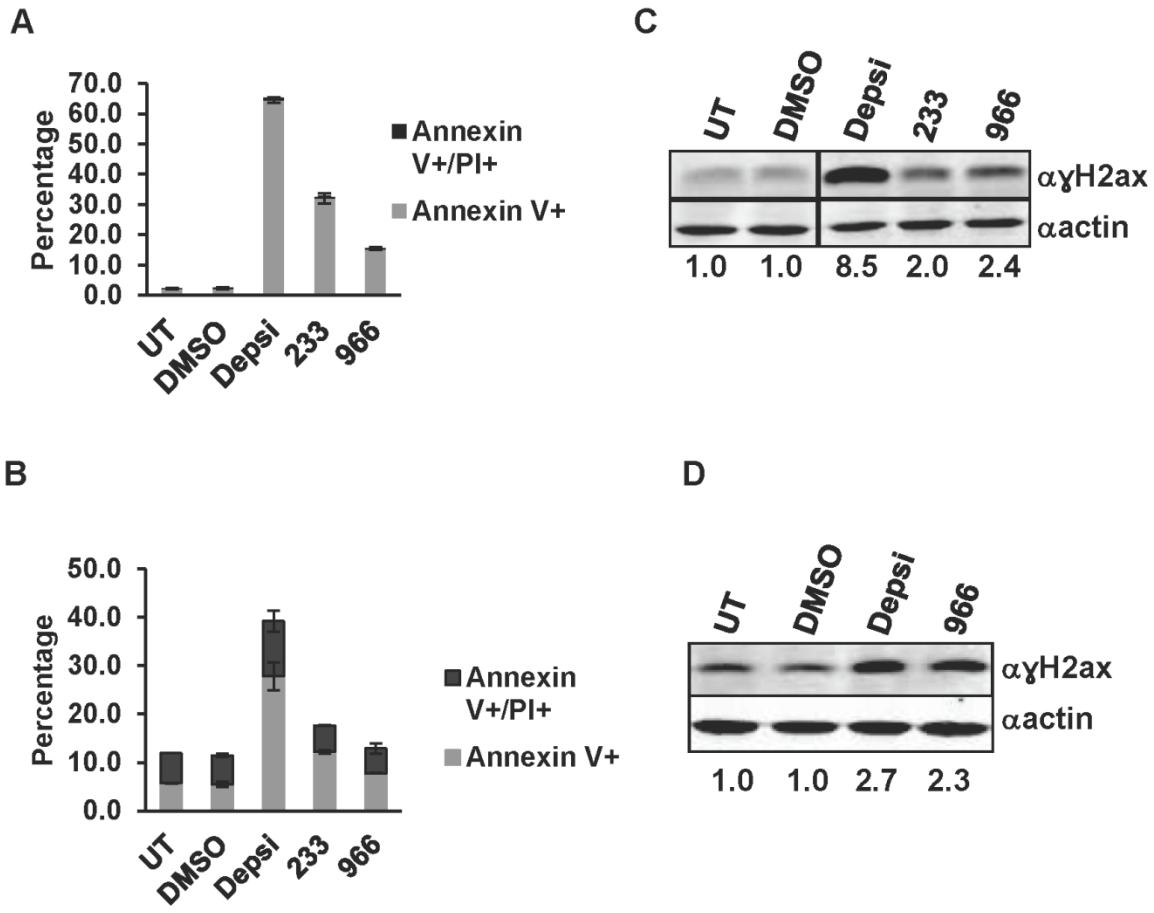

Figure 12. An HDAC3 selective inhibitor triggers apoptosis associated with increased DNA damage. (A) Hut78 and (B) HH cells were treated with DMSO, 10 nM Depsipeptide, 10 μM 233, or 10 μM 966 for 24 hr and apoptosis assessed by Annexin V staining and flow cytometry. Cells were also labeled with propidium iodide to assess DNA content. Untreated (UT) and DMSO treated cells were used as controls. Shown is a representative graph from an experiment performed in duplicate that is consistent with other biological replicates. Statistical analysis for both was performed using a two-tail T-test and resulting in the following p-values: (A) Depsi: p=0.0002, 233: p=0.003, and 966: p=0.0003. (B) Depsi: p=0.02, 233: p=0.01, and 966: p=0.06. (C &D) Western blot analysis of γH2aX levels in (C) Hut78 or (D) HH cells treated with DMSO, 10 nM Depsi, 10 μM 233, or 10 μM 966 for 8 hrs. Untreated and DMSO treated cells were used as controls. Samples were run on the same gel and probed on the same membrane. Intervening lanes (represented by a black bar) were removed for side by side comparison of DMSO and Depsipeptide.

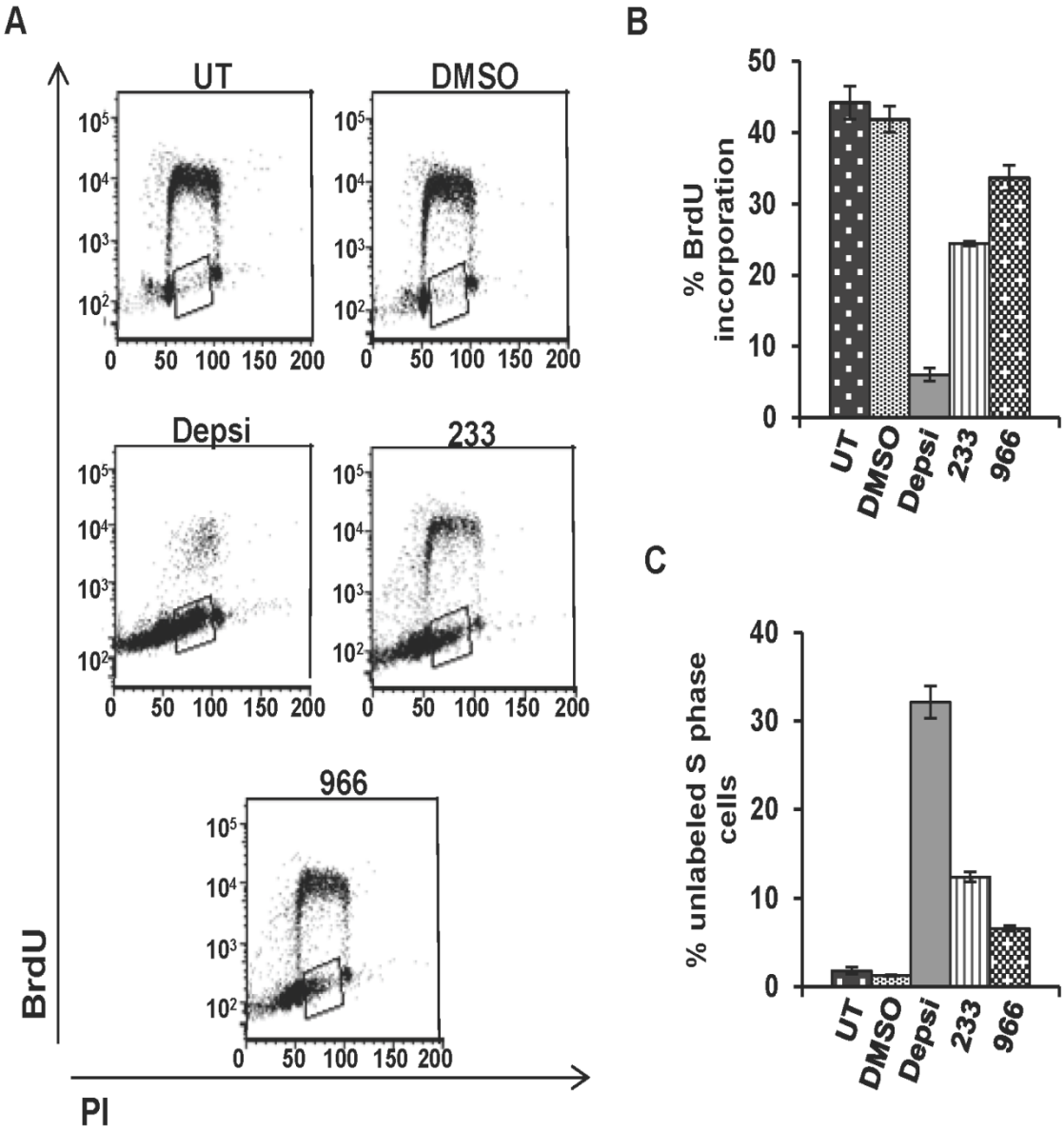

Figure 13. An HDAC3 selective inhibitor triggers cell cycle defects. (A) Cell cycle status was analyzed using BrdU incorporation and propidium iodide to assess DNA content by flow cytometry. Hut78 cells were treated with DMSO, 10 nM Depsipeptide, 10 μM 233, or 10 μM 966 for 24 hr and pulsed for an hour and a half with BrdU prior to cell harvest and analysis. Shown are representative flow cytometry plots performed in duplicate that is consistent with other biological replicates. (B) Graphical representation of BrdU incorporation from the experiment described in (A). (C) Graphical representation of the percent of S phase cells that did not incorporate BrdU (shown by box in (A)). Statistical analysis was performed using a two-tail T-test resulting in the following p-values: (B) Depsi: p=0.003, 233: p=0.01, and 966: p=0.08. (C) Depsi: p=0.003, 233: p=0.003, and 966: p=0.004.

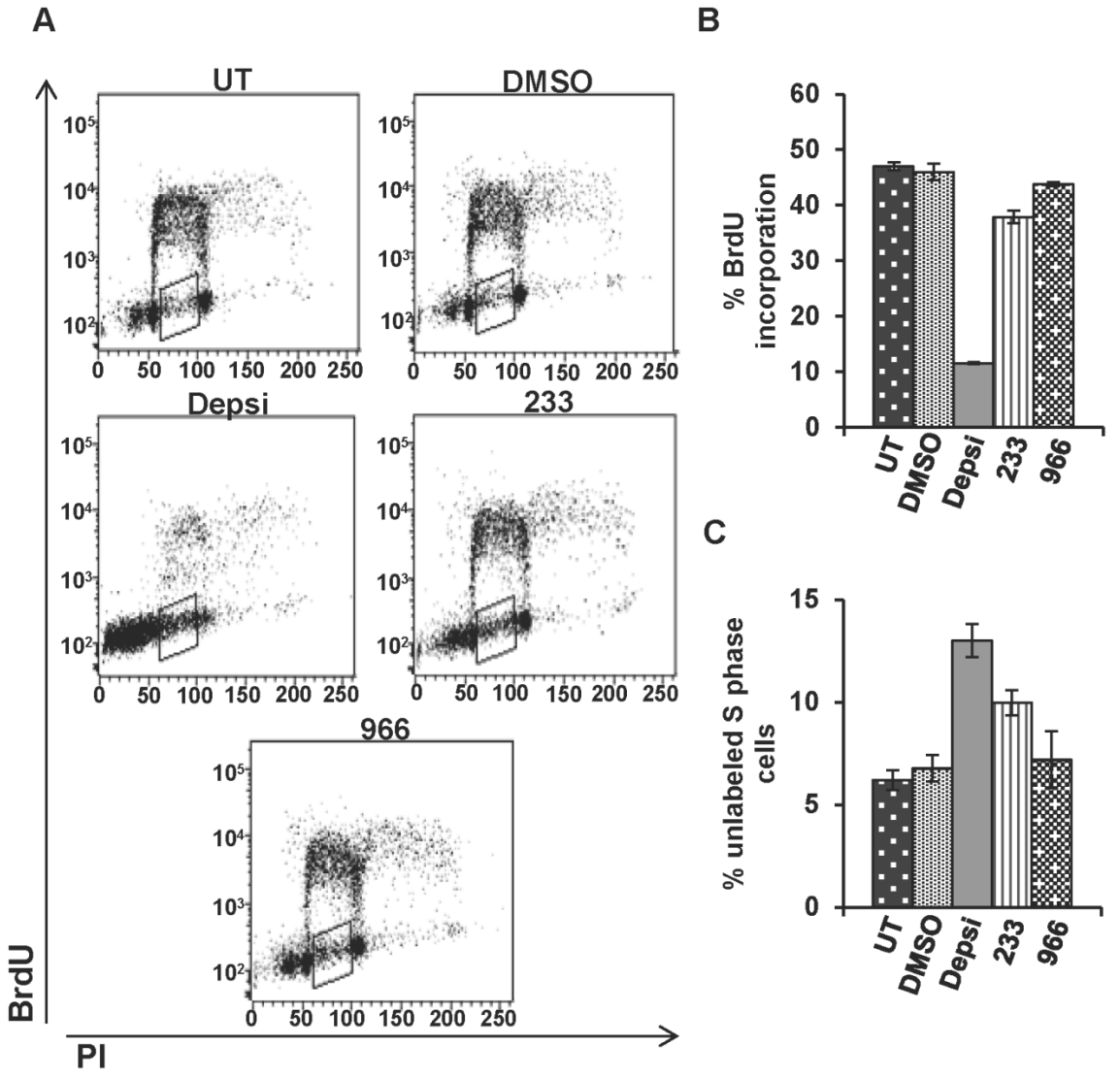

Figure 14. HDIs increased cell cycle defects in HH cells. (A) Cell cycle status was analyzed using BrdU/PI and flow cytometry. HH cells were treated with DMSO, 10nM Depsipeptide, 10 μM 233, or 10 μM 966 for 24 hr and pulsed for an hour and a half with BrdU prior to cell harvest and analysis. Shown are representative flow cytometry plots from an experiment performed in duplicate that is consistent with other biological replicates. (B) Graphical representation of BrdU incorporation from the experiment described in (A). (C) Graphical representation of the percent of S phase cells that did not incorporate BrdU (shown by box in panel (A)). Statistical analysis was performed using a two-tail T-test and comparing the HDI treated cells to the DMSO treated cells resulting in the following p-values: (B) Depsi: p=0.002, 233: p=0.05, and 966: p=0.3. (C) Depsi: p=0.03, 233: p=0.07, and 966: p=0.8.

Inhibition of Hdac3 leads to DNA replication defects

HDACs 1 and 2 regulate deacetylation of histones deposited on newly synthesized DNA during S phase and are enriched at replication forks [47, 124, 125] through association with histone chaperones like RbAp48 and CAF1 [25, 33, 126, 127]. Like HDAC1 and 2, HDAC3 also targets histone deposition marks ([47] and Figure 7), and yeast two-hybrid studies show that HDAC3 can also bind to RbAp48 [143]. Therefore, we tested whether HDAC3 could associate with RbAp48 in mammalian cells. Immunoprecipitation analysis of endogenous HDAC3 and RbAp48 from HeLa cells detected an association, suggesting that HDAC3 could be bound to histone chaperones on chromatin (Figure 15A). To extend this analysis, we used gel filtration to determine the sizes of native HDAC3-containing complexes. HDAC3 co-eluted with a portion of the RbAp48, but not PCNA, which marks DNA replication complexes (Figure 15B).

The gel filtration analysis suggested that HDAC3 might be associated with histone deposition machinery, yet not directly bound to the DNA replication machinery. Therefore, isolation of proteins on nascent DNA (iPOND) was used to further probe HDAC3 localization to DNA replication forks. A similar analysis in HEK293T cells suggested that, not only were HDAC1 and HDAC2 present at DNA replication forks, but HDAC3 was also detected [124]. To test whether HDAC3 was also present at replication forks in CTCL cells, Hut78 cells were pulsed for 15 minutes with EdU (5-Ethynyl-2'-deoxyuridine) only or pulsed with EdU for 15 minutes followed by a 60 minute thymidine chase. After the labeling, cells were cross-linked, and the nascent DNA with EdU incorporated was

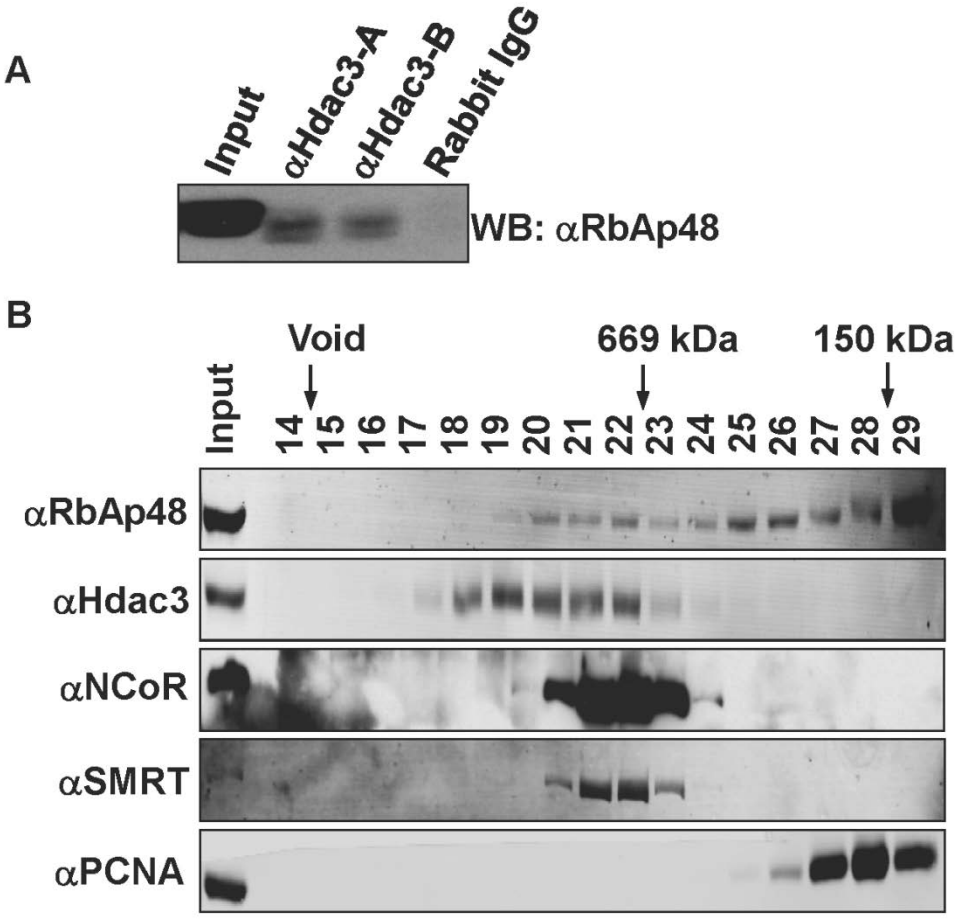

Figure 15. Hdac3 co-purifies with the histone chaperone, RbAp48, in mammalian cells. (A) Immunoprecipitation analysis of endogenous HDAC3 and RbAp48 from HeLa cells. Two different HDAC3 antibodies were used and labeled (A) or (B) and rabbit IgG was included as a negative control. (B) Gel Filtration analysis of HDAC3 containing protein complexes. Nuclear lysates were separated using a Superose 6 gel filtration column and the elution profile of the indicated proteins determined by western blot analysis. The elution of size markers is shown at the top of the blots.

conjugated to biotin using click chemistry. The newly synthesized DNA and the DNA-protein complexes were then purified using streptavidin beads. Proteins that move with the replication fork such as HDAC1 and PCNA [124, 129] were enriched immediately after EdU labeling (lanes labeled “0”, Figure 16) and then decreased with the thymidine chase. By contrast, western blot analysis showed that HDAC3 was bound to chromatin at and around replication forks, but like H2B, its levels did not significantly drop after the 60 minute chase, suggesting that it did not travel with replication forks (Figure 16).

Although HDAC3 did not appear to move with replication forks using iPOND, loss of HDAC3 activity using siRNA or gene deletion showed a requirement for this deacetylase for optimal DNA replication fork velocity [[128],Summers,unpublished data]. A major advantage of small molecules is that they allow the analysis of HDAC function in short timeframes that cannot be replicated by genetic methods. We started by assessing the minimal time required to achieve HDAC3 inhibition using 966. Hut78 cells were treated with DMSO, Depsipeptide, or 966 for 30 min, 1 hr, 2 hr, and 4 hr and western blot analysis for H4K5ac was used as a measure of HDAC3 inhibition (Figure 17). In purified enzyme assays, 966 is a slow on/slow off inhibitor when used at nanomolar concentrations, where full potency was observed within approximately 2 hr. Treatment with 10 μM 966 for 30 min did not significantly increase H4K5 acetylation levels, but by 1 hr a noticeable increase in H4K5 acetylation was apparent, and by 4 hr a dramatic accumulation of H4K5 acetylation was observed (Figure 17) suggesting full inhibition within 4 hr. This suggests that

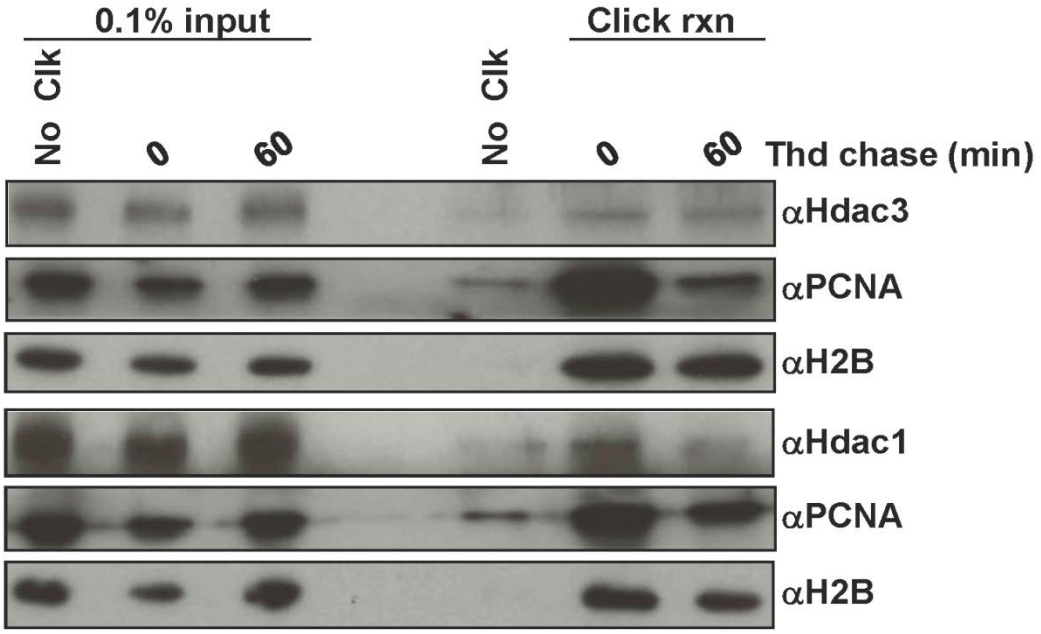

Figure 16. iPOND analysis reveals HDAC3 association with replication forks in Hut78 CTCL cells. Hut78 cells were pulsed for 15 minutes with EdU followed by either no thymidine chase or a 60 minute thymidine chase. The protein-DNA complexes were then cross-linked, nascent DNA was conjugated to biotin using click chemistry, and then protein-DNA complexes were purified using Streptavidin beads. The eluted proteins were then analyzed using western blot analysis. A no click reaction sample (No Clk) that did not include biotin azide was used as a negative control. 0.1% input samples were included for positive controls of each protein analyzed. PCNA served as a positive control for a replication fork bound protein and H2B served as a loading control and positive control for a chromatin bound protein.

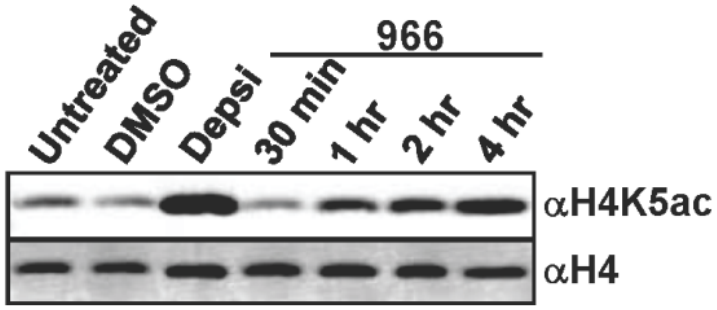

Figure 17. HDAC3-regulated histone acetylation is very dynamic but no global effects on histone acetylation seen within 30 min of 966 treatment. Western blot analysis of Hut78 cells treated with DMSO or 10 nM Depsipeptide (Depsi) for 4 hrs, or 10 μM 966 for 30 min, 1 hr, 2 hr, and 4 hr.

HDAC3-regulated histone acetylation is very dynamic with changes in histone acetylation detectable by western blot occurring within hours of treatment, but within 30 min of Hdac3 inhibition by 966 there were not global effects on histone acetylation.

Next, DNA fiber labeling analysis was used to visualize individual DNA fibers by sequential labeling of cells with IdU and CldU followed by immunofluorescence to detect the incorporation of these analogs [130] in strands of DNA to measure replication fork velocity. Treatment with Depsi or 966 for 4 hrs prior to labeling with IdU followed by CldU resulted in a shortening of the average length of fiber tracks (examples of fibers are shown on the right), which corresponds to slower replication fork progression than the DMSO control (Figure 18). To ensure that changes in chromatin structure did not affect fiber track length after replication fork progression, which would interfere with accurate measurement of DNA fibers, Hut78 cells were labeled with IdU followed by CldU, washed and then were either immediately treated with DMSO or HDIs for 25 min or incubated in fresh medium for 4hr and then treated with DMSO or HDIs for 25 min. Neither of these experiments showed significant changes in fiber track length or fork velocity (Figure 19), confirming that the effects on replication seen with inhibition of HDAC3 are not due to shortening of fiber track lengths due to global changes in chromatin structure.

Finally, to determine if this replication defect was due to a localized effect, we treated Hut78 cells for 5 min with either Depsi or 966 before labeling with IdU followed by CldU. Remarkably, even treatment within this short timeframe

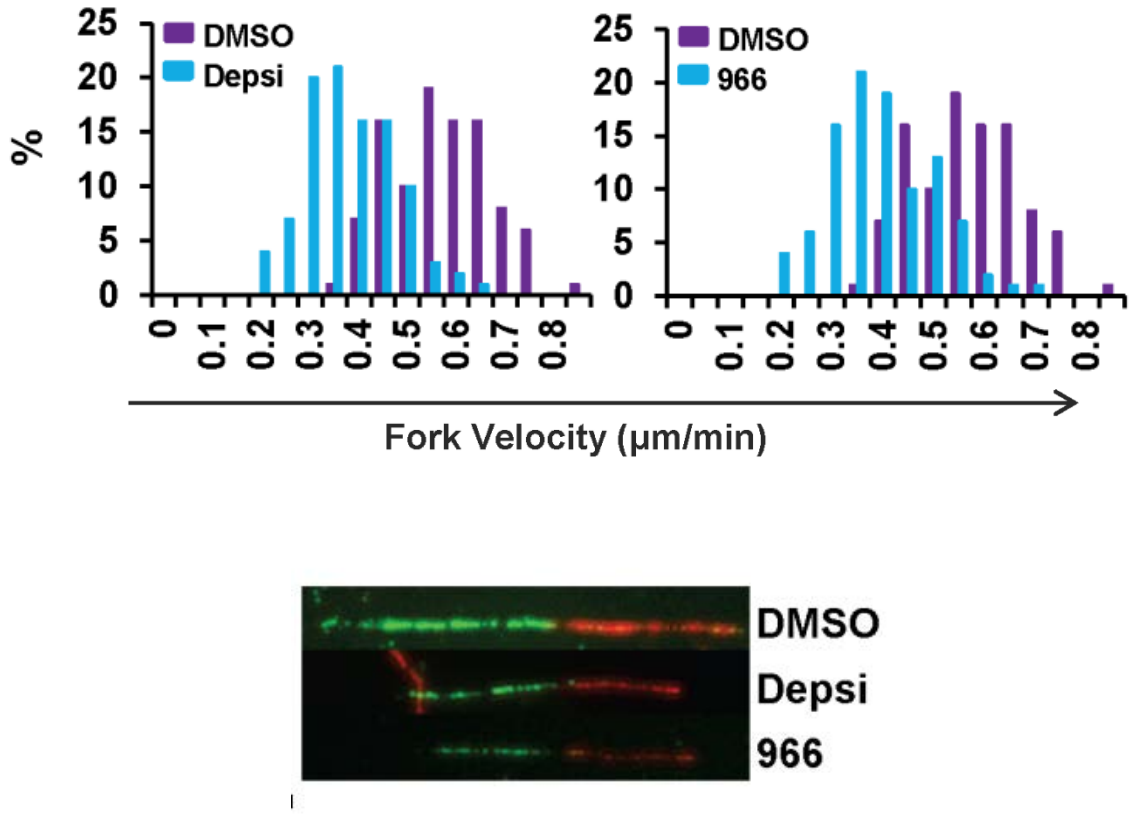

Figure 18. HDAC3 selective inhibitor causes defects in DNA replication with treatment 4hr prior to labeling with IdU and CldU. DNA fiber labeling analysis was used to assess DNA replication fork progression in Hut78 cells treated with DMSO, 10 nM Depsipeptide (left) or 10 µM 966 (right) for 4 hr prior to labeling with 20 mins of IdU (green) followed by 20 min of CldU (red). Graphical representation of fork velocity as determined by total length of fibers (IdU plus CldU) divided by 40 min pulse is shown. Representative fibers are shown. 100 fibers were measured for each sample. Statistical analysis was performed using Mann-Whitney test and standard deviations were calculated. HDI treated cells were compared to DMSO treated cells resulting in the following p-values: Depsi: $p<0.0001$; 966: $p<0.0001$. The average velocities for Depsi and 966 were greater than 3 standard deviations of the DMSO average velocity.

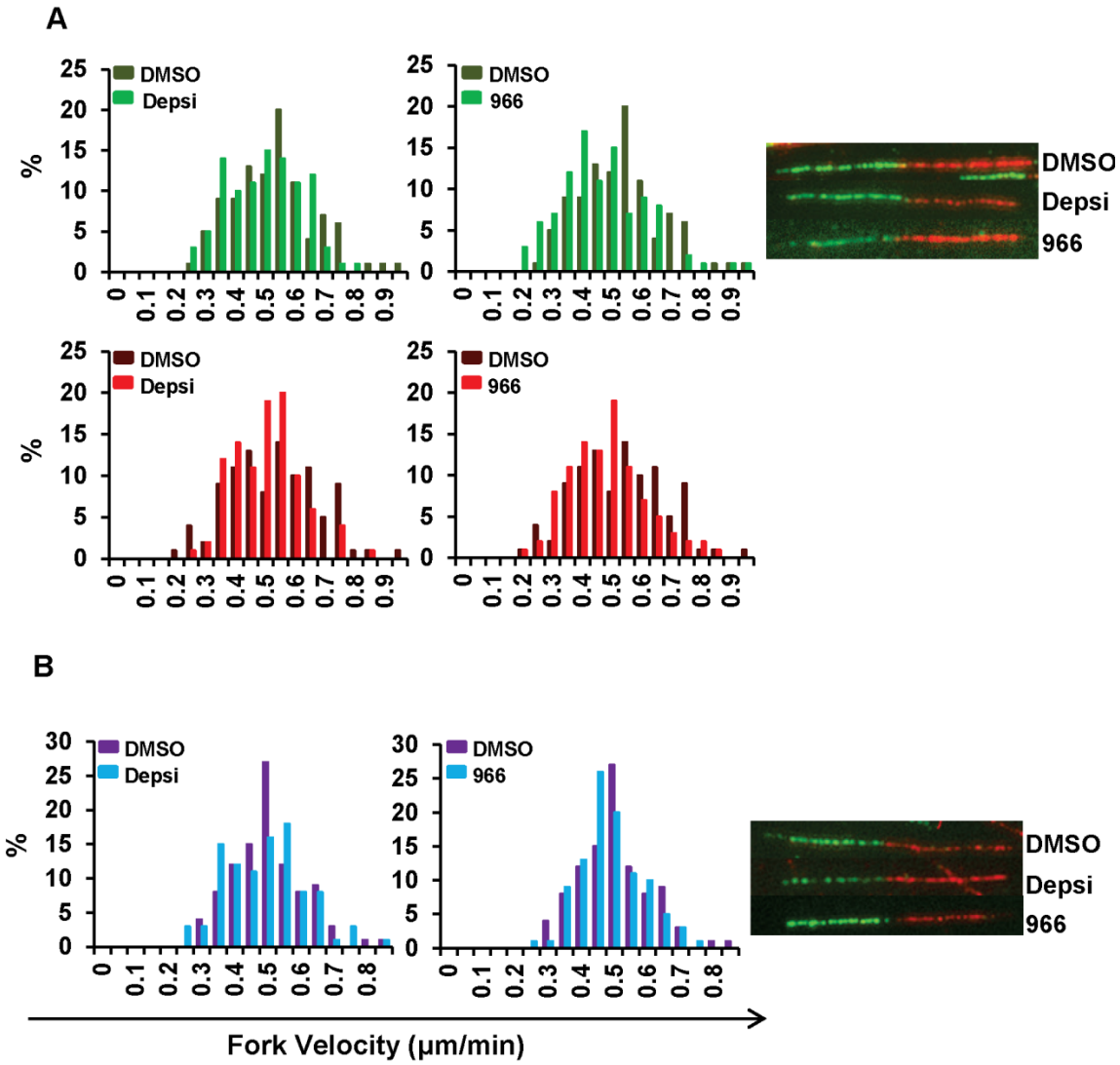

Figure 19. HDAC3 selective inhibitor does not affect replication after replication fork progression. DNA fiber labeling analysis of Hut78 cells treated with DMSO, 10 nM Depsipeptide (left) or 10 µM 966 (right) (A) immediately after or (B) 4 hrs after labeling cells with IdU followed by CldU. Graphical representation of fork velocity for either the IdU label or CldU label is shown. Fork velocity was determined by the length of either the IdU label or CldU label divided by 20 min pulse for (A) or the total length of fibers divided by 40 min pulse for (B). Representative fibers are shown. 100 fibers were measured for each sample. Statistical analysis was performed using Mann-Whitney test and standard deviations (SD) were calculated. P-values: (A) Depsi IdU (green): p=0.1, Depsi CldU (red): p=0.1; 966 IdU (green): p=0.0011; 966 CldU (red): p=0.01. Average velocities for IdU and CldU in Depsi treated cells were within 1 and 2 SD respectively of the DMSO average velocity. Average velocities for IdU and CldU in 966 treated cells were within 2 SD of the DMSO average velocity. (B) Depsi: p=0.5 and 966: p=0.4. The average velocities for both Depsi and 966 were within 1 SD of the average velocity for DMSO.

caused a shortening of DNA fiber track lengths and slower fork velocity (Figure 20). These data suggest that treatment with a HDAC3 selective inhibitor has localized effects on replication at or nearby the replication fork since global changes in H4K5ac were not seen within 30 min of treatment with 966 (Figure 17).

Discussion

Cutaneous T cell lymphoma (CTCL) diagnosed during early stage disease generally has an indolent course and good outcome [75-78, 131]. However, late stage, refractory, or aggressive CTCL (such as Sézary Syndrome) has a shortened survival expectancy [75-78, 131]. Two histone deacetylase inhibitors, SAHA and Depsipeptide, have been FDA approved for the treatment of late stage or refractory CTCL [75, 77, 93, 94, 136]. However, since these HDIs target multiple HDACs, it is unknown which of these HDACs must truly be inhibited to achieve the anti-tumor effects observed upon HDI treatment. Furthermore, it is likely that the unnecessary inhibition of other HDACs contributes to the side effects seen with HDI treatment (such as nausea, fatigue, and GI, cardiac and hematologic toxicities). By using selective HDIs, the efficacy of individual HDAC targeting can be assessed and side effects may be lessened, resulting in improved quality of life for patients undergoing treatment. Here, we show that the inhibition of HDAC1/2 or HDAC3 through the use of novel, selective inhibitors, caused decreased cell growth of the CTCL cell lines, HH and Hut78 by

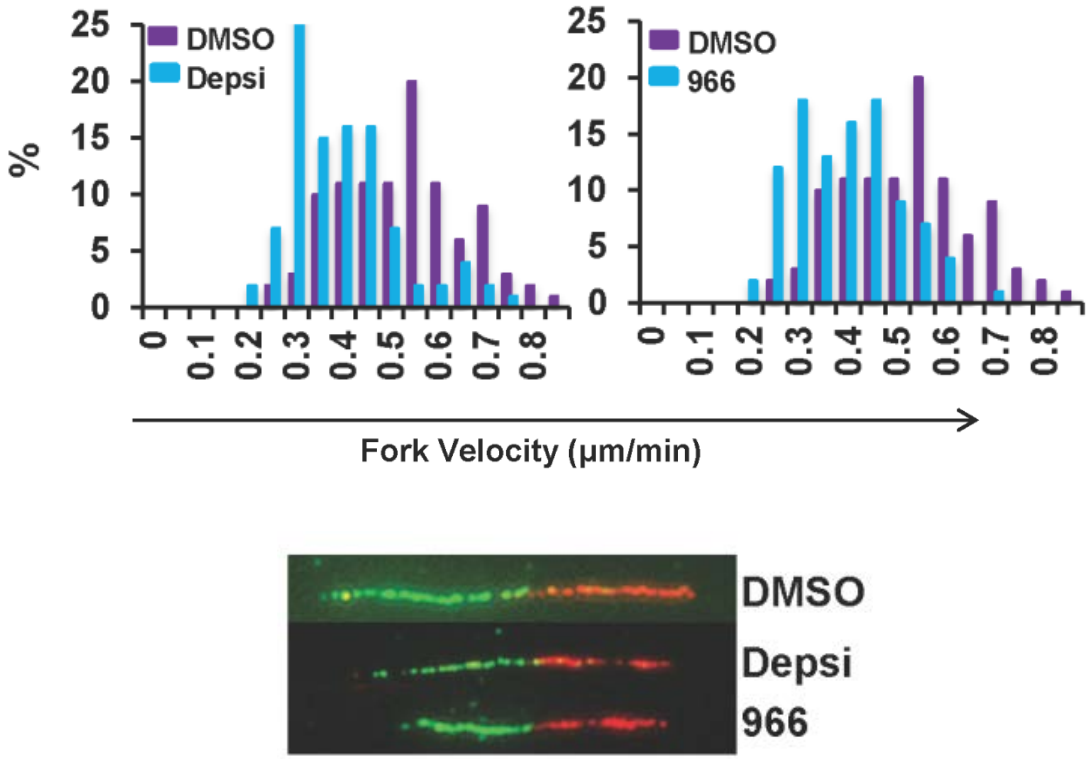

Figure 20. HDAC3 selective inhibitor rapidly causes defects in DNA replication. DNA fiber labeling analysis of Hut78 cells treated with DMSO, 10 nM Depsipeptide (left) or 10 µM 966 (right) for 5 mins prior to labeling with 20 mins of IdU (green) followed by 20 min of CldU (red). Graphical representation of fork velocity as determined by total length of fibers (IdU plus CldU) divided by 40 min pulse is shown. Representative fibers are shown. 100 fibers were measured for each sample. Statistical analysis was performed using Mann-Whitney test and standard deviations were calculated. P-values: Depsi: $p<0.0001$; 966: $p<0.0001$. The average velocities for Depsi and 966 were greater than 3 standard deviations of the DMSO average velocity.

triggering apoptosis (Figure 8). While it appears that inhibition of all three of these HDACs was more efficacious (e.g., Depsipeptide worked very well), more potent selective inhibitors may yield better results, or the lower toxicity may allow more intensive or longer-term treatments. Ultimately, having HDAC1/2 versus HDAC3 selective inhibitors will provide flexibility in defining the best schedules and combinations of these compounds to maximize the therapeutic benefit in the treatment of CTCL.

Mechanistically, the apoptosis observed was associated with the accumulation of DNA damage in HDI treated cells (Figure 12). BrdU-labeling studies showed decreased BrdU incorporation with pan HDAC inhibitors, inhibitors of HDAC1/2 and the HDAC3 selective inhibitors (Figure 13). These studies also revealed a significant increase in cells that did not incorporate BrdU, but showed increased DNA content, consistent with an S-phase arrest following HDI treatment, suggesting that the DNA damage was due to defects in DNA replication. This prompted an analysis of DNA replication fork velocity using DNA fiber labeling assays, which showed that Depsipeptide treatment and treatment with the Hdac3 selective inhibitor resulted in inefficient or slowed DNA replication (Figure 18-20). By examining DNA replication shortly after adding the HDIs, we were able to show that this is a very early event, occurring within the first hour of HDI treatment. These data suggest that HDI therapy first affects DNA replication (Figure 20), which would provide a therapeutic window by targeting the cycling cancer cells, and leaving normal, non-cycling cells intact.

The rapid effects of 966 on DNA replication suggest an important role for HDAC3 in DNA replication. In addition, by inhibiting HDAC3 at various times before DNA fiber labeling, we were able to narrow the possible mechanisms by which this might occur to localized effects at or around the DNA replication fork, as it took greater than 30 min before global changes in histone acetylation were observed (Figure 17). However, these studies cannot discriminate whether this is due to a local chromatin effect or whether HDAC3 directly targets the DNA replication machinery. For instance, chromatin in and around the DNA replication fork must be in an open configuration, which is more accessible to HDAC3 than nucleosomes in mature chromatin. Because the histones in newly placed nucleosomes are acetylated prior to deposition, inhibition of HDAC3 could cause the accumulation of acetylation of these histones within minutes of HDI treatment, whereas global accumulation of H4K5ac takes an hour or more (Figure 17). Alternatively, components of the DNA replication machinery may be regulated by acetylation and deacetylation and HDAC3 could play a regulatory role. One argument against this is that HDAC3 did not co-elute with PCNA in size exclusion chromatography (Figure 15) or move with the DNA replication fork in iPOND purifications (Figure 16). Thus, at this point in time, the evidence best supports a localized effect on chromatin at the replication fork.

Although endogenous HDAC3 can associate with histone chaperones such as RbAp48 (Figure 15), its role in deacetylation of newly formed nucleosomes is largely based on genetic, siRNA and chemical inhibition studies ([46, 47] and Figure 7). These studies indicate that HDAC3 targets the same

histone deposition marks that HDAC1/2 deacetylate and that HDAC3 is required at replication forks (Figure 16-20). Historically, HDAC1/2 were biochemically linked to histone deposition [47, 125]. These enzymes form nearly stoichiometric complexes with the histone deposition machinery and are thought to be the major enzymes responsible for the deacetylation of new nucleosomes. Moreover, siRNA or genetic impairment of HDAC1 is compensated by higher expression of HDAC2 (e.g., Figure 7C), whereas deletion of *Hdac3* is not compensated for by higher expression of other class 1 Hdacs. Thus, we conclude that HDAC3 plays a distinct role from HDAC1 and HDAC2 during chromatin maturation (Figure 16) and that targeting HDAC3 with small molecule inhibitors will provide additional therapeutic impact in the treatment of CTCL and other cancers.

Currently, SAHA and Depsipeptide are approved as single agents to treat refractory CTCL [75, 77, 93, 94, 136]. However, combinatorial treatment is almost always more beneficial than single agent therapy, so we tested HDAC3 inhibitors with other drugs currently used for CTCL. The combination of 966 and either bexarotene, methotrexate, or ATRA led to further reductions in cell growth than either agent alone in Hut78 cells (Figure 11), but these effects were additive, not synergistic. Nevertheless, these combinations did not negate the responses of these drugs, suggesting that these compounds could be used together in the clinic. Our studies show that individual HDACs can be targeted and that these inhibitors may be useful in the treatment of CTCL by rapidly targeting DNA replication. While the first effects of these compounds may be at replication forks (which provides a therapeutic window), within only 4 hr these

drugs also affected global histone acetylation, which indicates that HDAC3 plays a dynamic role in the regulation of histone acetylation and chromatin structure. Thus, these compounds may target multiple fundamental events in the cell cycle to trigger apoptosis in cycling tumor cells that would be beneficial in combination with current therapies for CTCL.

CHAPTER IV

SELECTIVE INHIBITION OF HISTONE DEACETYLASES 1 AND 2 OR HISTONE DEACETYLASES 1-3 CAUSES DEFECTS IN REPLICATION AND CELL DEATH

Background and Significance

For normal development, a cell must efficiently replicate its DNA in each cell cycle. This involves the disruption and reassembly of chromatin during each round of DNA replication. One important step of reassembly is the deacetylation of histones to allow for tight compaction of chromatin and reestablishment of proper chromatin structure [2, 3, 5, 123]. Inhibition of this deacetylation in yeast and mammalian cells has led to severe defects in chromatin stability and disruption of the cell cycle [3, 144]. However, it is unclear which individual HDACs are involved in DNA replication and chromatin condensation. HDACs play important roles in the modulation of chromatin accessibility during vital cell processes such as transcription, DNA replication and repair. However, the individual roles of each of the HDACs in these processes remain unclear. Selective inhibitors allow for elucidation of the roles of one or two HDACs at a time and could potentially lead to customized treatments by targeting only the necessary HDACs during treatment instead of treating with broad inhibitors that target multiple HDACs. This customized treatment would potentially reduce unnecessary side effects and provide for multiple avenues to avoid the

development of drug resistance. In Chapter III, inhibition of HDAC3 resulted in decreased cell growth associated with apoptosis, cell cycle arrest, and DNA replication defects. DNA replication fork velocity was significantly slowed when HDAC3 was inhibited in CTCL cells, even following short treatment times, suggesting that HDAC3 is essential for proper DNA replication. However, the role of HDACs 1 and 2 in replication remains to be answered. HDACs 1 and 2 are known to associate with certain replication or chromatin condensation factors [25, 33, 126, 127, 145], but it is unclear what happens to DNA replication when these HDACs are inhibited by HDIs. HDACs 1 and 2 are enriched at replication forks [124] through association with histone chaperones like RbAp48 and CAF1 [25, 33, 126, 127]. HDAC 1 also associates with PCNA (proliferating cell nuclear antigen), a loading platform for multiple proteins during DNA replication and repair, and through this association with PCNA, HDAC1 may play a role in the deacetylation required to compact chromatin after DNA replication [145]. Treatment with TSA (trichostatin A) inhibited the deacetylase activity of PCNA/HDAC1 [145]. However, TSA inhibits multiple class I HDACs and does not exclude the possibility that other class I HDACs also bind PCNA and play a role in this deacetylation.

Here, two other inhibitors are tested for their function during DNA replication. The inhibitor RGFP233, an inhibitor of HDACs 1 and 2, was introduced in Chapter III and also showed decreased cell growth associated with apoptosis and cell cycle arrest. However, at that time its effect in DNA replication was not assessed. The inhibitor RGFP963 is expected to inhibit HDACs 1, 2,

and 3 and is introduced here. In this chapter, RGFP963 will be tested in several assays to determine its effects on cell growth and during DNA replication.

Results

Selective inhibition of HDACs caused increases in acetylation

HDACs 1, 2, and 3 share a high degree of homology in their conserved deacetylase domains with HDACs 1 and 3 being 58% identical. This can pose challenges in designing selective inhibitors, however, progress has been made as demonstrated in Chapter III and [96, 97, 110, 111]. To begin examination of the new inhibitor RGFP963 (also known here as 963), the selectivity of this inhibitor needed to be confirmed. Changes in specific histone modifications can be used to determine the selectivity of HDIs (as established in Chapter III). Deletion or inhibition of HDAC3 caused increases in acetylation of residues such as H4K5, H4K16, H4K12, H3K27 and modest increases in H3K9K14 ([47] and Figure 7). HDACs 1 and 2 deacetylate these residues but in addition, deacetylate H3K56. This allows the use of antibodies against H3K56 to be used to distinguish an HDAC1 and 2 selective inhibitor from an HDAC3 selective inhibitor. To determine the selectivity of 963, HH and Hut78 CTCL cells were treated with DMSO, 10 nM Depsipeptide, 10 μM 963, 10 μM 233, or 10 μM 966 for 24 hrs. Depsipeptide, 233 and 966 were all included to serve as positive controls and full analysis of 233 and 966 can be seen in Chapter III. Western blot analysis was performed to examine changes in histone acetylation with

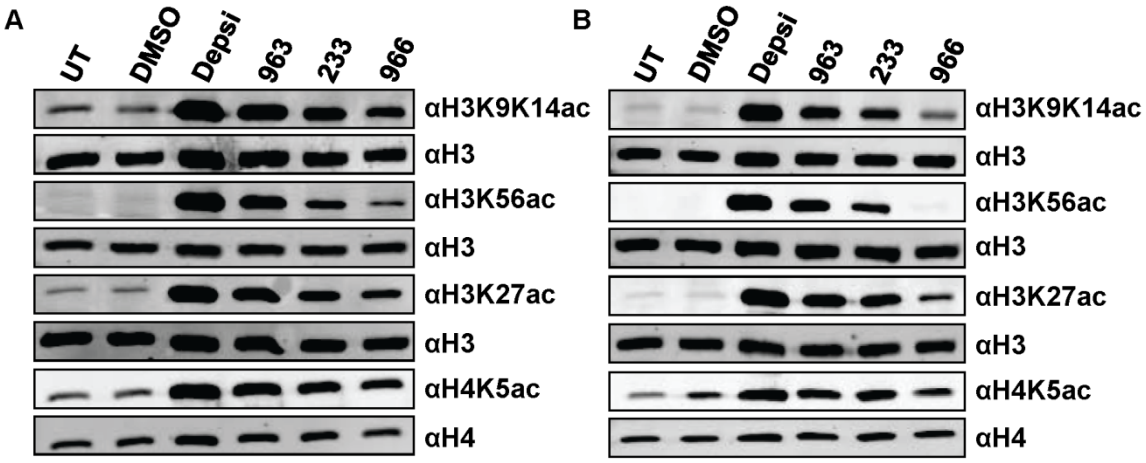

Figure 21. 963 shows selective inhibition of HDACs 1-3 in CTCL cell lines. (A & B) Western blot analysis of (A) HH or (B) Hut78 cell lines treated with DMSO, 10 nM Depsipeptide (Depsi), 10 µM 963, 10 µM 233, or 10 µM 966. Cells were treated for 24 hrs and then harvested for protein isolation. Histones H3 and H4 were used as loading controls.

treatment of the above listed HDIs (Figure 21). Treatment with 963 caused robust accumulations in acetylation of each histone mark tested including the HDAC1/2 specific histone mark, H3K56ac. Also, if the levels of H4K5ac are compared between 963 treated or 233 or 966 treated samples, there appears to be an additive amount of H4K5ac in the 963 treated samples, suggesting that 963 inhibits all 3 HDACs. However, the levels of H4K5ac were not quite as robust in 963 samples as in Depsipeptide. Correspondence with Repligen Corporation revealed that indeed 963 inhibits HDACs 1, 2, and 3 in *in vitro* substrate assays with comparable IC_{50} values, confirming that 963 inhibits HDACs 1, 2, and 3 with similar potencies.

HDI 963 caused dramatic decreased cell growth in CTCL cells

Next, the effect of 963 treatment on cell growth was determined. Due to the sensitivity seen in the clinic of CTCL to HDIs, HH and Hut78 cells were again used in these experiments. Cell proliferation assays using alamar blue to measure cell growth and viability in the presence of 963 were performed. HH and Hut78 cells were treated at hour 0 with either DMSO, 10 nM Depsipeptide, or varying concentrations of 963 and then analyzed at hours 0, 24, 48, and 72 for changes in cell proliferation as measured by changes in alamar blue-dependent fluorescence. Both cell lines were extremely sensitive to all concentrations of 963 as demonstrated by a dramatic decrease in cell growth over a 72 hour time period (Figure 22). Both cell lines were sensitive to Depsipeptide, while unaffected by the DMSO control. 2 µM 963 in comparison to treatment with 10

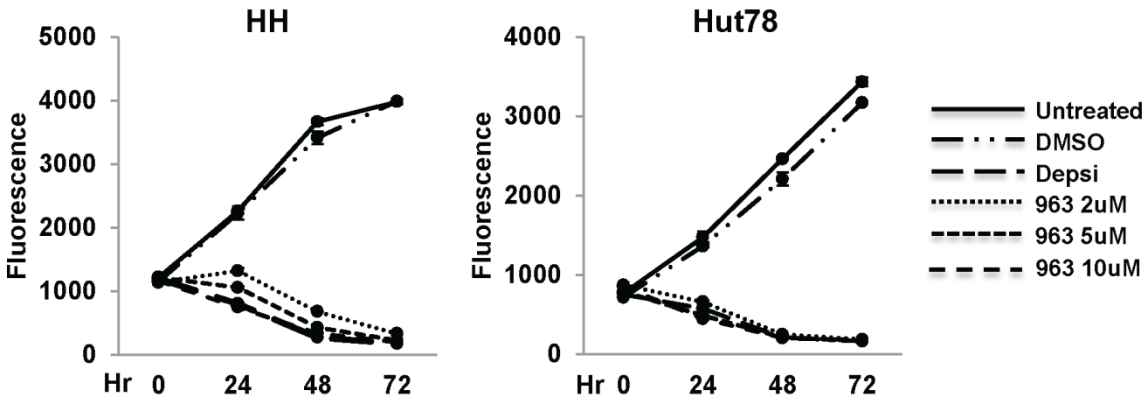

Figure 22. CTCL cell lines are sensitive to 963 treatment. Growth curves of HDI treated HH cells (left) or Hut78 cells (right). Cells were treated once with DMSO, 10 nM Depsipeptide (Depsi), 2 μM 963, 5 μM 963, or 10 μM 963 at hour 0. Untreated cells and DMSO treated cells were used as controls. Cell growth was assessed at 0, 24, 48, and 72 hours after treatment. Representative curves are shown from experiments performed in triplicate that are consistent with other biological replicates.

μM 233 or 966 (Figure 8 Chapter 3), was more potent, supporting that 963 inhibits HDACs 1, 2, and 3 versus either HDAC1/2 or HDAC3 alone.

Treatment with 963 caused increased apoptosis levels and cell cycle defects in CTCL cell lines

Next, to determine whether the decreased cell growth seen when HH and Hut78 cells were treated with selective and pan HDIs (Figure 22) was due to increased apoptosis, flow cytometry analysis using Annexin V versus propidium iodide (PI) was performed. HH and Hut78 cells were treated for 24 hrs with DMSO, 10 nM Depsipeptide, 10 μM 233, 10μM 966, or 10μM 963. HH and Hut78 cells both displayed increases in Annexin V levels following treatment with each HDI but not with DMSO (Figure 23). Hut78 cells displayed the greatest increase in Annexin V levels. These data confirm that CTCL cells underwent apoptosis when treated with these HDIs. Accordingly, there was a correlation between apoptosis levels and the number of HDACs inhibited. Depsipeptide had the highest apoptosis levels followed by 963, 233, and then 966 correlating very well with the inhibition of different numbers of HDACs at a time (Depsi inhibits the greatest number of HDACs and 966 inhibits a single HDAC).

In Chapter III, inhibition of HDAC3 caused cell cycle defects. To examine whether 963 causes these same defects, flow cytometry analysis of BrdU levels and cell cycle was performed. HH and Hut78 cells were treated with DMSO, 10 nM Depsipeptide, 10 μM 963, 10 μM 233, or 10 μM 966 for 24 hours and then pulsed with BrdU for 90 mins before harvest. Depsipeptide, 233, and 966 were

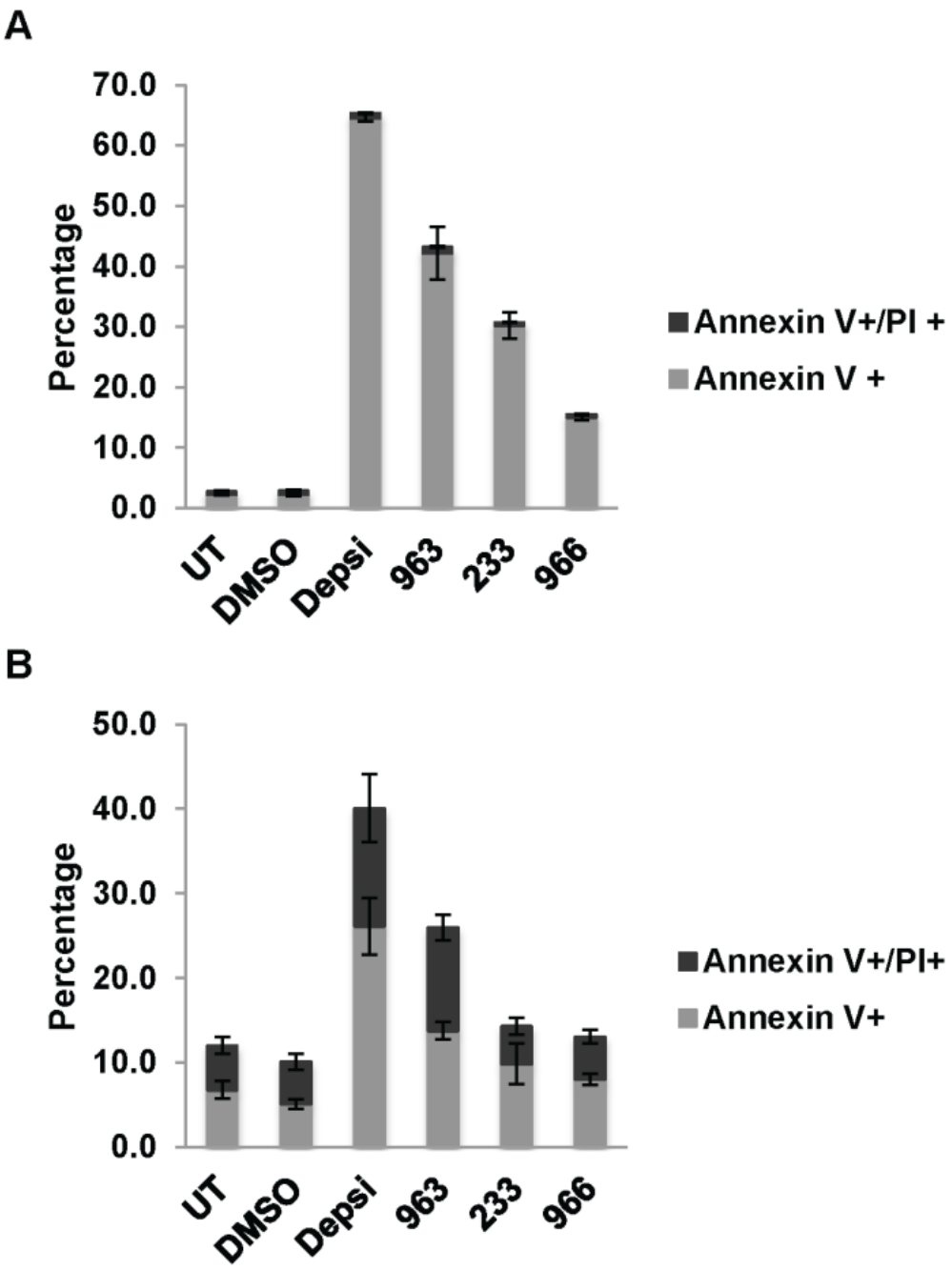

Figure 23. Selective inhibition of HDACs 1-3 triggers increased apoptosis in CTCL cells. (A) Hut78 and (B) HH cells were treated with DMSO, 10 nM Depsipeptide, 10 μM 963, 10 μM 233, or 10 μM 966 for 24 hr and apoptosis assessed by Annexin V staining and flow cytometry. Cells were also labeled with propidium iodide to assess DNA content. Untreated (UT) and DMSO treated cells were used as controls. Shown is a representative graph from an experiment performed in duplicate that is consistent with other biological replicates.

used as positive controls and comparisons for BrdU levels with inhibitors that target different numbers of HDACs while DMSO served as the negative control. Hut78 and HH cells both exhibited decreased BrdU incorporation upon treatment with 963 and also an increase in cells that were present in S phase but not actively incorporating BrdU (Figures 24 and 25). These S phase cells represent cells that are arrested in S phase, indicative of incomplete DNA replication. Again, a trend correlating to the number of HDACs inhibited was observed when comparing each inhibitor treatment.

Hut78 cells exhibited DNA damage and DNA replication defects with an HDAC1/2 selective inhibitor and an HDAC 1, 2, and 3 inhibitor

Deletion or inhibition of HDAC3 caused increased DNA damage in fibroblasts and CTCL cells (Figure 12 Chapter III and [46, 47]). To determine if 963 treatment caused a similar accumulation of DNA damage, Hut78 cells were treated with DMSO, 10 nM Depsipeptide, or 10 µM 963 for 8 hours and then western blot analysis using anti-ɣH2aX was performed. ɣH2aX is localized to sites of DNA double strand breaks and allows for the level of DNA damage to be assessed [142, 146]. Treatment with 963 caused increased ɣH2aX levels approximately 4.7 fold more than untreated or DMSO treated cells. This is indicative of an increase in DNA damage when all 3 HDACs are inhibited. This correlates nicely with the levels of DNA damage seen in Chapter III (Figure 12) which showed that both 233 and 966 treatment led to an approximate 2.4 fold increase in ɣH2aX

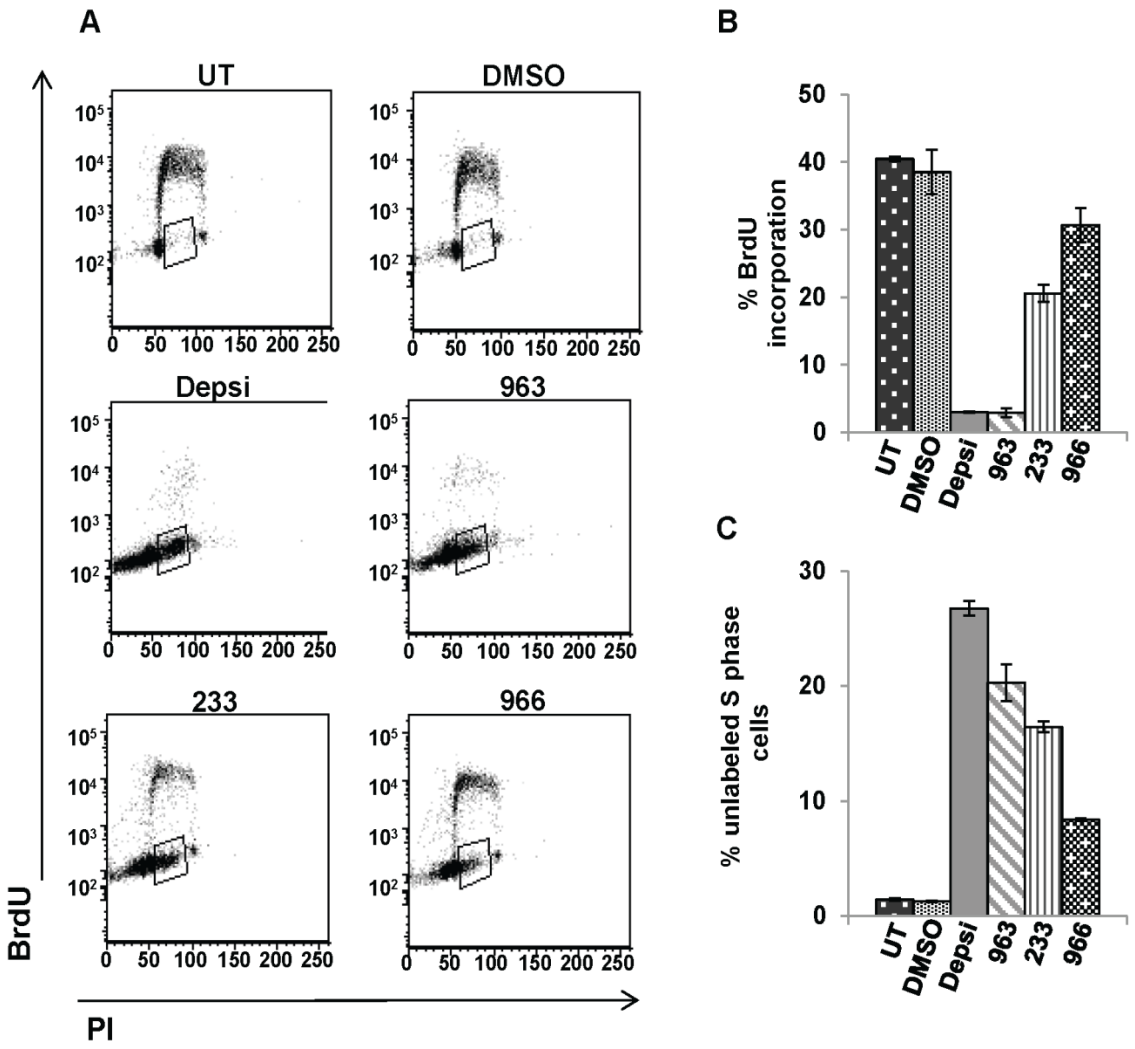

Figure 24. An HDACs 1-3 selective inhibitor triggers increased cell cycle defects in Hut78 cells. (A) Cell cycle status was analyzed using BrdU incorporation and propidium iodide to assess DNA content by flow cytometry. Hut78 cells were treated with DMSO, 10 nM Depsipeptide, 10 μM 963, 10 μM 233, or 10 μM 966 for 24 hr and pulsed for an hour and a half with BrdU prior to cell harvest and analysis. Shown are representative flow cytometry plots performed in duplicate that is consistent with other biological replicates. (B) Graphical representation of BrdU incorporation from the experiment described in (A). (C) Graphical representation of the percent of S phase cells that did not incorporate BrdU (shown by box in (A)).

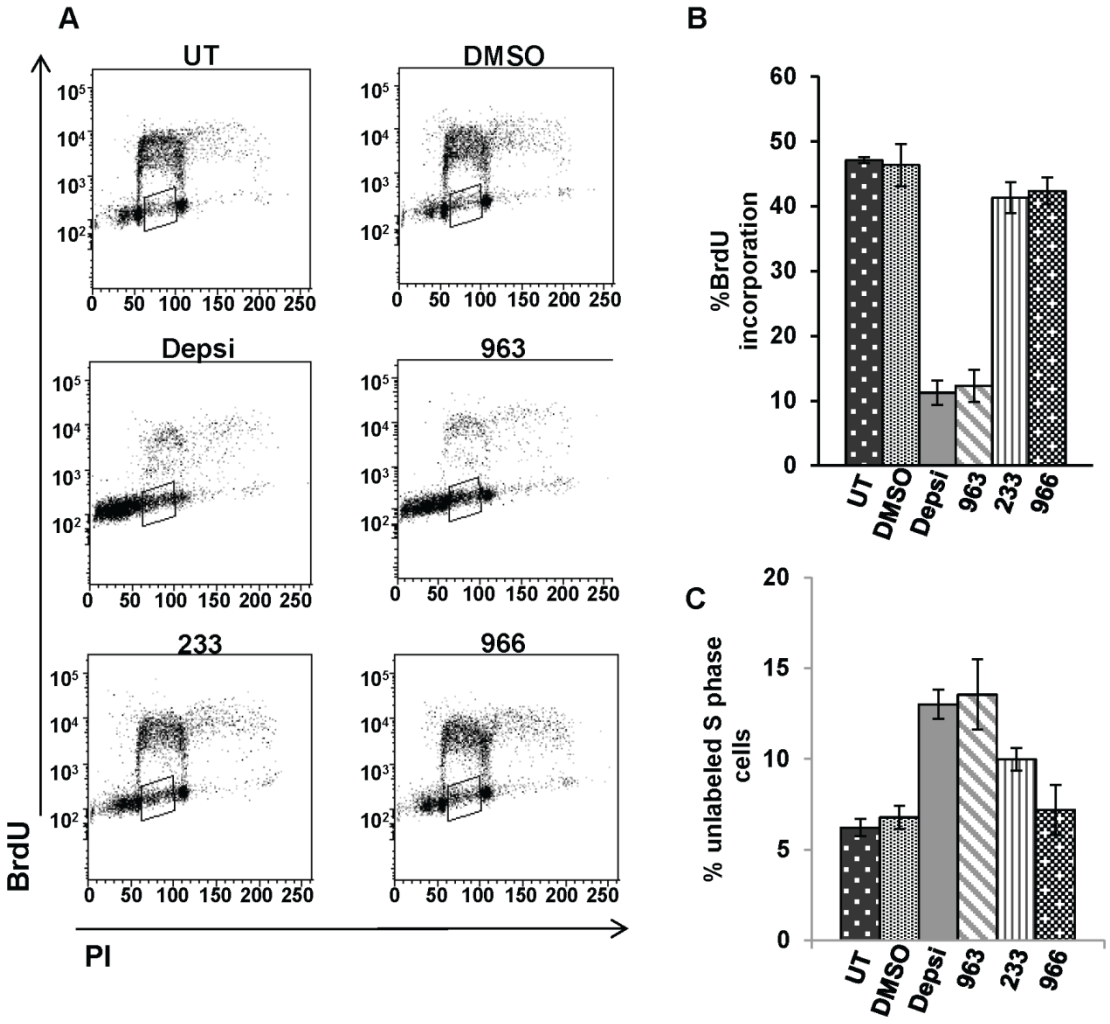

Figure 25. HH cells have increased cell cycle defects when treated with an HDACs 1-3 selective inhibitor. (A) Cell cycle status was analyzed using BrdU incorporation and propidium iodide to assess DNA content by flow cytometry. HH cells were treated with DMSO, 10 nM Depsipeptide, 10 µM 963, 10 µM 233, or 10 µM 966 for 24 hr and pulsed for an hour and a half with BrdU prior to cell harvest and analysis. Shown are representative flow cytometry plots performed in duplicate that is consistent with other biological replicates. (B) Graphical representation of BrdU incorporation from the experiment described in (A). (C) Graphical representation of the percent of S phase cells that did not incorporate BrdU (shown by box in (A)).

levels while Depsipeptide led to an 8.5 fold increase. Again this exhibits the stepwise trend of inhibiting different numbers of HDACs.

The observed DNA damage and S-phase arrest suggest that treatment with 963 disrupts replication. HDACs 1, 2, and 3 are present at and near replication forks and deletion or inhibition of HDAC3 causes decreased replication fork velocity indicative of DNA replication defects (Figure 18-20 Chapter III and [48, 124, 128]). Due to the fact that selective HDAC3 inhibition caused DNA replication defects, this raises the question of whether or not HDAC 1/2 inhibition would cause similar DNA replication defects. It would be expected that inhibition of HDAC 1/2 would cause DNA replication defects due to their presence at replication forks, the fact that HDACs 1 and 2 regulate deacetylation of histones deposited on newly synthesized DNA after replication, and given their association with histone chaperones (RbAp48 and CAF1) and replication fork factors (PCNA).

The use of these HDIs allow for the analysis of HDAC function in short time frames that cannot be replicated by genetic deletions in mice or siRNA. DNA fiber labeling assays were performed to determine the effects of these inhibitors on DNA replication fork velocity and replication. Replication fork velocity can be measure by DNA fiber labeling, which allows for the visualization of individual DNA fibers by sequential labeling of cells with IdU and CldU followed by immunofluorescence to detect incorporation of these thymidine analogs into DNA. Hut78 cells were treated with DMSO, 10 nM Depsipeptide, 10 μM 233, or 10 μM 966 for 1 hour before labeling with IdU followed by CldU. DMSO was

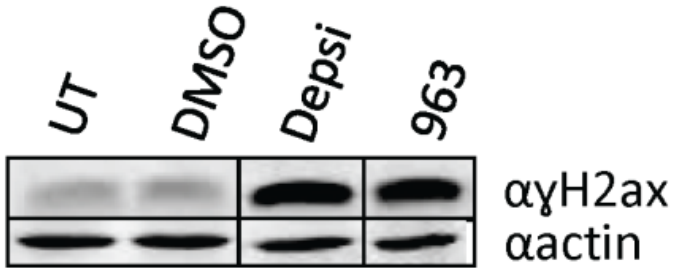

Figure 26. 963 treatment causes increased DNA damage in Hut78 cells. Western blot analysis of ɣH2aX levels in Hut78 cells treated with DMSO, 10 nM Depsi, or 10 μM 963 for 8 hrs. Untreated and DMSO treated cells were used as controls. Samples were run on the same gel and probed on the same membrane. Intervening lanes (represented by a black bar) were removed for side by side comparison of DMSO, Depsipeptide, and 963.

used as a negative control and all HDI treatments were compared to DMSO. Depsipeptide and 966 were included for direct comparison at 1 hr before labeling. Treatment with all HDIs resulted in shortening of the average length of fiber tracks, which corresponds to slower replication fork progression than DMSO (Figure 27). This suggests that HDACs 1 and 2 play a role at or near the replication fork.

Next, to determine whether combined inhibition of HDACs 1, 2, and 3 using 963 would cause additive DNA replication defects, we treated Hut78 cells for 1 hr with 963 before labeling with IdU (as described above). 963 treatment also caused decreases in fiber track length but did not show an additive effect (Figure 27). Possibly the fiber labeling assay is just not sensitive enough to detect an additive effect. Another possibility for not seeing an additive effect could be due to differences in IC_{50} values for the different inhibitors such that these selective inhibitors may be suppressing the activity of specific HDACs to varying degrees. However, this data with 233 and 963 provide evidence that these inhibitors (and 966 from this experiment and Chapter III) act by inhibiting proper DNA replication and suggest that selective inhibitors could be developed for treatment regimens.

Discussion

Proper DNA replication and chromatin condensation are required for normal cell proliferation. Furthermore, replication stress has been associated with the accumulation of DNA damage and reduced cell viability. HDACs are

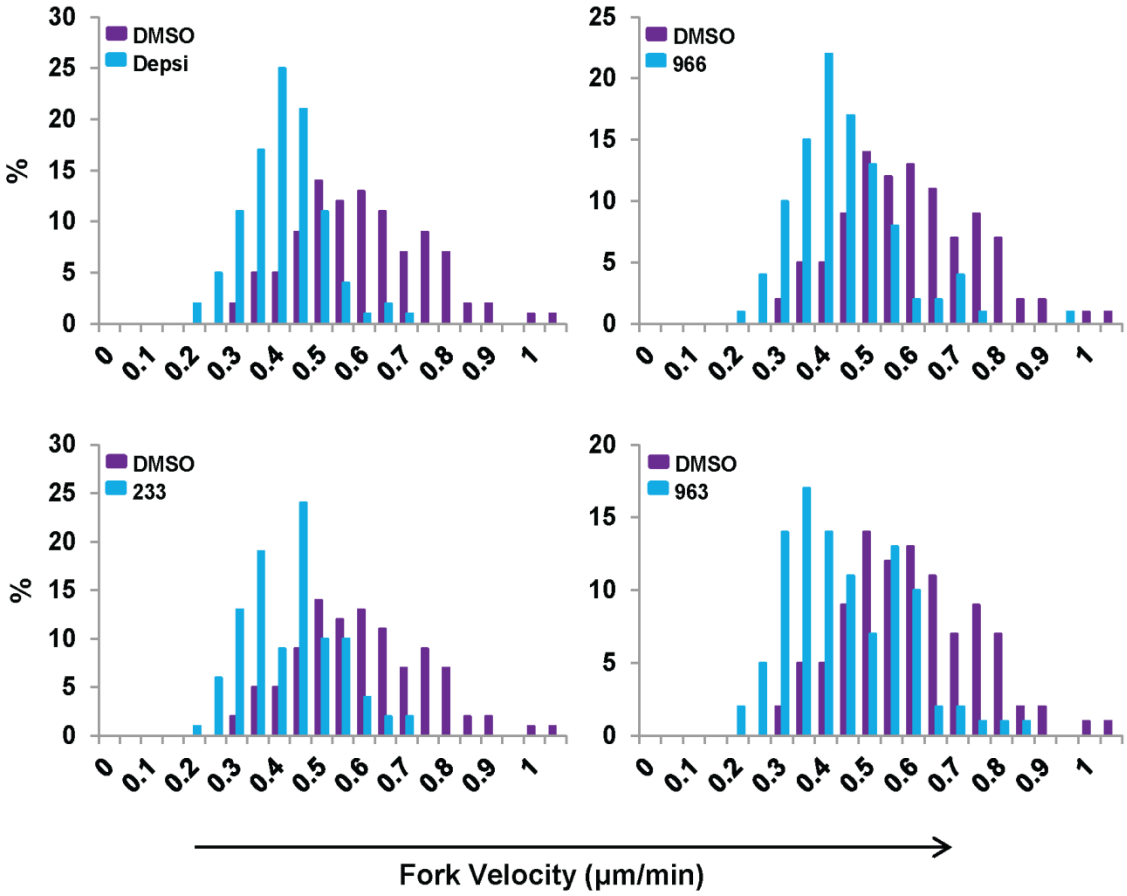

Figure 27. HDACs 1/2 and HDACs 1-3 inhibitors cause defects in DNA replication. DNA fiber labeling analysis was used to assess DNA replication fork progression in Hut78 cells treated with DMSO, 10 nM Depsipeptide (top left), 10 µM 966 (top right), 10 µM 233 (bottom left), or 10 µM 963 (bottom right) for 1 hr prior to labeling with 20 mins of IdU (green) followed by 20 min of CldU (red). Graphical representation of fork velocity as determined by total length of fibers (IdU plus CldU) divided by 40 min pulse is shown. 100 fibers were measured for each sample.

present at and near replication forks, associated with key histone chaperones and replication machinery components. Furthermore, deletion or inhibition of HDAC3 causes DNA replication defects [48, 128]. However, it is unclear whether short-term inhibition of other HDACs causes similar replication stress. The development of selective HDIs allows for the elucidation of the roles of individual HDACs in important cellular processes such as DNA replication and chromatin condensation. In this chapter, a new inhibitor, 963, was introduced that selectivity targets HDACs 1, 2, and 3. A second inhibitor, 233, was first introduced in Chapter III but is examined here along with 963 for their potential effects on DNA replication. 963 treatment in CTCL cells caused dramatic decreases in cell growth and viability by triggering apoptosis (Figure 22-23). Additionally, the number of HDACs inhibited correlated with increased death (e.g. Depsipeptide which targets 5 HDACs causing the most death and 966 which inhibits a single HDAC causing less). 963 showed comparable decreases in cell growth to that of Depsipeptide, albeit at higher concentrations used. This suggests the possibility, though, that an HDAC 1-3 selective inhibitor could be further developed for more comparable dosage levels and be used in treatment. This would allow for fewer HDACs to be targeted and possibly decrease toxicity associated with HDI treatment. Having multiple selective inhibitors allows for the customization of treatments such that different combinations of HDACs can be inhibited, possibly increasing the efficacy of treatment while decreasing toxicity.

Mechanistically, 963 treatment led to apoptosis that was associated with cell cycle defects (Figure 24-25) and increased DNA damage (Figure 26). Cell

cycle analysis showed decreased BrdU incorporation levels and a significant increase in the number of S phase cells that did not incorporate BrdU, suggesting an S phase arrest with 963 treatment. The cell cycle arrest plus DNA damage accumulation suggests DNA replication defects. DNA fiber labeling assays were performed to examine DNA replication fork velocity in 233 or 963 treated cells. Treatment with either of these inhibitors resulted in slowed DNA replication fork velocity indicative of DNA replication defects in HDI treated cells.

The results of the iPOND experiment and fiber labeling assays in Chapter III along with the fiber labeling assays in this chapter, suggest that HDACs 1/2 and HDAC3 play separate roles in DNA replication. HDAC3 inhibition led to DNA replication defects that could not be compensated by HDACs 1 and 2 while HDACs 1/2 inhibition could not be compensated by HDAC3. HDAC1 interacts with PCNA and appears to move with the replication fork while HDAC3 does not (Figure 16 iPOND). It is possible that HDAC1 or 1 and 2 associate with the fork and PCNA to deacetylate replication fork machinery, while HDAC3 plays a role in regulating localized chromatin at the replication fork. Further studies will need to be performed to try and determine whether these thoughts are true.

Surprisingly, while the inhibition of multiple HDACs by 963 appeared to have an additive effect on overall cell viability, this same additive effect was not observed with regards to replication fork velocity. As mentioned this may be due to differences in IC_{50} values for the different HDIs leading to different levels of inhibition of different HDACs. However, the DNA fiber labeling experiments executed in this chapter were performed with a short treatment of HDIs (1 hr)

while the apoptosis and cell cycle experiments were performed after 24 hr of HDI treatment. For example, it is possible that, the additive cell death seen with longer 963 treatment (24 hr) involves other mechanisms in addition to DNA replication that is killing the cells. DNA replication may be the first target of these HDIs (short treatments) that is then followed by compounding effects through other HDAC mediated mechanisms such as DNA repair defects or deregulated transcription (longer treatments).

HDACs 1, 2, and 3 have been linked to efficient DNA repair [47, 122]. For example, HDAC3 deletion in MEFs and hepatocytes led to impaired DNA repair with these cells not repairing the DNA damage and maintaining high levels of DNA damage caused by irradiation or DNA damaging agents [46, 47]. Over the course of a 24 hr treatment, possibly defects in DNA replication cause increased DNA damage and due to defects in DNA repair, these cells are unable to repair the damage and ultimately die. In cells that are treated with, for example, 233 (HDACs 1/2 are inhibited), HDAC3 may be able to compensate partially for the loss of HDACs 1/2 resulting in the repair of some of the damage associated with HDI treatment while if these cells were treated with 963, all three HDACs would be inhibited, DNA repair would be further disrupted, and an additive effect of cell death would be observed. This could explain why treatment with 963 in the cell death experiments would show an additive effect but short treatments as in the DNA fiber labeling experiments, which only measure the initial effects on DNA replication would not show an additive effect. Also, HDACs are traditionally transcriptional regulators thus in addition to DNA replication defects,

transcriptional effects (such as increases in the cell cycle inhibitor, p21) are likely to be seen after increased treatment time, again resulting in additive effects. Studies to determine the effects of these individual inhibitors on DNA repair and transcription would be helpful in answering the above theories.

Overall, this chapter provides more evidence that HDIs work through impairing proper DNA replication in cancer cells. It is reassuring that two classes of HDIs (Depsipeptide – cyclic peptides and 963, 233, and 966 – pimelic diphenylamides/ N-(o-amino-phenyl) carboxamides) behave very similarly with regards to their proposed mechanisms of action. This suggests an opportunity to target rapidly dividing cancer cells with HDIs while not harming the quiescent normal cells and provide new combinations of therapy in cancer treatment.

CHAPTER V

SUMMARY AND FUTURE DIRECTIONS

Histone deacetylases are required for normal development and function in crucial cell processes such as DNA replication, DNA repair, transcription, and even tumorigenesis. It is not surprising then that these proteins are being targeted as therapeutics for certain diseases. Currently, two HDIs are FDA approved for the treatment of refractory CTCL [75, 77, 93, 94, 136]. These inhibitors have shown great success in CTCL treatment but do have adverse effects such as nausea, fatigue, gastrointestinal and cardiac toxicity, and hematologic impairment [77, 93, 137] associated with them and, until this dissertation, the mechanism of action of these inhibitors was not known. Also, these HDIs inhibit multiple HDACs, possibly leading to unnecessary side effects. The development of selective HDIs would not only allow for the elucidation of the roles of individual HDACs in cell processes but also could potentially be used in the clinics to customize treatments and allow for combinatorial use with multiple HDIs or other cancer drugs. A class of selective inhibitors, the pimelic diphenylamides/ N-(o-amino-phenyl) carboxamides, that target individual members of the class I HDACs has been developed [96, 97, 110-112] and was the focus of this dissertation. Examination of these inhibitors using DNA fiber

labeling experiments (Figures 18-20,27) led to a better understanding of the mechanism of action of HDIs and their effects in cancer.

Changes in histone acetylation marks were analyzed using western blot analysis to determine the specificity of two selective inhibitors, 233 (HDAC 1/2 selective inhibitor) and 966 (HDAC3 selective inhibitor). Treatment with 966 caused accumulation of H4K5ac, H3K27ac, and modest increases in H3K9K14ac but not H3K56ac (a histone mark that is specific for HDACs 1 and 2 activity). On the other hand, treatment with 233 caused increases in all of the histone modification marks including H3K56ac. These data support that 966 is a HDAC3 selective inhibitor while 233 inhibits HDACs 1 and 2. Treatment with varying concentrations of either 233 or 966 in CTCL cell lines led to decreased cell growth. Further analysis of these HDI treated cells using flow cytometry (Annexin V and BrdU) and western blot analysis (to examine ɣH2aX levels) determined that the decrease in cell growth was associated with increased apoptosis, DNA damage, and cell cycle defects. HDI treated cells exhibited increased numbers of S phase cells that were not incorporating BrdU, suggesting that these cells did not complete DNA replication and were arrested in S phase.

To begin to elucidate a possible role of HDAC3 in DNA replication, the association of HDAC3 with histone chaperones was tested. HDAC3 was found to associate with the histone chaperone RbAp48 through immunoprecipitation and gel filtration assays, suggesting that HDACs3 may be associated with histone deposition machinery. HDAC3 was present at and around DNA replication forks using iPOND analysis. However, HDAC3 did not appear to

move with the replication fork machinery. Even though HDAC3 did not move with the fork, loss of HDAC3 using genetic and siRNA methods caused DNA replication defects determined by shorter DNA fiber length and slowed DNA replication fork velocity [48, 128]. The selective HDAC3 inhibitor was then tested at various time points in DNA fiber labeling experiments to determine whether HDAC3 was essential for DNA replication and whether any effects observed were due to a global chromatin effect or an effect localized at or near the replication fork. Global changes in histone acetylation were not observed until after 1 hr of treatment with 966 with a dramatic increase in acetylation by 4 hrs, as determined through western blot analysis of histone modification marks. Inhibition of HDAC3 led to a significant decrease in DNA fiber length and replication fork velocity even at short treatment times (5 min). This suggested that HDAC3 is essential for DNA replication and caused localized effects at or around the replication fork. However, this did not differentiate between whether HDAC3 affected the local chromatin around the replication fork or if HDAC3 directly deacetylated a component of the replication machinery.

Due to the high degree of heterogeneity of cancers, it is often beneficial to treat patients with multiple types of drugs. Some of the common treatments in CTCL therapies are Bexarotene (rexinoid), ATRA (retinoid), and Methotrexate (anti-folate). 966 was combined with each of these drugs and observed for combinatorial effects in CTCL cell lines. In Hut78 cells, combination of 966 with each of these drugs individually resulted in additive decreased cell growth. However, in HH cells, an additive effect was only seen with the combination of

966 and Bexarotene. The additive effects seen in these cells suggest that these inhibitors could be combined with other CTCL drugs for possible benefits in treatment.

Treatment with an HDAC 1, 2, and 3 inhibitor also caused increased acetylation levels of specific histone marks, H4K5ac, H3K9K14ac, H3K27ac, and H3K56ac, and decreased cell growth that was associated with apoptosis, DNA damage, and cell cycle arrest. Given the effects of HDAC3 inhibition on DNA replication and the roles of HDAC 1/2 in DNA replication, HDAC 1/2 and HDAC 1-3 selective inhibitors were tested for their effects on DNA replication. Treatment with either of these inhibitors caused significant decreases in fiber lengths and fork velocity.

The data presented in this dissertation, strongly suggest that the mechanism of action of HDIs is to first target DNA replication. There are multiple possibilities for the DNA replication defects that were seen in this dissertation and multiple functions of HDACs near and at the replication fork. One possibility for the DNA replication defects observed is that HDACs function in front of the fork to regulate the amount of acetylation on histones and maintain some organized structure to the chromatin and DNA (Figure 28). If, for example, HDAC3 is inhibited, then there may be an accumulation of acetylation causing the chromatin to unpack too loosely and the DNA may be under wound causing alternative DNA structures, which may cause the DNA to “tangle” in front of the fork [147, 148]. This would not allow the replication machinery to move through

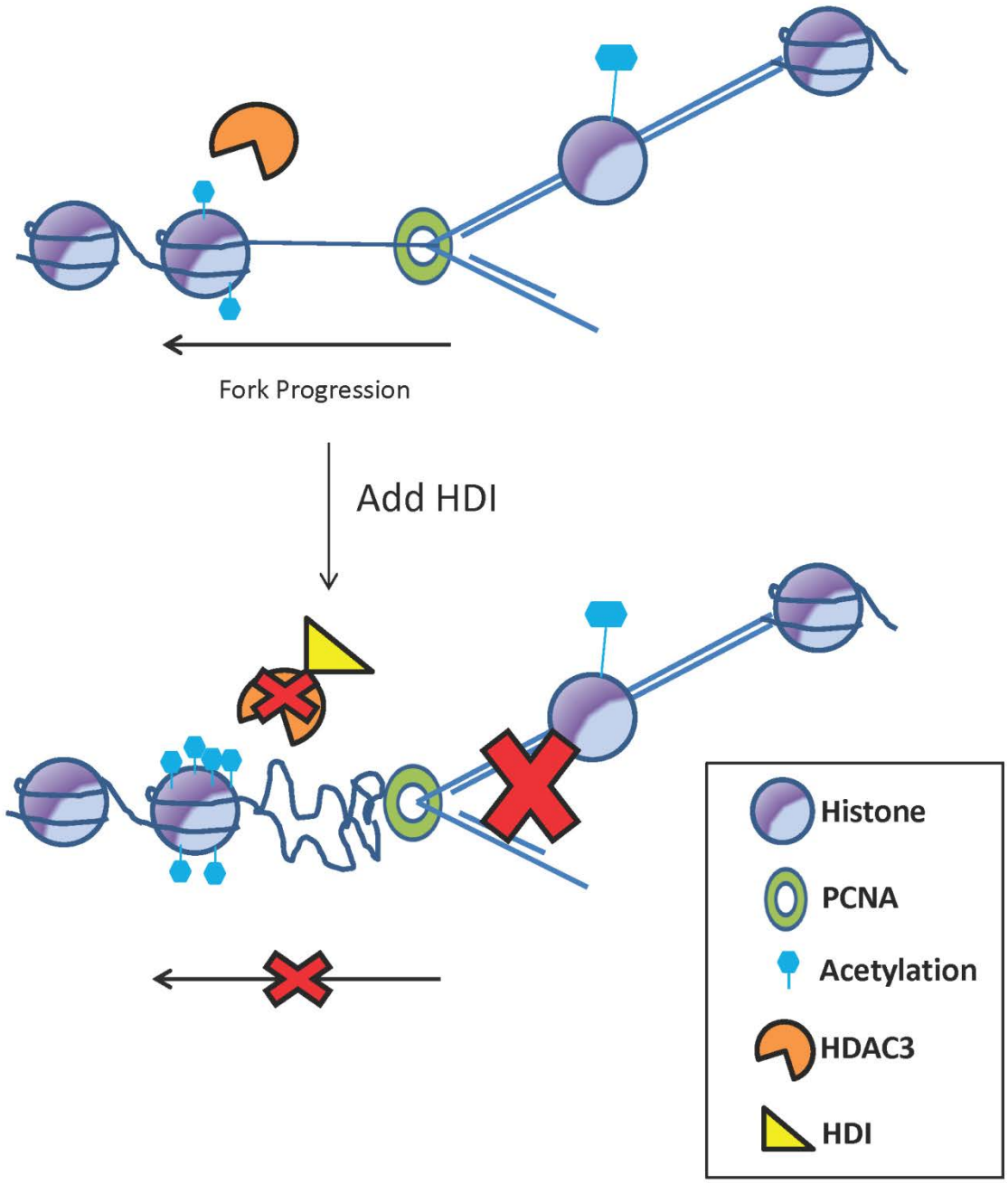

Figure 28. Model of HDAC function that affects replication in front of the replication fork.

the DNA as efficiently, thus causing slowed or stalled DNA replication. Also many proteins bind to supercoiled DNA rather than relaxed DNA so hyperacetylation may inhibit replication proteins from binding DNA [147, 148].

Another possibility is that HDACs may function to deacetylate replication machinery components directly at the fork (Figure 29) to allow for recruitment of other factors or affect the activity of a specific protein. HDACs 1 and 2 regulate the deacetylation of histones during histone deposition after DNA replication, and accumulation of acetylation behind the fork with treatment of an HDI could cause inefficient packaging of chromatin and DNA replication defects (Figure 30). Based on our DNA fiber labeling experiments that involved adding an HDAC3 selective inhibitor at different times during the assays and the iPOND data (Figures 16-20,27), we hypothesize that HDAC3 functions in front of the fork and plays a role in regulating local chromatin around the replication fork and does not directly function at the replication fork. However, more studies will need to be performed.

Future work to determine the exact roles of these HDACs in DNA replication will require a more in depth look at replication fork machinery and acetylated chromatin around the fork. It would be interesting to perform additional iPOND experiments with these selective inhibitors to examine changes in acetylation at and around the fork of histone modification marks when each HDAC is inhibited. Also, one could examine the changes in known acetylated replication machinery proteins using iPOND and these inhibitors to determine

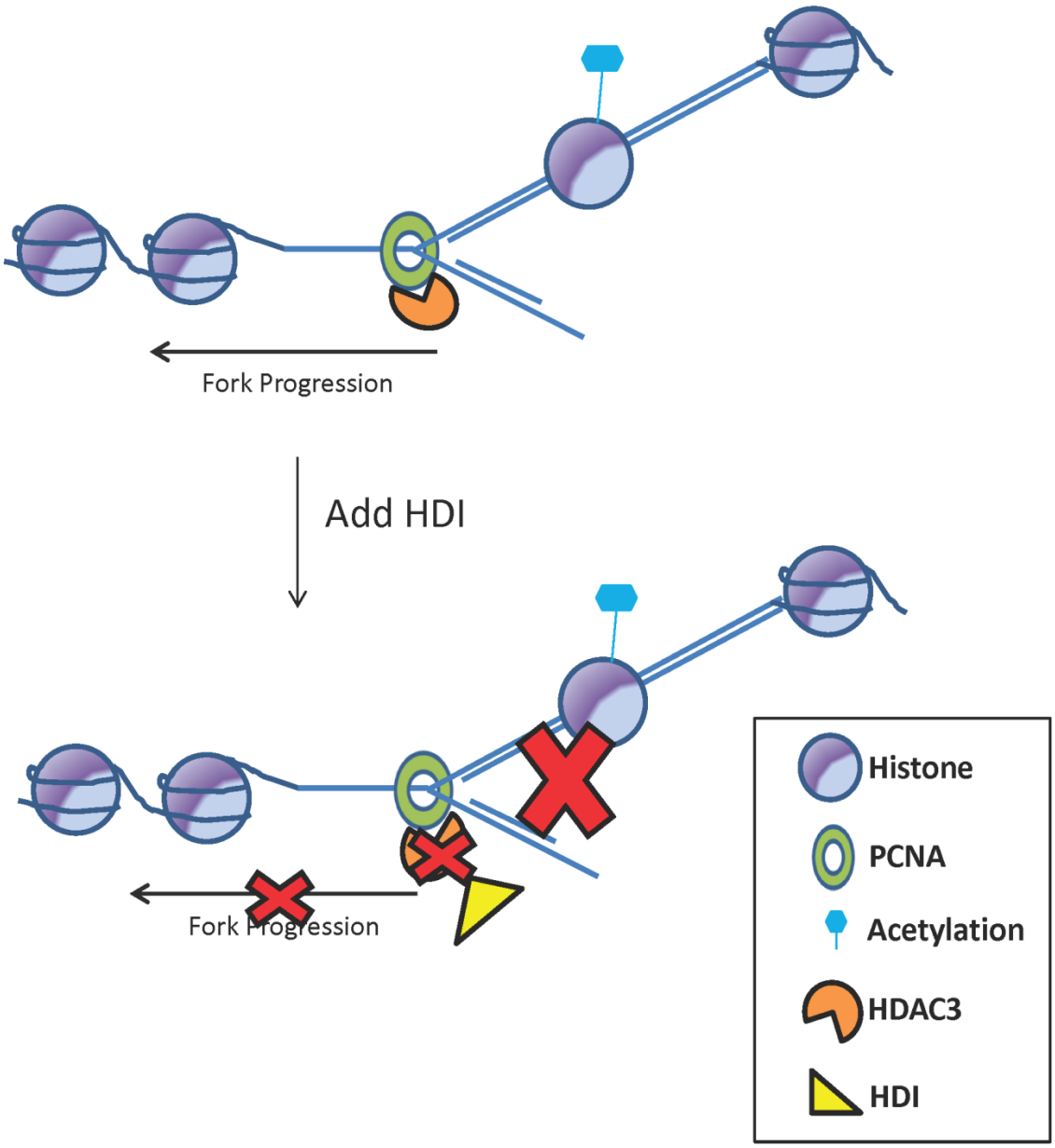

Figure 29. Model of HDAC function that affects replication directly at the replication fork.

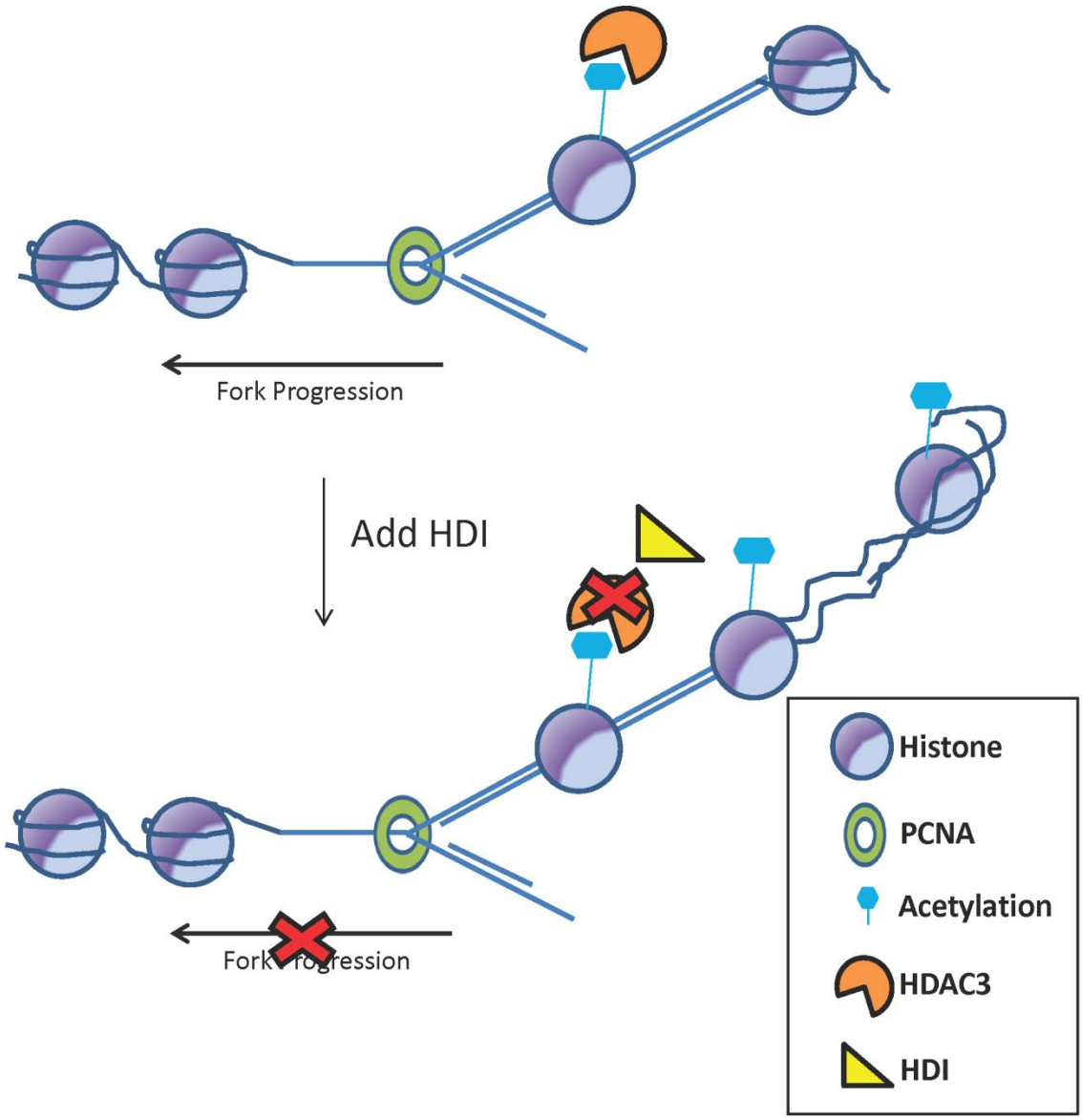

Figure 30. Model of HDAC function that affects replication behind the replication fork.

whether any of these HDACs directly deacetylate replication proteins and possibly affect DNA replication in this way. Also, to potentially discover new targets of HDAC activity around the replication fork or in general, a SILAC mass spectrometry analysis could be performed with an acetyl lysine antibody in cells that were treated with and without these selective inhibitors to determine changes in acetylated proteins with treatment.

Selective HDIs need to be further tested in *in vivo* models to determine their potential in treating cancers or other diseases. Studies of long term memory and neurodegenerative disease have shown promising results with these selective HDIs and little to no toxicity in mice [96, 110, 111]. It would be interesting to study xenograft models where nude mice were injected with CTCL cell lines and then treated with the different selective HDIs to determine if these HDIs caused decreased tumor burden and/or increased survival. Monitoring these mice for different levels of toxicities with different HDIs or combinations of HDIs would be helpful to determine if it would be feasible for clinical trials in patients after further development of these drugs.

Selective inhibitors allow for the combination of different HDIs at varying doses to possibly achieve the same or better efficacy than pan-HDIs but with fewer side effects. For example, an HDAC 1/2 selective inhibitor could be combined with an HDAC3 selective inhibitor at the IC_{50} dose (instead of a maximal dose) and tested for comparable decreases in growth to a pan- or HDAC 1-3 inhibitor. For example, the combination of 233 and 966 resulted in

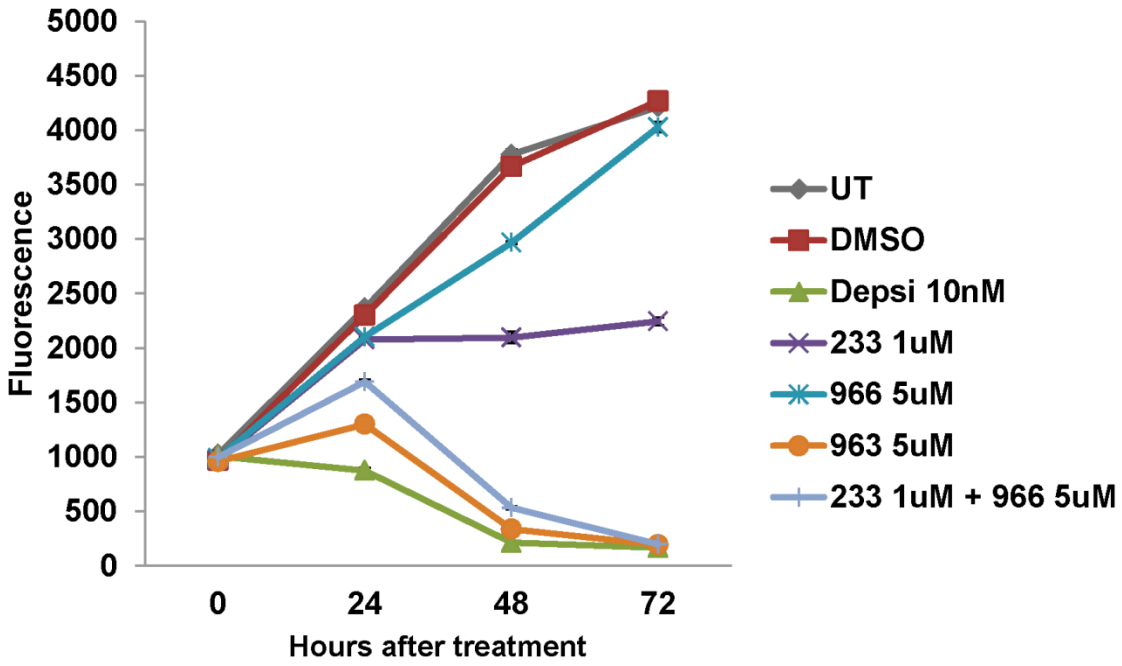

Figure 31. Combined treatment of 233 and 966 results in decreased cell growth comparable to 963 treatment. Growth curves of HDI treated Hut78 cells. Cells were treated once with DMSO, 10 nM Depsipeptide, 1 µM 233, 5 µM 966, 5 µM 963 or a combination of 1 µM233 plus 5 µM 966 at hour 0. Untreated cells and DMSO treated cells were used as controls. Cell growth was assessed at 0, 24, 48, and 72 hours after treatment. Experiment was performed in triplicate.

decreased growth comparable to 963 (Figure 31), suggesting that the combination of selective HDIs may be feasible in treatment plans.

It would also be of interest to test the effects of sequential administration of these selective HDIs to determine whether treatment with one HDI could potentially sensitize the cells to treatment with another HDI. For example, treating cells with a lower dose of 233 for a given time (possibly 12-24hrs) and then treating the cells with a low dose of 966 might result in a more dramatic effect than administering these HDIs together, due to increased sensitization from the first HDI treatment. It may be possible to treat cells with one HDI at a low dose to cause DNA replication defects or DNA damage and then treat cells with a second low dose HDI to cause dramatic accumulation of DNA damage and inhibit any functional DNA repair pathways thus causing increased cell death.

Overall, new, more targeted therapies are needed for treatment of cancer. Due to the many roles of HDACs and the proven success of HDIs in the treatment of CTCL, they are attractive targets for further therapeutic development. However, understanding the mechanisms of action of these HDIs is important for treatment strategies, dosages, and combinatorial studies. The work in this dissertation provided mechanistic information for the action of selective and pan histone deacetylase inhibitors and provided support for the further development of these inhibitors.

REFERENCES

1. Dawson, M.A. and T. Kouzarides, *Cancer epigenetics: from mechanism to therapy.* Cell, 2012. **150**(1): p. 12-27.
2. Groth, A., et al., *Chromatin challenges during DNA replication and repair.* Cell, 2007. **128**(4): p. 721-33.
3. Kouzarides, T., *Chromatin modifications and their function.* Cell, 2007. **128**(4): p. 693-705.
4. Horn, P.J. and C.L. Peterson, *Molecular biology. Chromatin higher order folding--wrapping up transcription.* Science, 2002. **297**(5588): p. 1824-7.
5. Munshi, A., et al., *Histone modifications dictate specific biological readouts.* J Genet Genomics, 2009. **36**(2): p. 75-88.
6. Fierz, B. and T.W. Muir, *Chromatin as an expansive canvas for chemical biology.* Nat Chem Biol, 2012. **8**(5): p. 417-27.
7. Musselman, C.A., et al., *Perceiving the epigenetic landscape through histone readers.* Nat Struct Mol Biol, 2012. **19**(12): p. 1218-27.
8. Waldmann, T. and R. Schneider, *Targeting histone modifications-epigenetics in cancer.* Curr Opin Cell Biol, 2013.
9. Delmore, J.E., et al., *BET bromodomain inhibition as a therapeutic strategy to target c-Myc.* Cell, 2011. **146**(6): p. 904-17.
10. Filippakopoulos, P., et al., *Selective inhibition of BET bromodomains.* Nature, 2010. **468**(7327): p. 1067-73.
11. Kimura, A., K. Matsubara, and M. Horikoshi, *A decade of histone acetylation: marking eukaryotic chromosomes with specific codes.* J Biochem, 2005. **138**(6): p. 647-62.
12. Marmorstein, R., *Structure of histone acetyltransferases.* J Mol Biol, 2001. **311**(3): p. 433-44.
13. Shahbazian, M.D. and M. Grunstein, *Functions of site-specific histone acetylation and deacetylation.* Annu Rev Biochem, 2007. **76**: p. 75-100.
14. Nagy, Z. and L. Tora, *Distinct GCN5/PCAF-containing complexes function as co-activators and are involved in transcription factor and global histone acetylation.* Oncogene, 2007. **26**(37): p. 5341-57.
15. Lafon, A., et al., *MYST opportunities for growth control: yeast genes illuminate human cancer gene functions.* Oncogene, 2007. **26**(37): p. 5373-84.
16. Grant, P.A., et al., *Yeast Gcn5 functions in two multisubunit complexes to acetylate nucleosomal histones: characterization of an Ada complex and the SAGA (Spt/Ada) complex.* Genes Dev, 1997. **11**(13): p. 1640-50.
17. Peterson, C.L. and J. Cote, *Cellular machineries for chromosomal DNA repair.* Genes Dev, 2004. **18**(6): p. 602-16.
18. Vidal, M. and R.F. Gaber, *RPD3 encodes a second factor required to achieve maximum positive and negative transcriptional states in Saccharomyces cerevisiae.* Mol Cell Biol, 1991. **11**(12): p. 6317-27.

19. Rundlett, S.E., et al., *HDA1 and RPD3 are members of distinct yeast histone deacetylase complexes that regulate silencing and transcription.* Proc Natl Acad Sci U S A, 1996. **93**(25): p. 14503-8.
20. Rine, J., et al., *A suppressor of mating-type locus mutations in Saccharomyces cerevisiae: evidence for and identification of cryptic mating-type loci.* Genetics, 1979. **93**(4): p. 877-901.
21. Ivy, J.M., A.J. Klar, and J.B. Hicks, *Cloning and characterization of four SIR genes of Saccharomyces cerevisiae.* Mol Cell Biol, 1986. **6**(2): p. 688-702.
22. Blander, G. and L. Guarente, *The Sir2 family of protein deacetylases.* Annu Rev Biochem, 2004. **73**: p. 417-35.
23. Landry, J., et al., *The silencing protein SIR2 and its homologs are NAD-dependent protein deacetylases.* Proc Natl Acad Sci U S A, 2000. **97**(11): p. 5807-11.
24. Denu, J.M., *The Sir 2 family of protein deacetylases.* Curr Opin Chem Biol, 2005. **9**(5): p. 431-40.
25. Taunton, J., C.A. Hassig, and S.L. Schreiber, *A mammalian histone deacetylase related to the yeast transcriptional regulator Rpd3p.* Science, 1996. **272**(5260): p. 408-11.
26. Bernstein, B.E., J.K. Tong, and S.L. Schreiber, *Genomewide studies of histone deacetylase function in yeast.* Proc Natl Acad Sci U S A, 2000. **97**(25): p. 13708-13.
27. Emiliani, S., et al., *Characterization of a human RPD3 ortholog, HDAC3.* Proc Natl Acad Sci U S A, 1998. **95**(6): p. 2795-800.
28. Hodawadekar, S.C. and R. Marmorstein, *Chemistry of acetyl transfer by histone modifying enzymes: structure, mechanism and implications for effector design.* Oncogene, 2007. **26**(37): p. 5528-40.
29. Yang, X.J. and E. Seto, *The Rpd3/Hda1 family of lysine deacetylases: from bacteria and yeast to mice and men.* Nat Rev Mol Cell Biol, 2008. **9**(3): p. 206-18.
30. Hagelkruys, A., et al., *The biology of HDAC in cancer: the nuclear and epigenetic components.* Handb Exp Pharmacol, 2011. **206**: p. 13-37.
31. Yang, W.M., et al., *Isolation and characterization of cDNAs corresponding to an additional member of the human histone deacetylase gene family.* J Biol Chem, 1997. **272**(44): p. 28001-7.
32. Yang, W.M., et al., *Functional domains of histone deacetylase-3.* J Biol Chem, 2002. **277**(11): p. 9447-54.
33. Zhang, Y., et al., *Histone deacetylases and SAP18, a novel polypeptide, are components of a human Sin3 complex.* Cell, 1997. **89**(3): p. 357-64.
34. Ahringer, J., *NuRD and SIN3 histone deacetylase complexes in development.* Trends Genet, 2000. **16**(8): p. 351-6.
35. Silverstein, R.A. and K. Ekwall, *Sin3: a flexible regulator of global gene expression and genome stability.* Curr Genet, 2005. **47**(1): p. 1-17.
36. Tong, J.K., et al., *Chromatin deacetylation by an ATP-dependent nucleosome remodelling complex.* Nature, 1998. **395**(6705): p. 917-21.

37. Xue, Y., et al., *NURD, a novel complex with both ATP-dependent chromatin-remodeling and histone deacetylase activities.* Mol Cell, 1998. **2**(6): p. 851-61.
38. Takami, Y. and T. Nakayama, *N-terminal region, C-terminal region, nuclear export signal, and deacetylation activity of histone deacetylase-3 are essential for the viability of the DT40 chicken B cell line.* J Biol Chem, 2000. **275**(21): p. 16191-201.
39. Cohen, R.N., et al., *The nuclear corepressors recognize distinct nuclear receptor complexes.* Mol Endocrinol, 2000. **14**(6): p. 900-14.
40. Watson, P.J., et al., *Structure of HDAC3 bound to co-repressor and inositol tetraphosphate.* Nature, 2012. **481**(7381): p. 335-40.
41. Ma, P. and R.M. Schultz, *Histone deacetylase 1 (HDAC1) regulates histone acetylation, development, and gene expression in preimplantation mouse embryos.* Dev Biol, 2008. **319**(1): p. 110-20.
42. Lagger, G., et al., *Essential function of histone deacetylase 1 in proliferation control and CDK inhibitor repression.* EMBO J, 2002. **21**(11): p. 2672-81.
43. Knutson, S.K., et al., *Liver-specific deletion of histone deacetylase 3 disrupts metabolic transcriptional networks.* EMBO J, 2008. **27**(7): p. 1017-28.
44. Trivedi, C.M., et al., *Hdac2 regulates the cardiac hypertrophic response by modulating Gsk3 beta activity.* Nat Med, 2007. **13**(3): p. 324-31.
45. Haberland, M., et al., *Epigenetic control of skull morphogenesis by histone deacetylase 8.* Genes Dev, 2009. **23**(14): p. 1625-30.
46. Bhaskara, S., et al., *Deletion of histone deacetylase 3 reveals critical roles in S phase progression and DNA damage control.* Mol Cell, 2008. **30**(1): p. 61-72.
47. Bhaskara, S., et al., *Hdac3 is essential for the maintenance of chromatin structure and genome stability.* Cancer Cell, 2010. **18**(5): p. 436-47.
48. Summers, A.R., Fischer, M.A., Zhao, Y., Kaiser, J.F., Wells, C.E., Stengel, K.R., Hunt, A., Bhaskara, S. Luzwick, J.W., Cortez, D., Hiebert, S.W., *Hdac3 is essential for DNA replication and differentiation of hematopoietic stem and progenitor cells.* Submitted.
49. Verdin, E., F. Dequiedt, and H.G. Kasler, *Class II histone deacetylases: versatile regulators.* Trends Genet, 2003. **19**(5): p. 286-93.
50. Yang, X.J. and S. Gregoire, *Class II histone deacetylases: from sequence to function, regulation, and clinical implication.* Mol Cell Biol, 2005. **25**(8): p. 2873-84.
51. Chang, S., et al., *Histone deacetylases 5 and 9 govern responsiveness of the heart to a subset of stress signals and play redundant roles in heart development.* Mol Cell Biol, 2004. **24**(19): p. 8467-76.
52. Vega, R.B., et al., *Histone deacetylase 4 controls chondrocyte hypertrophy during skeletogenesis.* Cell, 2004. **119**(4): p. 555-66.
53. Chang, S., et al., *Histone deacetylase 7 maintains vascular integrity by repressing matrix metalloproteinase 10.* Cell, 2006. **126**(2): p. 321-34.

54. Davis, F.J., et al., *Calcium/calmodulin-dependent protein kinase activates serum response factor transcription activity by its dissociation from histone deacetylase, HDAC4. Implications in cardiac muscle gene regulation during hypertrophy.* J Biol Chem, 2003. **278**(22): p. 20047-58.
55. McKinsey, T.A., C.L. Zhang, and E.N. Olson, *Activation of the myocyte enhancer factor-2 transcription factor by calcium/calmodulin-dependent protein kinase-stimulated binding of 14-3-3 to histone deacetylase 5.* Proc Natl Acad Sci U S A, 2000. **97**(26): p. 14400-5.
56. Grozinger, C.M. and S.L. Schreiber, *Regulation of histone deacetylase 4 and 5 and transcriptional activity by 14-3-3-dependent cellular localization.* Proc Natl Acad Sci U S A, 2000. **97**(14): p. 7835-40.
57. McKinsey, T.A., C.L. Zhang, and E.N. Olson, *MEF2: a calcium-dependent regulator of cell division, differentiation and death.* Trends Biochem Sci, 2002. **27**(1): p. 40-7.
58. Lu, J., et al., *Signal-dependent activation of the MEF2 transcription factor by dissociation from histone deacetylases.* Proc Natl Acad Sci U S A, 2000. **97**(8): p. 4070-5.
59. Dittenhafer-Reed, K.E., J.L. Feldman, and J.M. Denu, *Catalysis and mechanistic insights into sirtuin activation.* Chembiochem, 2011. **12**(2): p. 281-9.
60. Lin, S.J., P.A. Defossez, and L. Guarente, *Requirement of NAD and SIR2 for life-span extension by calorie restriction in Saccharomyces cerevisiae.* Science, 2000. **289**(5487): p. 2126-8.
61. Cheng, H.L., et al., *Developmental defects and p53 hyperacetylation in Sir2 homolog (SIRT1)-deficient mice.* Proc Natl Acad Sci U S A, 2003. **100**(19): p. 10794-9.
62. Vakhrusheva, O., et al., *Sirt7 increases stress resistance of cardiomyocytes and prevents apoptosis and inflammatory cardiomyopathy in mice.* Circ Res, 2008. **102**(6): p. 703-10.
63. Mostoslavsky, R., et al., *Genomic instability and aging-like phenotype in the absence of mammalian SIRT6.* Cell, 2006. **124**(2): p. 315-29.
64. Lombard, D.B., et al., *Mammalian Sir2 homolog SIRT3 regulates global mitochondrial lysine acetylation.* Mol Cell Biol, 2007. **27**(24): p. 8807-14.
65. Haigis, M.C., et al., *SIRT4 inhibits glutamate dehydrogenase and opposes the effects of calorie restriction in pancreatic beta cells.* Cell, 2006. **126**(5): p. 941-54.
66. Gao, L., et al., *Cloning and functional characterization of HDAC11, a novel member of the human histone deacetylase family.* J Biol Chem, 2002. **277**(28): p. 25748-55.
67. Hahnen, E., et al., *Histone deacetylase inhibitors: possible implications for neurodegenerative disorders.* Expert Opin Investig Drugs, 2008. **17**(2): p. 169-84.
68. Berry, J.M., et al., *Histone deacetylase inhibition in the treatment of heart disease.* Expert Opin Drug Saf, 2008. **7**(1): p. 53-67.
69. Cress, W.D. and E. Seto, *Histone deacetylases, transcriptional control, and cancer.* J Cell Physiol, 2000. **184**(1): p. 1-16.

70. Barneda-Zahonero, B. and M. Parra, *Histone deacetylases and cancer.* Mol Oncol, 2012. **6**(6): p. 579-89.
71. Grignani, F., et al., *Fusion proteins of the retinoic acid receptor-alpha recruit histone deacetylase in promyelocytic leukaemia.* Nature, 1998. **391**(6669): p. 815-8.
72. Lin, R.J., et al., *Role of the histone deacetylase complex in acute promyelocytic leukaemia.* Nature, 1998. **391**(6669): p. 811-4.
73. Amann, J.M., et al., *ETO, a target of t(8;21) in acute leukemia, makes distinct contacts with multiple histone deacetylases and binds mSin3A through its oligomerization domain.* Mol Cell Biol, 2001. **21**(19): p. 6470-83.
74. Gelmetti, V., et al., *Aberrant recruitment of the nuclear receptor corepressor-histone deacetylase complex by the acute myeloid leukemia fusion partner ETO.* Mol Cell Biol, 1998. **18**(12): p. 7185-91.
75. Lansigan, F. and F.M. Foss, *Current and emerging treatment strategies for cutaneous T-cell lymphoma.* Drugs, 2010. **70**(3): p. 273-86.
76. Wilcox, R.A., *Cutaneous T-cell lymphoma: 2011 update on diagnosis, risk-stratification, and management.* Am J Hematol, 2011. **86**(11): p. 928-48.
77. Li, J.Y., et al., *Management of cutaneous T cell lymphoma: new and emerging targets and treatment options.* Cancer Manag Res, 2012. **4**: p. 75-89.
78. Wollina, U., *Cutaneous T cell lymphoma: update on treatment.* Int J Dermatol, 2012. **51**(9): p. 1019-36.
79. Olsen, E.A., et al., *Sezary syndrome: immunopathogenesis, literature review of therapeutic options, and recommendations for therapy by the United States Cutaneous Lymphoma Consortium (USCLC).* J Am Acad Dermatol, 2011. **64**(2): p. 352-404.
80. Campbell, J.J., et al., *Sezary syndrome and mycosis fungoides arise from distinct T-cell subsets: a biologic rationale for their distinct clinical behaviors.* Blood, 2010. **116**(5): p. 767-71.
81. Narducci, M.G., et al., *Skin homing of Sezary cells involves SDF-1-CXCR4 signaling and down-regulation of CD26/dipeptidylpeptidase IV.* Blood, 2006. **107**(3): p. 1108-15.
82. Picchio, M.C., et al., *CXCL13 is highly produced by Sezary cells and enhances their migratory ability via a synergistic mechanism involving CCL19 and CCL21 chemokines.* Cancer Res, 2008. **68**(17): p. 7137-46.
83. Kempf, W., et al., *EORTC, ISCL, and USCLC consensus recommendations for the treatment of primary cutaneous CD30-positive lymphoproliferative disorders: lymphomatoid papulosis and primary cutaneous anaplastic large-cell lymphoma.* Blood, 2011. **118**(15): p. 4024-35.
84. Duvic, M., *CD30+ neoplasms of the skin.* Curr Hematol Malig Rep, 2011. **6**(4): p. 245-50.
85. Axelrod, P.I., B. Lorber, and E.C. Vonderheid, *Infections complicating mycosis fungoides and Sezary syndrome.* JAMA, 1992. **267**(10): p. 1354-8.

86. Saed, G., et al., *Mycosis fungoides exhibits a Th1-type cell-mediated cytokine profile whereas Sezary syndrome expresses a Th2-type profile.* J Invest Dermatol, 1994. **103**(1): p. 29-33.
87. Heald, P., S.L. Yan, and R. Edelson, *Profound deficiency in normal circulating T cells in erythrodermic cutaneous T-cell lymphoma.* Arch Dermatol, 1994. **130**(2): p. 198-203.
88. Zhang, C. and M. Duvic, *Retinoids: therapeutic applications and mechanisms of action in cutaneous T-cell lymphoma.* Dermatol Ther, 2003. **16**(4): p. 322-30.
89. Zhang, C., et al., *Induction of apoptosis by bexarotene in cutaneous T-cell lymphoma cells: relevance to mechanism of therapeutic action.* Clin Cancer Res, 2002. **8**(5): p. 1234-40.
90. Bertino, J.R., *Cancer research: from folate antagonism to molecular targets.* Best Pract Res Clin Haematol, 2009. **22**(4): p. 577-82.
91. Shen, S., et al., *The use of methotrexate in dermatology: a review.* Australas J Dermatol, 2012. **53**(1): p. 1-18.
92. Chan, E.S. and B.N. Cronstein, *Methotrexate--how does it really work?* Nat Rev Rheumatol, 2010. **6**(3): p. 175-8.
93. Mann, B.S., et al., *FDA approval summary: vorinostat for treatment of advanced primary cutaneous T-cell lymphoma.* Oncologist, 2007. **12**(10): p. 1247-52.
94. Mann, B.S., et al., *Vorinostat for treatment of cutaneous manifestations of advanced primary cutaneous T-cell lymphoma.* Clin Cancer Res, 2007. **13**(8): p. 2318-22.
95. Jain, S. and J. Zain, *Romidepsin in the treatment of cutaneous T-cell lymphoma.* J Blood Med, 2011. **2**: p. 37-47.
96. Rai, M., et al., *Two new pimelic diphenylamide HDAC inhibitors induce sustained frataxin upregulation in cells from Friedreich's ataxia patients and in a mouse model.* PLoS One, 2010. **5**(1): p. e8825.
97. Malvaez, M., et al., *HDAC3-selective inhibitor enhances extinction of cocaine-seeking behavior in a persistent manner.* Proc Natl Acad Sci U S A, 2013.
98. Riggs, M.G., et al., *n-Butyrate causes histone modification in HeLa and Friend erythroleukaemia cells.* Nature, 1977. **268**(5619): p. 462-4.
99. Vidali, G., et al., *Butyrate suppression of histone deacetylation leads to accumulation of multiacetylated forms of histones H3 and H4 and increased DNase I sensitivity of the associated DNA sequences.* Proc Natl Acad Sci U S A, 1978. **75**(5): p. 2239-43.
100. Sealy, L. and R. Chalkley, *The effect of sodium butyrate on histone modification.* Cell, 1978. **14**(1): p. 115-21.
101. Phiel, C.J., et al., *Histone deacetylase is a direct target of valproic acid, a potent anticonvulsant, mood stabilizer, and teratogen.* J Biol Chem, 2001. **276**(39): p. 36734-41.
102. Kim, T.Y., Y.J. Bang, and K.D. Robertson, *Histone deacetylase inhibitors for cancer therapy.* Epigenetics, 2006. **1**(1): p. 14-23.

103. Tsuji, N., et al., *A new antifungal antibiotic, trichostatin.* J Antibiot (Tokyo), 1976. **29**(1): p. 1-6.
104. Yoshida, M., et al., *Potent and specific inhibition of mammalian histone deacetylase both in vivo and in vitro by trichostatin A.* J Biol Chem, 1990. **265**(28): p. 17174-9.
105. Richon, V.M., et al., *Second generation hybrid polar compounds are potent inducers of transformed cell differentiation.* Proc Natl Acad Sci U S A, 1996. **93**(12): p. 5705-8.
106. Richon, V.M., et al., *A class of hybrid polar inducers of transformed cell differentiation inhibits histone deacetylases.* Proc Natl Acad Sci U S A, 1998. **95**(6): p. 3003-7.
107. Rosato, R.R. and S. Grant, *Histone deacetylase inhibitors in cancer therapy.* Cancer Biol Ther, 2003. **2**(1): p. 30-7.
108. Rosato, R.R., J.A. Almenara, and S. Grant, *The histone deacetylase inhibitor MS-275 promotes differentiation or apoptosis in human leukemia cells through a process regulated by generation of reactive oxygen species and induction of p21CIP1/WAF1 1.* Cancer Res, 2003. **63**(13): p. 3637-45.
109. Saito, A., et al., *A synthetic inhibitor of histone deacetylase, MS-27-275, with marked in vivo antitumor activity against human tumors.* Proc Natl Acad Sci U S A, 1999. **96**(8): p. 4592-7.
110. Chou, C.J., D. Herman, and J.M. Gottesfeld, *Pimelic diphenylamide 106 is a slow, tight-binding inhibitor of class I histone deacetylases.* J Biol Chem, 2008. **283**(51): p. 35402-9.
111. Xu, C., et al., *Chemical probes identify a role for histone deacetylase 3 in Friedreich's ataxia gene silencing.* Chem Biol, 2009. **16**(9): p. 980-9.
112. McQuown, S.C., et al., *HDAC3 is a critical negative regulator of long-term memory formation.* J Neurosci, 2011. **31**(2): p. 764-74.
113. Khan, O. and N.B. La Thangue, *HDAC inhibitors in cancer biology: emerging mechanisms and clinical applications.* Immunol Cell Biol, 2012. **90**(1): p. 85-94.
114. Xu, W.S., R.B. Parmigiani, and P.A. Marks, *Histone deacetylase inhibitors: molecular mechanisms of action.* Oncogene, 2007. **26**(37): p. 5541-52.
115. Rosato, R.R. and S. Grant, *Histone deacetylase inhibitors: insights into mechanisms of lethality.* Expert Opin Ther Targets, 2005. **9**(4): p. 809-24.
116. Butler, L.M., et al., *The histone deacetylase inhibitor SAHA arrests cancer cell growth, up-regulates thioredoxin-binding protein-2, and down-regulates thioredoxin.* Proc Natl Acad Sci U S A, 2002. **99**(18): p. 11700-5.
117. Almenara, J., R. Rosato, and S. Grant, *Synergistic induction of mitochondrial damage and apoptosis in human leukemia cells by flavopiridol and the histone deacetylase inhibitor suberoylanilide hydroxamic acid (SAHA).* Leukemia, 2002. **16**(7): p. 1331-43.
118. Sasakawa, Y., et al., *Effects of FK228, a novel histone deacetylase inhibitor, on human lymphoma U-937 cells in vitro and in vivo.* Biochem Pharmacol, 2002. **64**(7): p. 1079-90.

119. Insinga, A., et al., *Inhibitors of histone deacetylases induce tumor-selective apoptosis through activation of the death receptor pathway.* Nat Med, 2005. **11**(1): p. 71-6.
120. Insinga, A., S. Minucci, and P.G. Pelicci, *Mechanisms of selective anticancer action of histone deacetylase inhibitors.* Cell Cycle, 2005. **4**(6): p. 741-3.
121. Rosato, R.R., et al., *Simultaneous activation of the intrinsic and extrinsic pathways by histone deacetylase (HDAC) inhibitors and tumor necrosis factor-related apoptosis-inducing ligand (TRAIL) synergistically induces mitochondrial damage and apoptosis in human leukemia cells.* Mol Cancer Ther, 2003. **2**(12): p. 1273-84.
122. Miller, K.M., et al., *Human HDAC1 and HDAC2 function in the DNA-damage response to promote DNA nonhomologous end-joining.* Nat Struct Mol Biol, 2010. **17**(9): p. 1144-51.
123. Alabert, C. and A. Groth, *Chromatin replication and epigenome maintenance.* Nat Rev Mol Cell Biol, 2012. **13**(3): p. 153-67.
124. Sirbu, B.M., et al., *Analysis of protein dynamics at active, stalled, and collapsed replication forks.* Genes Dev, 2011. **25**(12): p. 1320-7.
125. Yamaguchi, T., et al., *Histone deacetylases 1 and 2 act in concert to promote the G1-to-S progression.* Genes Dev, 2010. **24**(5): p. 455-69.
126. Tyler, J.K., et al., *The p55 subunit of Drosophila chromatin assembly factor 1 is homologous to a histone deacetylase-associated protein.* Mol Cell Biol, 1996. **16**(11): p. 6149-59.
127. Ahmad, A., Y. Takami, and T. Nakayama, *WD dipeptide motifs and LXXLL motif of chicken HIRA are necessary for transcription repression and the latter motif is essential for interaction with histone deacetylase-2 in vivo.* Biochem Biophys Res Commun, 2003. **312**(4): p. 1266-72.
128. Conti, C., et al., *Inhibition of histone deacetylase in cancer cells slows down replication forks, activates dormant origins, and induces DNA damage.* Cancer Res, 2010. **70**(11): p. 4470-80.
129. Sirbu, B.M., F.B. Couch, and D. Cortez, *Monitoring the spatiotemporal dynamics of proteins at replication forks and in assembled chromatin using isolation of proteins on nascent DNA.* Nat Protoc, 2012. **7**(3): p. 594-605.
130. Dorn, E.S., et al., *Analysis of re-replication from deregulated origin licensing by DNA fiber spreading.* Nucleic Acids Res, 2009. **37**(1): p. 60-9.
131. Willemze, R., et al., *WHO-EORTC classification for cutaneous lymphomas.* Blood, 2005. **105**(10): p. 3768-85.
132. Barneda-Zahonero, B. and M. Parra, *Histone deacetylases and cancer.* Mol Oncol, 2012.
133. Cotto, M., et al., *Epigenetic therapy of lymphoma using histone deacetylase inhibitors.* Clin Transl Oncol, 2010. **12**(6): p. 401-9.
134. Melnick, A. and J.D. Licht, *Histone deacetylases as therapeutic targets in hematologic malignancies.* Curr Opin Hematol, 2002. **9**(4): p. 322-32.

135. Yoshida, M., et al., *Histone deacetylase as a new target for cancer chemotherapy.* Cancer Chemother Pharmacol, 2001. **48 Suppl 1**: p. S20-6.
136. Prince, H.M., M.J. Bishton, and S.J. Harrison, *Clinical studies of histone deacetylase inhibitors.* Clin Cancer Res, 2009. **15**(12): p. 3958-69.
137. Whittaker, S.J., et al., *Final results from a multicenter, international, pivotal study of romidepsin in refractory cutaneous T-cell lymphoma.* J Clin Oncol, 2010. **28**(29): p. 4485-91.
138. Gallinari, P., et al., *HDACs, histone deacetylation and gene transcription: from molecular biology to cancer therapeutics.* Cell Res, 2007. **17**(3): p. 195-211.
139. Goodarzi, A.A., A.T. Noon, and P.A. Jeggo, *The impact of heterochromatin on DSB repair.* Biochem Soc Trans, 2009. **37**(Pt 3): p. 569-76.
140. Drogaris, P., et al., *Histone deacetylase inhibitors globally enhance h3/h4 tail acetylation without affecting h3 lysine 56 acetylation.* Sci Rep, 2012. **2**: p. 220.
141. Abbott, R.A., et al., *Bexarotene therapy for mycosis fungoides and Sezary syndrome.* Br J Dermatol, 2009. **160**(6): p. 1299-307.
142. Fernandez-Capetillo, O. and A. Nussenzweig, *Linking histone deacetylation with the repair of DNA breaks.* Proc Natl Acad Sci U S A, 2004. **101**(6): p. 1427-8.
143. Rual, J.F., et al., *Towards a proteome-scale map of the human protein-protein interaction network.* Nature, 2005. **437**(7062): p. 1173-8.
144. Ejlassi-Lassallette, A. and C. Thiriet, *Replication-coupled chromatin assembly of newly synthesized histones: distinct functions for the histone tail domains.* Biochem Cell Biol, 2012. **90**(1): p. 14-21.
145. Milutinovic, S., Q. Zhuang, and M. Szyf, *Proliferating cell nuclear antigen associates with histone deacetylase activity, integrating DNA replication and chromatin modification.* J Biol Chem, 2002. **277**(23): p. 20974-8.
146. Fernandez-Capetillo, O., et al., *H2AX: the histone guardian of the genome.* DNA Repair (Amst), 2004. **3**(8-9): p. 959-67.
147. Lionberger, T.A., et al., *Cooperative kinking at distant sites in mechanically stressed DNA.* Nucleic Acids Res, 2011. **39**(22): p. 9820-32.
148. Bae, S.H., et al., *Structural and dynamic basis of a supercoiling-responsive DNA element.* Nucleic Acids Res, 2006. **34**(1): p. 254-61.